

The Octagonal PET I: Renormalization and Hyperbolic Symmetry

Richard Evan Schwartz *

December 5, 2018

Abstract

We introduce a family of polytope exchange transformations acting on parallelotopes in \mathbf{R}^{2n} , for $n = 1, 2, 3, \dots$. These PETs are constructed using a pair of lattices in \mathbf{R}^{2n} . The moduli space of these PETs is $GL_n(\mathbf{R})$. We study the case $n = 1$ in detail. In this case, we show that the 2-dimensional family is completely renormalizable and that the $(2, 4, \infty)$ hyperbolic reflection triangle group acts (by linear fractional transformations) as the renormalization group on the moduli space. These results have a number of geometric corollaries for the system.

1 Introduction

1.1 Background

A *polytope exchange transformation* (or PET) is defined by a polytope X which has been partitioned in two ways into smaller polytopes:

$$X = \bigcup_{i=1}^m A_i = \bigcup_{i=1}^m B_i.$$

For each i there is some vector V_i such that $B_i = A_i + V_i$. That is, some translation carries A_i to B_i . One then defines a map $f : X \rightarrow X$ by the formula $f(x) = x + V_i$ for all $x \in \text{int}(A_i)$. It is understood that f is not

* Supported by N.S.F. Research Grant DMS-0072607

defined for points in the boundaries of the small polytopes. The inverse map is defined by $f^{-1}(y) = y - V_i$ for all $y \in \text{int}(B_i)$.

The simplest examples of PETs are 1-dimensional systems, known as *interval exchange transformations* (or IETs). These systems have been extensively studied in the past 30 years, and there are close connections between IETs and other areas of mathematics such as Teichmüller theory. See, for instance, [Y] and [Z] and the many references mentioned therein.

The *Rauzy renormalization* [R] gives a satisfying renormalization theory for the family of IETs all having the same number of intervals in the partition. The idea is that one starts with an n -interval IET, and then considers the first return map to a specially chosen sub-interval. This first return map turns out to give another n -interval IET. This mechanism sheds a lot of light on IETs. Some examples of polygon exchange maps have been studied in [AG], [AKT], [H], [Hoo], [LKV], [Low], [S2], [S3], and [T]. Some definitive theoretical work concerning the (zero) entropy of such systems is done in [GH1], [GH2], and [B].

Often, renormalization phenomena are found in these systems: The first return to some subset is conjugate to the original system, and this allows for a detailed understanding of the system. In [S1] and [Hoo], a renormalizable family of polygon exchange maps is constructed. In this setting, like in Rauzy renormalization, the first return map to a subset of one system is conjugate to the first return map of another system in the family. The family in [Hoo] is 2-dimensional and the family in [S1] is 1-dimensional.

In [S1] we introduced a class of PETs which we called *double lattice PETs*. See §2 for a definition. These PETs are defined in terms of a pair of Euclidean lattices, and in each dimension there is a large space of them. We originally found (some of) the double lattice PETs as compactifications of polygonal outer billiards systems, but it seems reasonable to study these objects for their own sake. One motivation for studying these objects is to search for good examples of renormalization schemes for families of higher dimensional PETs.

In this paper we introduce a family of double lattice PETs in every even dimension. In dimension $2n$, the objects are indexed by $GL_n(\mathbf{R})$. In the two-dimensional setting, there is a 1-parameter family. In this paper we will study the 1-parameter family of 2-dimensional examples in detail, showing that it has a complete renormalization scheme. The $(2, 4, \infty)$ reflection triangle group acts on the parameter space, and points in the same orbit have closely related dynamics - e.g., their limit sets have the same Hausdorff dimension.

1.2 The Planar Construction

We will describe the $2n$ -dimensional examples systematically in §2.2. Here we explain the 2-dimensional case in a visual way. Our construction depends on a parameter $s \in (0, \infty)$. Usually, but not always, we take $s \in (0, 1)$. Below we suppress s from most of our notation.

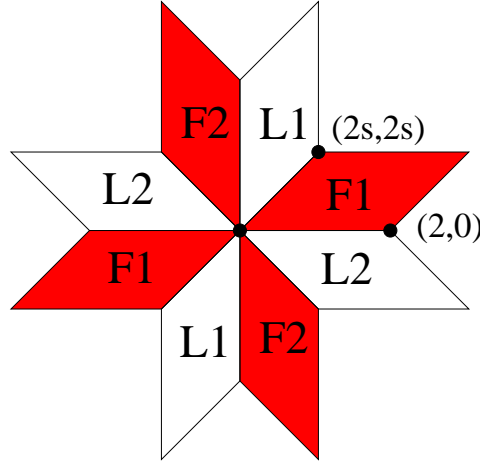


Figure 1.1: The scheme for the PET.

The 8 parallelograms in Figure 1.1 are the orbit of a single parallelogram P under a dihedral group of order 8. Two of the sides of P are determined by the vectors $(2, 0)$ and $(2s, 2s)$. For $j = 1, 2$, let F_j denote the parallelogram centered at the origin and translation equivalent to the ones in the picture labeled F_j . Let L_j denote the lattice generated by the sides of the parallelograms labeled L_j . (Either one generates the same lattice.)

In §2 we will check the easy fact that F_i is a fundamental domain for L_j , for all $i, j \in \{1, 2\}$. We define a system (X', f') , with $X' = F_1 \cup F_2$, and $f' : X' \rightarrow X'$, as follows. Given $p \in F_j$ we let

$$f'(p) = p + V_p \in F_{3-j}, \quad V_p \in L_{3-j}. \quad (1)$$

The choice of V_p is almost always unique, on account of F_{3-j} being a fundamental domain for L_{3-j} . When the choice is not unique, we leave f' undefined. When $p \in F_1 \cap F_2$ we have $V_p = 0 \in L_1 \cap L_2$. We will show in §2 that (X', f') is a PET.

We prefer the map $f = (f')^2$, which preserves both F_1 and F_2 . We set $X = F_1$. Our system is $f : X \rightarrow X$, which we denote by (X, f) .

1.3 The Tiling and the Limit Set

We define a *periodic tile* for (X, f) as a maximal convex polygon on which f and its iterates are completely defined and periodic. So, every point in a periodic tile has the same period and every periodic point is contained in a nontrivial periodic tile. We call the union Δ of the periodic tiles the *tiling*.

We define the *aperiodic set* Λ to be the set of aperiodic points of f . The aperiodic set is a subset of a somewhat more natural set which we call the *limit set* and denote by $\hat{\Lambda}$. The set $\hat{\Lambda}$ is the set of weakly aperiodic points. We call a point $p \in X$ *weakly aperiodic* if there is a sequence $\{q_n\}$ converging to p with the following property. The first iterates of f are defined on q_n and the points $f^k(q_n)$ for $k = 1, \dots, n$ are distinct. When Δ is dense (and it turns out that this always happens for our system) we can say alternately that $\hat{\Lambda}$ consists of those points p such that every neighborhood of p intersects infinitely many tiles of Δ . See Lemma 8.3. One advantage $\hat{\Lambda}$ has over Λ is that $\hat{\Lambda}$ is compact.

Figures 1.2 and 1.3 show (approximations of) Δ and $\hat{\Lambda}$ for two quadratic irrational parameters. In Figure 1.2, the picture is the same (locally) as what one sees for outer billiards on the regular octagon. In Figure 1.3, $\hat{\Lambda}$ is the union of two curves (though we do not give a proof in this paper). Isometric copies of these curves arise in Pat Hooper's system [Hoo]. Hooper and I plan to explore this "coincidence" later.

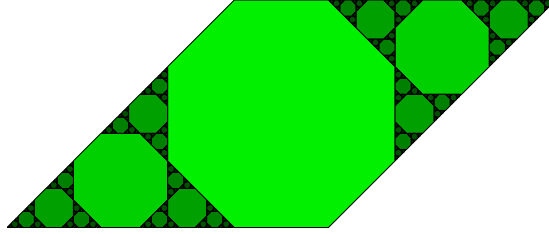


Figure 1.2: The tiling associated to $s = \sqrt{2}/2$

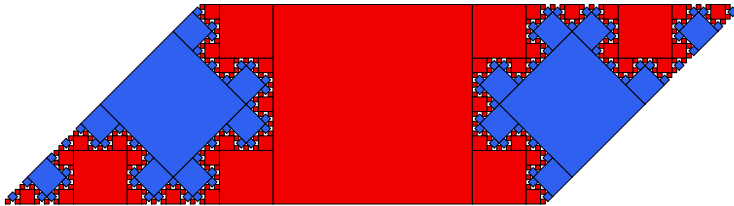


Figure 1.3: The tiling associated to $s = \sqrt{3}/2 - 1/2$.

Here are some results about the tiling.

Theorem 1.1 *When s is rational, Δ_s is a finite union of squares, semi-regular octagons, and right-angled isosceles triangles. When s is irrational, Δ_s is an infinite union of squares and semi-regular octagons. Moreover, the following is true.*

1. Δ_s has at least one square unless $s = \sqrt{2}/2$.
2. Δ_s has only squares if and only if the continued fraction expansion of s has the form $[a_0, a_1, a_2, a_3, \dots]$ where a_k is even for all odd k .
3. Δ_s has infinitely many squares and a dense set of shapes of semi-regular octagons, for almost all s .

A *semi-regular octagon* is an octagon with 8-fold dihedral symmetry. Theorem 1.1 is a corollary of a more precise statement about Δ_s , Theorem 1.4 below. We defer the statement of Theorem 1.4 because it requires a build-up of terminology.

Here are some results about the limit set and the aperiodic set. We only care about the irrational case. These sets are empty when s is rational. See Lemma 2.4.

Theorem 1.2 *Suppose s is irrational.*

1. $\widehat{\Lambda}_s$ has zero area.
2. The projection of $\widehat{\Lambda}_s$ onto a line parallel to any 8th root of unity contains a line segment. Hence $\widehat{\Lambda}_s$ has Hausdorff dimension at least 1.
3. $\widehat{\Lambda}_s$ is not contained in a finite union of lines.
4. $\widehat{\Lambda}_s - \Lambda_s$ has zero length for almost all s . Hence Λ_s has Hausdorff dimension at least 1 for almost all s .

Remark: In §8.5 we prove a more precise result about when $\widehat{\Lambda}_s - \Lambda_s$ has zero length.

The results above are consequences of the renormalization properties of the family $\{(X_s, f_s) \mid s \in (0, 1)\}$. We explain this next.

1.4 Renormalization

We define the *renormalization map* $R : (0, 1) \rightarrow [0, 1)$ as follows.

- $R(x) = 1 - x$ if $x > 1/2$
- $R(x) = 1/(2x) - \text{floor}(1/(2x))$ if $x < 1/2$.

R relates to the $(2, 4, \infty)$ reflection triangle much in the way that the classical Gauss map relates to the modular group.

Define

$$Y = F_1 - F_2 = X - F_2 \subset X. \quad (2)$$

For any subset $S \subset X$, let $f|S$ denote the first return map to S , assuming that this map is defined. When we use this notation, it means implicitly that the map is actually defined, at least away from a finite union of line segments. We call S *clean* if no point on ∂S has a well defined orbit. This means, in particular, that no tile of Δ crosses over ∂S .

Theorem 1.3 (Main) *Suppose $s \in (0, 1)$ and $t = R(s) \in (0, 1)$. There is a clean set $Z_s \subset X_s$ such that $f_t|Y_t$ is conjugate to $f_s^{-1}|Z_s$ by a map ϕ_s .*

1. ϕ_s commutes with reflection in the origin and maps the acute vertices of X_t to the acute vertices of X_s .
2. When $s < 1/2$, the restriction of ϕ_s to each component of Y_t is an orientation reversing similarity, with scale factor $s\sqrt{2}$.
3. When $s < 1/2$, either half of ϕ_s extends to the trivial tile of Δ_t and maps it to a tile in Δ_s .
4. When $s < 1/2$, the only nontrivial orbits which miss Z_s are contained in the ϕ_s -images of the trivial tile of Δ_t . These orbits have period 2.
5. When $s > 1/2$ the restriction of ϕ_s to each component of Y_s is a translation.
6. When $s > 1/2$, all nontrivial orbits intersect Z_s .

The Main Theorem is an example of a result where a picture says a thousand words. Figures 1.4 and 1.5 show the Main Theorem in action for $s < 1/2$. Figures 1.6 and 1.7 show the Main Theorem in action for $s > 1/2$.

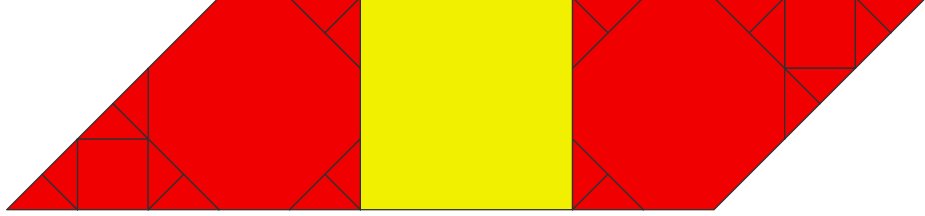


Figure 1.4: Y_t in red for $t = 3/10 = R(5/13)$.

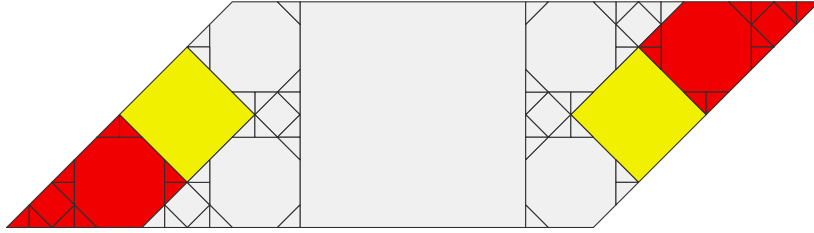


Figure 1.5: Z_s in red $s = 5/13$.

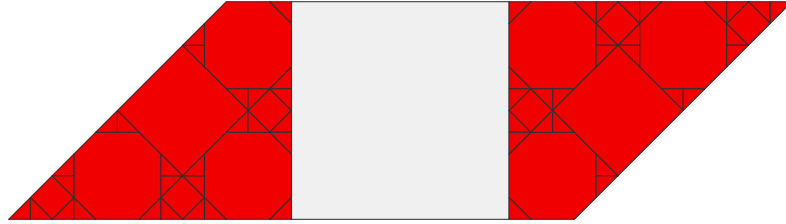


Figure 1.6: Y_t in red for $t = R(8/13) = 5/13$.

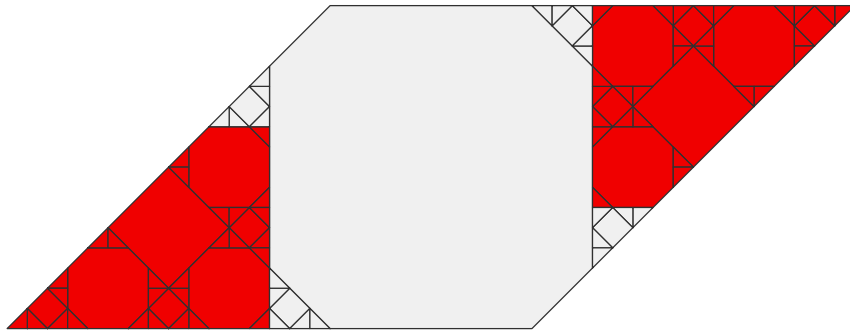


Figure 1.7: Z_s in red for $s = 8/13$.

Now we explain the result behind Theorem 1.1. When $s > 1/2$, the intersection

$$O_s = (F_1)_s \cap (F_2)_s \quad (3)$$

is the semi-regular octagon with vertices

$$(\pm s, \pm(1-s)), \quad (\pm(1-s), \pm s). \quad (4)$$

When $s < 1/2$, the intersection O_s is the square with vertices $(\pm s, \pm s)$.

Suppose we fix some irrational $s = s_0 \in (0, 1)$. Let $s_n = R^n(s)$. Let T_0 be the identity map and, referring to the Main Theorem, let T_n be the linear part of the composition

$$\phi_{s_0} \circ \dots \circ \phi_{s_{n-1}}. \quad (5)$$

The map T_n is a similarity whose exact nature can be computed using the information given in the Main Theorem.

Theorem 1.4 *When $s \in (0, 1)$ is irrational, a polygon arises in Δ_s if and only if it is translation equivalent to $T_n(O_{s_n})$ for some $n = 0, 1, 2, \dots$*

Remark: When s is rational, we get a very similar result, except that Δ_s also contains some right-angled isosceles triangles. See Lemma 6.1.

1.5 Hyperbolic Symmetry

Let $\mathbf{H}^2 \subset \mathbf{C}$ denote the upper half plane model of the hyperbolic plane. Let Γ denote the $(2, 4, \infty)$ reflection triangle group, generated by reflections in the sides of the hyperbolic triangle with vertices

$$\frac{i}{\sqrt{2}}, \quad \frac{1}{2} + \frac{i}{2}, \quad \infty. \quad (6)$$

We extend our parameter range so that our system is defined for all $s \in \mathbf{R}$. The systems at s and $-s$ are identical. Γ acts on the parameter set by linear fractional transformations.

We call the two systems (X_s, f_s) and (X_t, f_t) *locally equivalent* if the following is true. There is a finite union L of lines such that, for each point $p_s \in \widehat{\Lambda}_s - L$, there is a point $p_t \in \widehat{\Lambda}_t$, together with open neighborhoods U_s and U_t of p_s and p_t respectively, such that $\Delta_s \cap U_s$ is equivalent to $\Delta_t \cap U_t$ by a similarity. We also require the same statement to be true with the roles of s and t reversed.

Local equivalence is strong: For instance, the limit sets of locally equivalent systems have the same Hausdorff dimension.

Theorem 1.5 *Suppose s and t are in the same orbit of Γ . Then (X_s, f_s) and (X_t, f_t) are locally equivalent. In particular, the Hausdorff dimension of the limit set, as a function of the parameter, is a Γ -invariant function.*

Remarks:

- (i) Γ is contained with index 4 in the group generated by reflections in the ideal triangle with vertices $0, 1, \infty$. Using this fact, together with a classic result about continued fractions, we will show that the forward orbit $\{R^n(s)\}$ is dense in $(0, 1)$ for almost all $s \in (0, 1)$.
- (ii) The need to exempt a finite union of lines in the definition of local equivalence seems partly to be an artifact of our proof, but in general one needs to disregard some points to make everything work.
- (iii) Given the ergodic nature of the action of Γ , we can say that there is some number δ_0 such that $\dim(\widehat{\Lambda}_s) = \delta_0$ for almost all s . However, we don't know the value of δ_0 .

1.6 Further Results and Claims

This paper now has a sequel [S0]. Here is the main result of that paper.

Theorem 1.6 *Let $s \in (0, 1)$ be irrational.*

1. $\widehat{\Lambda}_s$ is a disjoint union of two arcs if and only if Δ_s contains only squares.
(This happens if and only if $R^n(s) < 1/2$ for all n .)
2. $\widehat{\Lambda}_s$ is a finite forest if and only if Δ_s contains finitely many octagons.
(This happens if and only if $R^n(s) > 1/2$ for finitely many n .)
3. $\widehat{\Lambda}_s$ is a Cantor set if and only if Δ_s contains infinitely many octagons.
(This happens if and only if $R^n(s) > 1/2$ for infinitely many n .)

It turns out that our system here is intimately related to outer billiards on semi-regular octagons. Recall that O_s is the octagon from Equation 4.

Claim 2: *For any $s \in (1/2, 1)$, the limit set and periodic tiling produced by outer billiards on O_s are locally isometric to $\widehat{\Lambda}_s$ and Δ_s , respectively, except at finitely many points.*

This claim is amply supported by computer evidence, and I basically know how to prove it. I hope to prove this claim in a sequel paper.

1.7 Organization

This paper is organized as follows. In §2 we will define our PETs in every even dimension and give some basic information about them.

In §3 we prove some basic results about our PETs, most of which have to do with the stability of orbits under the perturbation of the parameter.

In §4 we prove some symmetry results about our PETs, modulo 2 computer calculations.

In §5 we prove the Main Theorem, modulo 6 more computer calculations.

In §6 we prove Theorem 1.4 and Theorem 1.1.

In §7 we deduce some length and area estimates for the limit set.

In §8 we prove Theorem 1.5 and Theorem 1.2.

In §9 we will do the 8 calculations left over from §4-5. These are exact integer arithmetic calculations.

In §10 we list the raw data needed for the calculations done in §9.

1.8 OctaPET

This paper has a companion java program, called *OctaPET*. I discovered practically everything in the paper while developing and using this program. Also, the calculations mentioned in §9 are all done using OctaPET. I encourage you to use OctaPET while reading the paper. OctaPET relates to this paper much like a song relates to musical notes written on a page. You can download OctaPET from

<http://www.math.brown.edu/~res/Java/OCTAPET.tar>

This is a tarred directory, which untars to a directory called OctaPET. This directory contains a java program which you can compile and then run.

1.9 Acknowledgements

I would like to thank Nicolas Bedaride, Pat Hooper, Injee Jeong, John Smillie, and Sergei Tabachnikov for interesting conversations about topics related to this work. Some of this work was carried out at ICERM in Summer 2012, and some was carried out during my sabbatical in 2012-13. This sabbatical was funded from many sources. I would like to thank the National Science Foundation, All Souls College, Oxford, the Oxford Maths Institute, the Simons Foundation, the Leverhulme Trust, and Brown University for their support during this time period.

2 The Examples

2.1 Double Lattice PETs

Generalizing the construction made in the introduction, we will define what we mean by a double lattice PET. The input to an n -dimensional double lattice PET is a quadruple (L_1, L_2, F_1, F_2) , where

- L_1 and L_2 are lattices in \mathbf{R}^n .
- F_1 and F_2 are parallelotopes.
- F_i is a fundamental domain for L_j for all $i, j \in \{1, 2\}$.

Given (F_1, F_2, L_1, L_2) we have a PET defined on $X' = F_1 \cup F_2$ as follows. For each $x \in F_i$ we define (if possible) $f'(x) = x + V_x$, where $V_x \in F_{3-i}$ is the unique vector such that $x + V_x \in F_{3-i}$. It may happen that V_x is not uniquely defined. In these cases, we leave f undefined. Note that $V_x = 0 \in L_1 \cap L_2$ when $x \in F_1 \cap F_2$, so that our definition is not ambiguous for such points.

Lemma 2.1 (X', f') is a PET.

Proof: First, we check that f is invertible. The inverse map $(f')^{-1}$ is defined just as f' is defined, but with the roles of L_1 and L_2 reversed: For each $x \in F_i$ we define (if possible) $f'(x) = x + W_x$, where $W_x \in F_i$ is the unique vector such that $x + W_x \in F_{3-i}$.

The set X' is partitioned as follows. Let $U \subset X'$ denote the set of points for which the assignment $p \rightarrow V_p$ is defined. The set $X' - U$ is contained in a finite union of hyperplanes. Let $U' \subset X'$ denote the complement of these hyperplanes. Then U' is a finite union of convex polytopes which partitions X' .

The assignment $p \rightarrow V_p$ is constant on each component of U' . Hence $V' = f'(U')$ is also a finite union of polytopes. But construction, the polytopes in V' have disjoint interior, and their union has full measure. Hence V' is a second partition of X' . The two partitions U' and V' determine f in the manner of a PET. ♠

As in the introduction, it is convenient to set $f = (f')^2$ and $X = F_1$. Then (X, f) is also a PET, and the domain of f is the parallelotope X .

2.2 Basic Construction

In this section we construct examples of double lattice PETs in every even dimension. To describe the examples in a natural way, it is useful to work in \mathbf{C}^n , complex n -space. Note, however, that when it comes time to do calculations in the case of interest, \mathbf{C} , we will revert to working in \mathbf{R}^2 .

Let J denote multiplication by i . Consider the following totally real subspaces

$$H = \{(z_1, \dots, z_n) \mid \Im(z_j) = 0 \ \forall j\} \quad D = \{(z_1, \dots, z_n) \mid \Im(z_j) = \Re(z_j) \ \forall j\}. \quad (7)$$

H and D respectively are the fixed point sets of the reflections

$$R_H(z_1, \dots, z_n) = (\bar{z}_1, \dots, \bar{z}_n) \quad R_D(z_1, \dots, z_n) = (i\bar{z}_1, \dots, i\bar{z}_n). \quad (8)$$

Clearly $J = R_D \circ R_H$.

Let $\{H_1, \dots, H_n\}$ and $\{D_1, \dots, D_n\}$ be any \mathbf{R} -bases for H and D respectively. Let F_1 be the parallelogram centered at the origin, whose sides are spanned by the vectors $\{H_1, \dots, H_n, D_1, \dots, D_n\}$. We let $F_2 = J(F_1)$. Since $J^2 = -I$, and F_j is centrally symmetric, we have $J(F_2) = F_1$.

We let L_1 be the lattice spanned by the vectors

$$H_1, \dots, H_n, R_H(D_1), \dots, R_H(D_n).$$

We let L_2 be the lattice spanned by the vectors

$$D_1, \dots, D_n, R_D(H_1), \dots, R_D(H_n).$$

Lemma 2.2 $J(L_1) = L_2$ and $J(L_2) = L_1$.

Proof: Since $J^2 = -\text{Identity}$, we have $J^2(L_j) = L_j$ for $j = 1, 2$. So, it suffices to prove that $J(L_1) = L_2$. We have

$$J(H_j) = R_D R_H(H_j) = R_D(H_j) \in L_2,$$

$$J(R_H(D_j)) = R_D R_H R_H(D_j) = R_D(D_j) = D_j \in L_2.$$

This does it. ♠

In the next result we will use the notation of \mathbf{C}^n but we point out in advance that our argument only uses the \mathbf{R} -structure of \mathbf{C}^n .

Lemma 2.3 F_1 is a fundamental domain for both L_1 and L_2 .

Proof: The proof works the same way for both L_1 and L_2 . So, we will just prove that F_1 is a fundamental domain for L_1 . Let L'_1 denote the lattice generated by the sides of F_1 . A \mathbf{Z} -basis for L'_1 is $\{H_1, \dots, H_n, D_1, \dots, D_n\}$. Let $L''_1 \subset L_1 \cap L'_1$ be the \mathbf{Z} -span of $\{H_1, \dots, H_n\}$.

Note that L_1 and L'_1 have the same co-volume, by symmetry. But the volume of F_1 coincides with the co-volume of L'_1 . Hence, the volume of F_1 coincides with the co-volume of L_1 . To finish the proof we just have to show the following: For any $p \in \mathbf{C}^n$ there is some vector $V \in L_1$ such that $p + V \in F_1$.

Let $\pi : \mathbf{C}^n \rightarrow H^\perp$ be orthogonal projection. The kernel of π is exactly H . Moreover, $\pi(F_1)$ is a fundamental domain for $\pi(L'_1)$ in H^\perp . However $\pi(L_1) = \pi(L'_1)$. So, $\pi(F_1)$ is a fundamental domain for $\pi(L_1)$ as well. Since $\pi(L_1)$ is a fundamental domain for $\pi(F_1)$, there is some $V_1 \in L_1$ such that the translate H' of H , through $p + V_1$, intersects F_1 .

Since F_1 is a parallelotope which intersects H in a parallelotope, the intersection $H' \cap F_1$ is isometric to $H \cap F_1$, and hence is a fundamental domain for L''_1 . Hence, there is some $V_2 \in L''_1$ such that $p + V_1 + V_2 \in F_1$. But $V = V_1 + V_2 \in L_1$. So, $p + V \in F_1$. This proves what we want. ♠

Since J swaps F_1 with F_2 and also swaps L_1 with L_2 , the preceding lemma shows that F_i is a fundamental domain for L_j for all $i, j \in \{1, 2\}$. Now we know that the quadruple (F_1, F_2, L_1, L_2) defines a double lattice PET. We imagine that these higher dimensional examples are interesting, but so far the 2-dimensional case is hard enough for us.

Remark: In our examples, both F_1 and F_2 are centered at the origin. One can define a PET without this property, but some computer experimentation suggests that the character of the PET is much different when F_1 and F_2 are not centered at the origin. In the 2-dimensional example, which is the only one we've looked at, these "exotic" examples all have limit sets which contain open sets. That is, there are aperiodic orbits which are dense in open sets. Indeed, in the 2 dimensional example, this seems to happen for every placement of F_1 and F_2 except for the case when they have a common center (which we might as well take as the origin.)

2.3 The Moduli Space

We keep the notation from the previous section. Let $M \in GL_n(\mathbf{R})$ denote any invertible real $n \times n$ matrix. Note that M commutes with both R_H and R_D . In particular $M(H) = H$ and $M(D) = D$. The system (F_1, F_2, L_1, L_2) is conjugate to the system $(M(F_1), M(F_2), M(L_1), M(L_2))$. So, up to conjugacy, we might as well consider systems in which $\{H_1, \dots, H_n\}$ is the standard basis for \mathbf{R}^n .

We can specify one of our PETs by giving a lattice $\mathbf{s} \subset D$. In case $n = 1$, the lattice \mathbf{s} is 1 dimensional and generated by its shortest vector $s + is$. Identifying \mathbf{C} with \mathbf{R}^2 , this shortest vector becomes (s, s) . For later convenience, we scale everything by a factor of 2, and this gives us the same collection of objects as discussed in connection with Figure 1.1.

We can always take $s \in (0, 1)$ because the case $s > 1$ can be reduced to the case $s \in (0, 1)$ by interchanging the roles of D and H . More precisely, the two parameters s and $s' = 1/(2s)$ give rise to conjugate systems. We will formalize this idea in §4, in the Inversion Lemma. Technically, we could take $s \in (0, \sqrt{2}/2)$, but this further restriction is not convenient to us.

Fixing n , let \mathcal{F} denote the set of PETs which arise from our construction in \mathbf{C}^n . It seems worth pointing out that \mathcal{F} contains a natural collection of rational points. These correspond to taking \mathbf{s} as a sub-lattice of $(\mathbf{Q}[i])^n$. We call such systems rational. In case $n = 1$, this just amounts to taking $s \in \mathbf{Q}$. Here is an easy observation.

Lemma 2.4 *For any rational system, all the orbits are periodic.*

Proof: Let $G = (\mathbf{Z}[i])^n$ be the usual lattice of Gaussian integers. We can conjugate a rational system by a dilation so that $L_1, L_2 \subset G$ and also the vertices of F_1 and F_2 belong to G .

Letting (X, f) denote the associated PET, we observe that all the points in an orbit of f differ from each other by vectors of G . Moreover, such orbits are bounded. Hence, they are finite. ♠

Consider the 2-dimensional case, setting $s = p/q$. In this case, we can dilate so that $H_1 = q$ and $H_2 = p + ip$. Then F_1 and F_2 have volume $(pq)^2$. In this case, the maximum period of any point in the system is $(pq)^2$.

3 Stability and Limiting Considerations

3.1 Intersection of the Lattices

For the rest of the paper, we will consider the case $n = 1$ discussed in the previous chapter. We will work in \mathbf{R}^2 . Our main goals in this chapter are the Stability Lemma and the Convergence Lemma, stated below.

Lemma 3.1 *If s is irrational, then $L_1 \cap L_2 = 0$.*

Proof: L_1 is the \mathbf{Z} -span of $(2, 0)$ and $(2s, -2s)$. and L_2 is the \mathbf{Z} -span of $(0, 2)$ and $(2s, 2s)$. If this lemma is false, then we can find an equation of the form

$$(A + Bs, Bs) = (D, C + D). \quad (9)$$

for integers A, B, C, D . This forces

$$s = \frac{A}{D - B} = \frac{-C}{B + D}, \quad (10)$$

which is only possible if s is rational. ♠

We say that (X, f) is *sharp* if, for any vector V , the sets

$$\{p \mid f(p) = p + V\} \quad (11)$$

are open and convex. The issue is that such a set, if nonempty, might be a finite union of open convex polygons. The systems (X_s, f_s) are not sharp for $s = 1/n$ and $n = 2, 3, 4, \dots$

Lemma 3.2 *Suppose that $s \in [1/4, 1]$. Then (X_s, f_s) is sharp unless $s = 1/n$ for $n = 1, 2, 3, 4$.*

Proof: we first observe that (X_s, f_s) has the following property for all s . Suppose we specify a pair of vectors $(V_1, V_2) \in L_1 \times L_2$. Then the set of points

$$S(V_1, V_2) = \{p \in F_1 \mid p + V_2 \in F_2, p + V_1 + V_2 \in F_1\}$$

is always convex: It is the intersection of 3 parallelograms. So, if (X_s, f_s) is not sharp, then we can find vectors $(V_1, V_2) \in L_1 \times L_2$ and $(V'_1, V'_2) \in L_1 \times L_2$ such that

- $S(V_1, V_2)$ and $S(V'_1, V'_2)$ are both nonempty,
- $V_1 + V_2 = V'_1 + V'_2$
- $(V_1, V_2) \neq (V'_1, V'_2)$.

In this situation, we get a relation like the one in Equation 9.

Both L_1 and L_2 have a standard basis. Let $\{v_{j1}, v_{j2}\}$ be the standard basis for L_j . For instance $v_{11} = (2, 0)$ and $v_{12} = (2s, -2s)$. Since $s \geq 1/4$, the vectors V_j and V'_j must be fairly short. Specifically, we have

$$V_1 = av_{11} + bv_{12}, \quad |a| \leq 1 \quad |b| \leq 2. \quad (12)$$

Similar bounds hold for the other vectors. This means that the relation in Equation 9 satisfies

$$\max(|A|, |C|) \leq 2, \quad \min(|B + D|, |B - D|) \leq 4.$$

But then Equation 10 forces $s = p/q$ where $q \leq 4$. This leaves only the cases $s = 1/n$ for $n = 1, 2, 3, 4$. ♠

Let $p \in X$ be a periodic point of period n . We define the *displacement list* of p to be the list of vectors V_1, \dots, V_n so that

$$f^k(p) = p + \sum_{i=1}^k V_i, \quad k = 1, \dots, n. \quad (13)$$

Corollary 3.3 *Suppose $s \in [1/4, 1]$ and s does not have the form $1/n$ for $n = 1, 2, 3, 4$. Then the set of periodic points in X_s having the same period and displacement list is a single tile of Δ_s .*

.

Proof: We check the result by hand for $s = 1/n$, $n = 1, 2, 3, 4$. For the remaining parameters, the system is sharp, and the set in question is the intersection of n convex polygons. ♠

Remark: In Corollary 4.5, we promote Lemma 3.2 and Corollary 3.3 to results about all $s \in (0, 1)$.

3.2 The Arithmetic Graph

Suppose that $p_0 \in X$ is some point on which the orbit of f is well defined. Call this orbit $\{p_i\}$. There are unique vectors $V_i \in L_1$ and $W_i \in L_2$ such that

$$f'(p_i) = p_i + V_i, \quad f'(p_i + V_i) = p_i + V_i + W_i = p_{i+1}.$$

We call the sequence $\{(V_i, W_i)\}$ the *symbolic encoding* of the orbit. We define the *arithmetic graph* to be the polygon whose i th vertex is $V_0 + \dots + V_i$. We define the *conjugate arithmetic graph* to be the polygon whose i th vertex is $W_0 + \dots + W_i$.

Remark: The displacement list is determined from the arithmetic graph, but the reverse is not *a priori* true. One way to interpret Corollary 3.3 (and the more general Corollary 4.5) is that, unless $s = 1/n$, we can determine the graph from the displacement list.

We hope to explain the structure of the arithmetic graphs associated to systems such as these in a later paper. In this paper, we are mainly interested in using the graph to detect when an orbit is stable under perturbation of the parameter.

Lemma 3.4 (Stability) *If s is irrational and p is a periodic point of f , then both the arithmetic graph of p is a closed polygon.*

When the orbit is periodic, of period n , we have

$$\sum_{i=1}^n (V_i + W_i) = 0. \tag{14}$$

We can re-write this as

$$\sum_{i=1}^n V_i = - \sum_{i=1}^n W_i.$$

But then the common sum belongs to $L_1 \cap L_2$. When s is irrational, Lemma 3.1 then tells us that

$$\sum_{i=1}^n V_i = 0, \quad \sum_{i=1}^n W_i = 0. \tag{15}$$

These two equations are equivalent to the lemma. ♠

3.3 Convergence Properties

We say that a sequence of (solid) polygons P_n converges to a (solid) polygon P_∞ if the sequence converges in the *Hausdorff metric* on the set of compact sets. Concretely, for every $\epsilon > 0$ there should be an N such that $n > N$ implies that every point of P_n is within ϵ of P_∞ and *vice versa*. In the next lemma, we write $\Delta_\infty = \Delta_{s_\infty}$ and $\Delta_n = \Delta_{s_n}$ for ease of notation.

Lemma 3.5 (Approximation) *Let $s_\infty \in (0, 1)$ be irrational, and let $\{s_n\}$ be a sequence of rationals converging to s_∞ . Let P_∞ be a tile of Δ_∞ . Then for all large n there is a tile P_n of Δ_n such that $\{P_n\}$ converges to P_∞ .*

Proof: For any object A that depends on a parameter, we let $A(n)$ denote the object corresponding to the parameter s_n .

Let $p \in P_\infty$ be a periodic point of period N . Let $\{(V_i(\infty), W_i(\infty))\}$ be the symbolic encoding of the orbit. The lattice $L_j(n)$ converges to the lattice $L_j(\infty)$. So, we can uniquely choose vectors $V_i(n) \in L_1(n)$ and $W_i(n) \in L_2(n)$ which converge respectively to $V_i(\infty)$ and $W_i(\infty)$.

By the Stability Lemma, $\sum_{i=1}^N V_i(\infty) = 0$. Hence $\sum_{i=1}^N V_i(n) \rightarrow 0$ as $n \rightarrow \infty$. But, independent of n , there is some ϵ so that the ϵ balls centered on lattice points of $L_1(n)$ are disjoint. This shows that $\sum_{i=1}^N V_i(n) = 0$ for large n . The same argument works with W in place of V . For n large, the symbolic encoding of p starts out

$$V_1(n), W_1(n), \dots, V_N(n), W_N(n).$$

But then p is a periodic point of period N for n large, and the above list is the whole symbolic encoding. In short, p is a periodic point of the same period relative to f_n as it is relative to f_∞ . Let P_n denote the periodic tile containing p .

The size of n required for this continuity argument depends only on the distance from p to ∂P_∞ . For this reason, P_∞ is contained in the ϵ neighborhood of P_n for n sufficiently large. On the other hand, if q lies just outside P_∞ , the symbolic encoding of q relative to f_∞ differs from the symbolic encoding of p relative to f_∞ . But then, by continuity, the same goes for large n in place of ∞ . This shows that P_n is contained in an arbitrarily small neighborhood of P_∞ , once n is sufficiently large.

Putting everything together, we see that $\{P_n\}$ converges to P_∞ , as desired. ♠

4 Symmetry

4.1 Rotational Symmetry

In this chapter we discuss the symmetry of the system (X_s, f_s) . We begin with an obvious result. Define

$$\iota(x, y) = (-x, -y) \quad (16)$$

Note that $\iota(X) = X$ for every parameter.

Lemma 4.1 (Rotation) *ι and f_s commute for all $s \in (0, 1)$.*

Proof: ι preserves F_1, F_2, L_1 , and L_2 . For this reason ι commutes with f . ♠

The subsets of Δ_s and Λ_s lying to the right of the central tiles are reflected images of the subsets of Δ_s and Λ_s lying to the left of the central tiles. For this reason, we will usually consider the picture just on the left hand side.

4.2 Inversion Symmetry

As we have already remarked, we usually take the parameter s to lie in $(0, 1)$ but we can define all the objects for any $s \in (0, \infty)$.

Lemma 4.2 (Inversion) *(X_t, f_t) and (X_s, f_s) are conjugate if $t = 1/2s$.*

Proof: An easy calculation shows that there is a similarity $\phi : R_t \rightarrow R_s$ which maps the horizontal (respectively diagonal) side of R_t to the diagonal (respectively horizontal) side of R_s .

We denote F_1 , at the parameter s , by F_1^s . We make similar notations for the other parameters. We already know that $\phi(F_1^t) = F_1^s$. Let J be rotation by $\pi/2$ clockwise. The map ϕ conjugates J to J^{-1} . For this reason, we have $\phi(F_j^t) = F_j^s$ and $\phi(L_j^t) = L_j^s$ for $j = 1, 2$. This does it. ♠

Lemma 4.2 is really the source of the renormalization map R . However, Lemma 4.2 does not directly apply to our situation. Let's consider the situation in some detail. Let $\rho(s) = 1/2s$. The map ρ is an involution of the parameter interval $[1/2, 1]$. However, the Main Theorem requires us to use the map $R(s) = 1 - s$ on this interval. When $s \in 1/2$ we have $R(s) = t_1$ and $\rho(s) = t_2$, where $t_1 = t_2 - k$, where k is the integer such that $t_2 - k \in (0, 1]$. However, it is not yet clear that the two systems at t_1 and t_2 are related.

4.3 Insertion Symmetry

When $s \in (1/2, 1)$, the intersection $F_1 \cap F_2$ is an octagon, which we call the *central tile*. When $s \leq 1/2$ or $s \geq 1$, the intersection $F_1 \cap F_2$ is a square. This square generates a grid in the plane, and finitely many squares in this grid lie in $X = F_1$. We call these squares the *central tiles*. See Figure 4.1.

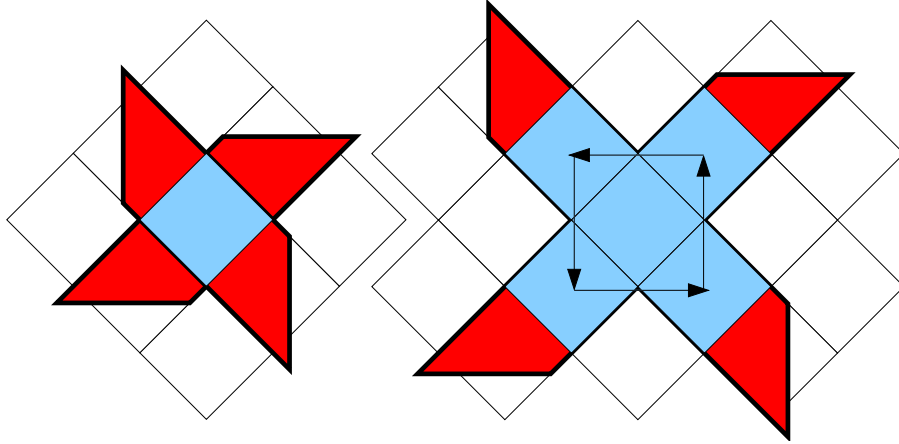


Figure 4.1: The central tiles (blue) for $s = 5/4$ and $t = 9/4$.

Let X^0 denote the portion of X which lies to the left of the central tiles. The set $\iota(X^0)$ is the portion of X which lies to the right of the central tiles. The union $X^0 \cup \iota(X)$ is an f -invariant set.

Lemma 4.3 (Insertion) *Suppose $s \geq 1$ and $t = s + 1$, or suppose $s \leq 1/2$ and $t = s/(2s + 1)$. The restriction of f_s to $X_s^0 \cup \iota(X_s^0)$ is conjugate to the restriction of f_t to $X_t^0 \cup \iota(X_t^0)$. The conjugacy is a piecewise similarity.*

Proof: The case when $s < 1/2$ is equivalent to the case $s > 1$ by the Inversion Lemma. So, we will take $s > 1$ and $t = s + 1$.

We consider how X_s and X_t sit relative to the grid of diamonds mentioned above. When $s, t > 1$, the squares in the grid are diagonals of length 2. Significantly, the diagonals of the diamonds are parallel to the vectors $(\pm 2, 0) \in L_1$ and $(0, \pm 2) \in L_2$. This is true independent of the parameters. There are two more diamonds contained in X_t than there are in X_s . On the central tile, the map f has the obvious action shown in Figure 4.1.

The sets X_s^0 and X_s^t have the same relative position relative to the diamond grid, and there is an obvious translation carrying the one set to the

other. This translation extends to give piecewise translation from the complement of the diamonds in X_s to the complement of the diamonds in X_t . Call points related by this piecewise translation *partners*

Let $p_s \in X_s^0$ and $p_t \in X_s^t$ be partners. Let λ_s and λ_t respectively be the vectors in $(L_2)_s$ and $(L_2)_t$ such that $p_s + \lambda_s \in (F_2)_s$ and $p_t + \lambda_t \in (F_2)_t$. We have either $\lambda_s = \lambda_t + (2, 0)$ or $\lambda_s = \lambda_t + (0, 2)$, depending on whether or not $p_s + \lambda_s$ and $p_t + \lambda_t$ lie in the top or bottom of $(F_2)_s$ and $(F_2)_t$ respectively. The answer (top/bottom) is the same for s as it is for t . In short, the two new points $p_s + \lambda_s$ and $p_t + \lambda_t$ are again partner points. Repeating this construction again, we see that $f_s(p_s)$ and $f_t(p_t)$ are partner points. This is what we wanted to prove. ♠

Remark: Informally, what Insertion Lemma says is that, for $s \geq 1$, the tiling Δ_{s+1} is obtained from the tiling Δ_s by inserting two new large diamonds.

Lemma 4.4 Δ_s consists entirely of squares and right-angled isosceles triangles when $s = 1, 2, 3, \dots$ and when $s = 1/2, 1/4, 1/6, \dots$

Proof: We check this for $n = 1$ just by a direct calculation. See Figure 4.2.

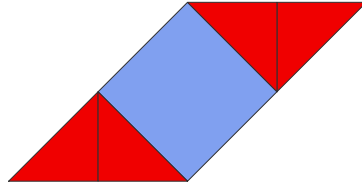


Figure 4.2: The tiling Δ_s for $s = 1$.

The cases $n = 2, 3, 4, \dots$ now follow from the Insertion Lemma. The cases $n = 1/2, 1/4, 1/6, \dots$ follow from the cases $n = 1, 2, 3, \dots$ and the Inversion Lemma. ♠

Combining the Insertion Lemma with Lemmas 3.2 and Corollary 3.3, we have

Corollary 4.5 Let $s \in (0, 1)$. Suppose s does not have the form $1/n$ for $n = 1, 2, 3, \dots$. Then (X_s, f_s) is clean, and the set of periodic points in X_s having the same period and displacement list is a single tile of Δ_s .

4.4 Bilateral Symmetry

In this section we always take $s \in (0, 1)$. We say that a line L is a *line of symmetry* for Δ_s if

$$\Delta_s \cap (X_s \cap \rho(X_s)) \quad (17)$$

is invariant under the reflection ρ in L . Note that X_s itself need not be invariant under L .

Figure 4.3 shows 3 lines. H is the line $y = 0$ and V is the line $x = -1$ and D_s is the line of slope -1 through the bottom vertex of the leftmost central square of Δ_s .

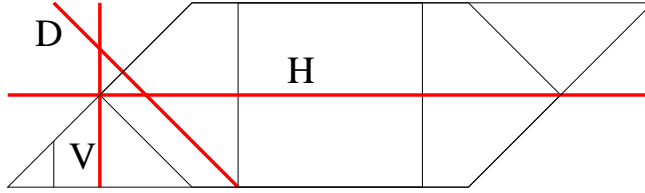


Figure 4.3 H and V and D_s for the parameter $s = 2/5$.

In this section we will prove (modulo 2 finite calculations) the following result.

Lemma 4.6 (Bilateral) *For all $s \in (0, 1)$, the lines H , V , and D_s are lines of symmetry of Δ_s .*

We will prove this result through a series of smaller lemmas.

Define

$$A = X \cap \rho_H(X), \quad B = X \cap \rho_V(X). \quad (18)$$

Here ρ_H is the reflection in H and ρ_V is the reflection in V . A is the green hexagon shown in Figure 4.4. The complement $X - A$ consists of two triangles, B and $\iota(B)$ as shown in Figure 4.4.

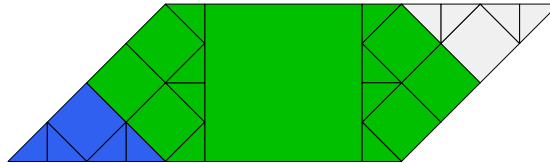


Figure 4.4 A_s (green) and B_s (blue) and $\iota(B_s)$ (white) for $s = 2/5$.

Each of the pieces A , B and $\iota(B)$ has a vertical line of bilateral symmetry. The reflections across these vertical lines gives rise to a piecewise isometry of X . We call this map μ . If $p \in A$ we define $\mu(p)$ to be reflection in the vertical line of symmetry for A , etc.

The Insertion Lemma allows us to turn many infinite-appearing calculations into finite calculations. The problem with trying to compute something for every parameter in $(0, 1)$ is that the number of domains of continuity for the map f_s tends to ∞ as $s \rightarrow 0$. However, if we restrict our attention to $s \in [1/4, 1)$, then there is a uniform bound on the number of regions of continuity. In this range, we can establish identities using a finite calculation. The picture for any parameter $s < 1/4$ is the same as some picture for $s' > 1/4$, up to the insertion of finitely many central tiles. In §9 we prove the following result by direct calculation.

Lemma 4.7 (Calculation 1) *If $s \in [1/4, 1]$ then $\mu_s \circ f_s \circ \mu_s = f_s^{-1}$ wherever both maps are defined.*

Combining this calculation with the Insertion Lemma, we have

Corollary 4.8 *Suppose $s \in (0, 1)$ then $\mu_s \circ f_s \circ \mu_s = f_s^{-1}$ wherever both maps are defined.*

Proof of Statements 1 and 2: Now we prove Statements 1 and 2 of the Bilateral Lemma. Using the rotational symmetry, it suffices to prove that $\Delta \cap A$ and $\Delta \cap B$ are invariant under the action of μ . We will consider the situation in the Hexagon A . The situation in the other regions has a similar treatment.

Let τ be a tile of Δ that is contained in A . All iterates of f are defined on the interior of τ . Let n be the order of f on the interior of τ . The first n iterates of $\mu f \mu$ are defined on an open set $\tau' = \tau - L$. Here L is a finite union of line segments. For each $p \in \tau'$, the period of $\mu f \mu$ on p is n . Since μ is everywhere defined in the interior of A , we see that f^{-1} is defined on all points of $\mu(\tau')$. But all the points in $\mu(\tau')$ have the same displacement list. Hence $\mu(\tau')$ is convex. This is only possible if $\tau' = \tau$. ♠

Define

$$P = X \cap \rho_D(X), \quad Q = X^0 - P. \quad (19)$$

When $s < 1/2$, the set P_s is a pentagon and Q_s is an isosceles triangle. When $s > 1/2$, the set P_s is a triangle and Q_s is empty. Figures 4.5 shows the case $s < 1/2$.

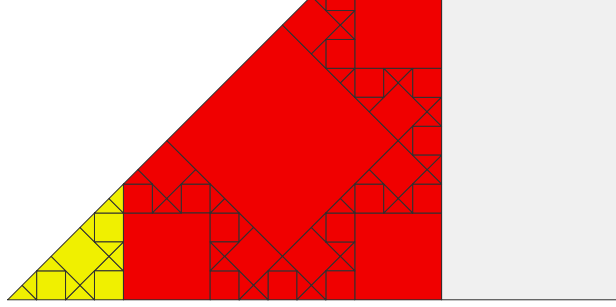


Figure 4.5: P_s (red) and Q_s (yellow) for $s = 11/30$.

X_s is partitioned into square central tiles and the additional tiles P_s , Q_s , $\iota(P_s)$ and $\iota(Q_s)$. (When $s > 1/2$, the tiles Q_s and $\iota(Q_s)$ do not exist.) Each tile in this partition has reflection symmetry, in a line of slope -1 . Let $\nu_s : X_s \rightarrow X_s$ be the piecewise isometry which does this reflection on each piece.

In §9 we prove the following result by direct calculation.

Lemma 4.9 (Calculation 2) *If $s \in [1/4, 1]$, then $\nu_s \circ f_s \circ \nu_s = f_s^{-1}$ wherever both maps are defined.*

Combining this calculation with the Insertion Lemma, we have

Corollary 4.10 *If $s \in (0, 1)$ then $\nu_s \circ f_s \circ \nu_s = f_s^{-1}$ wherever both maps are defined.*

Proof of Statement 3: Statement 3 of the Bilateral Lemma is deduced from Corollary 4.10 in the same way that Statements 1 and 2 are deduced from Corollary 4.8. ♠

5 Proof of the Main Theorem

5.1 Discussion and Overview

The Inversion Lemma and the Insertion Lemma go part of the way towards proving the Main Theorem. These two results say that the systems (X_s, f_s) and (X_t, f_t) are related, in the appropriate sense, for pairs $(s, 1/2s)$ and, assuming $s > 1$, for pairs $(s, s - 1)$. These results are not strong enough to establish the Main Theorem. For instance, when $s = 2/5$ we have $R(s) = 1/4$. We can say that the parameters $2/5$ and $5/4$ are related by Condition 1 above. However, Condition 2 does not apply to $(s, t) = (1/4, 5/4)$ because $s < 1$. Similarly, if $s = 3/4$ we have $R(s) = 1/4$. Here, neither condition applies.

The reader might wonder why we care about R in the first place. Perhaps we can prove all the corollaries to the Main Theorem just with the limited symmetries we have already established. The virtue of R is that, for every rational parameter p/q , one of the two iterates $R(p/q)$ or $R^2(p/q)$ has denominator smaller than q . Thus, the map R gives us an inductive mechanism for understanding our system at all rational values. Once we have a good understanding of what happens at rational values, we can take limits. We cannot do this much with just the two conditions listed above.

Referring to Theorem 1.5, the existence of Γ sheds light on what we have said above. The way we prove the Main Theorem, roughly speaking, is to verify certain facts on the generators of Γ , by computation or symmetry, and then use the group structure to extract global statements about the renormalization map R . What we are saying, in a sense, is that we haven't checked *enough* of Γ yet. What is missing is a statement about what happens for pairs $(s, s - 1)$ with $s \in (1, 2)$ and for pairs $(s, 1 - s)$ with $s \in (1/2, 1)$.

Here are the two results we prove in this chapter. The first is equivalent to the half of the Main Theorem corresponding to $s \in (0, 1/2)$.

Lemma 5.1 *Suppose $s \in (1, 2)$ and $t = s - 1$. Let $\phi_s : Y_t \rightarrow X_s$ be the map which is a translation on each half of Y_t and maps the acute vertices of Y_t to the acute vertices of X_s . Let $Z_s = \phi_s(Y_t)$. Then ϕ_s conjugates $f_t|_{Y_t}$ to $f_s|_{Z_s}$, and Z_s is a clean set. Either half of ϕ_s extends to the trivial tile of Δ_t and maps it to tiles τ_1 and τ_2 . The only nontrivial f_s -orbits which miss Z_s are contained in $\tau_1 \cup \tau_2$ and have period 2.*

Our other result is just a restatement of the half of the Main Theorem corresponding to $s \in (1/2, 1)$.

Lemma 5.2 *Suppose $s \in (1/2, 1)$ and $t = 1 - s$. Let $\phi_s : Y_t \rightarrow X_s$ be the map which is a translation on each half of Y_t and maps the acute vertices of Y_t to the acute vertices of X_s . Let $Z_s = \phi_s(Y_t)$. Then ϕ_s conjugates $f_t|_{Y_t}$ to $f_s^{-1}|_{Z_s}$, and Z_s is a clean set. All nontrivial f_s -orbits intersect Z_s .*

To be sure, let's deduce the Main Theorem from these results.

Proof of the Main theorem: Lemma 5.2 is just a restatement of the Main Theorem for $s \in (1/2, 1)$. Suppose that $s < 1/2$. By the Insertion Lemma, it suffices to consider the case when $s \in (1/4, 1/2)$. By the Inversion Lemma, the system (X_s, f_s) is conjugate to the system (X_t, f_t) , where $t = 1/2s$. Here $t \in (1, 2)$. But now Lemma 5.1 applies to the pair $(t, t - 1)$ and $t - 1 = R(s)$. When we combine the conjugacy given by the Inversion Lemma with the one given by Lemma 5.1, we get the statement of the Main Theorem. ♠

We would like to have conceptual proofs of Lemmas 5.1 and 5.2, but we do not. Instead, we will give computational proofs. The difficulty in giving a computational proof is that it seems to involve an infinite amount of calculation. Consider, for instance, what happens in Lemma 5.1 as $s \rightarrow 1$. In this case, the area of Y_t tends to 0. But then, the proportion of X_s taken up by Z_s tends to 0. But then the amount of time it takes for some orbits to return to X_s probably tends (and, in fact, does tend) to ∞ . This makes a direct computer verification difficult. A similar problem happens for Lemma 5.2 as $t \rightarrow 1$.

In §9 we will prove the following results by a direct and finite calculation.

Lemma 5.3 (Calculation 3) *Lemma 5.1 holds for all $t \in [5/4, 2]$.*

Lemma 5.4 (Calculation 4) *Lemma 5.2 holds for all $t \in [1/2, 3/4]$.*

The trick is to relate the system on the intervals $[1/2, 3/4]$ and $[5/4, 2]$ to the larger intervals $[1/2, 1)$ and $(1, 2]$. We will do this by establishing some auxilliary symmetry results. One can view these auxilliary results as statements about some of the other elements in the group Γ .

5.2 First Modular Symmetry

Define the maps

$$T(s) = \frac{s-2}{2s-3}, \quad \omega_s(x, y) = (3-2s)(x, y) \pm (2-2s, 0). \quad (20)$$

We take $s \in (1, 4/3]$, so that $u = T(s) \in (1, 2]$. The domain of ω_s is the set Y_u from the Main Theorem. The (+) option for ω_s is taken when $x < 0$ and the (-) option is taken then $x > 0$. We set $W_s = \omega_s(Y_u)$. A picture says a thousand words. In the picture W_s^0 is the left half of W_s and Y_u^0 is the left half of Y_u .

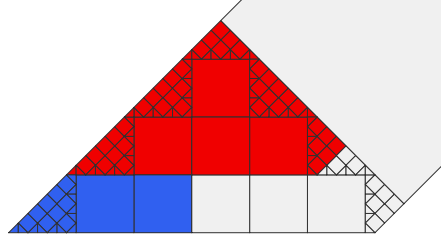


Figure 5.1: $\Delta_s \cap W_s^0$ (red) for $s = 22/19$.

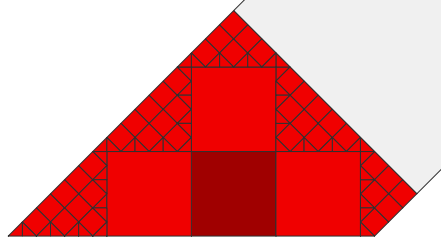


Figure 5.2: $\Delta_u \cap Y_u^0$ (red) for $u = T(22/19) = 16/13$.

Lemma 5.5 (Calculation 5) *Let $s \in (1, 4/3]$ and $u = T(s)$. Then ω_s conjugates $f_u|Y_u$ to $f_s|W_s$. Moreover, Z_s is a clean set.*

Remarks:

- (i) As a corollary, we see that ω_s maps $\Delta_u \cap Y_u^0$ to $\Delta_s \cap W_s^0$. This explains why the tilings in the red regions in Figures 5.1 and 5.2 look the same.
- (ii) We only need Calculation 5 for $s \in (1, 5/4]$, but it is more convenient to make the calculation on the larger interval.

The blue set in Figure 5.1 is isometric the left half of Y_{s-1} . We denote this set by Z_s^0 and we set $Z_s = Z_s^0 \cup \iota(Z_s)$. Here ι is reflection in the origin. We let τ denote the square whose left side coincides with the right side of Z_u^0 . The square τ_u is a darker red than the others in Figure 5.1. We define τ_s just as we defined τ_u , with s in place of u . Let δ_s be the vector which spans the diagonal of τ_s , pointing from the bottom left vertex to the top right vertex.

Lemma 5.6 (Calculation 6) *Let $s \in (1, 5/4]$, so that $u = T(s) \in (1, 3/2]$. Then*

1. τ_u is a tile of Δ_u , having period 2.
2. $f_s^{-1}(p) = p + \delta_s$ for all $p \in Z_s^0$.
3. $f_s^{-1}(X_s - Z_s - W_s) \subset Z_s \cup \tau_s \cup \iota(\tau_s)$.

We will establish these results in §9. Calculation 6 really just amounts to inspecting the partitions for f_u and f_s .

5.3 Proof of Lemma 5.1

Let T be the map from Equation 20.

Lemma 5.7 *Let $s \in (1, 5/4)$ be any point. Then there is some positive k such that $T^k(s) \in (5/4, 3/2)$.*

Proof: T is a parabolic linear fractional transformation fixing 1 and having the property that $T(5/4) = 3/2$. So, the iterates $T^j(s)$, $j = 1, 2, 3, \dots$ are increasing, but then cannot avoid the interval $(5/4, 3/2)$. ♠

Lemma 5.1 follows immediately from Lemma 5.7 and from the following result.

Lemma 5.8 *If Lemma 5.1 is true for some $u \in (1, 3/2)$, then Lemma 5.1 is also true for $s = T^{-1}(u)$.*

The rest of this section is devoted to proving Lemma 5.8. Let $s' = s - 1$ and $u' = u - 1$. A calculation shows that

$$s' = \frac{u'}{2u' + 1}. \quad (21)$$

In other words, s' and u' are related exactly as in the Insertion Lemma. So, the dynamics relative to s' is the same as the dynamics relative to u' , except that two more central squares are inserted for s' . These central squares have period 2. We need to establish the same relation between $f_u|_{Z_u}$ and $f_s|_{Z_s}$.

Define

$$Z_u^* = Z_u \cup \tau_u \cup \iota(\tau_u). \quad (22)$$

We are augmenting Z_u by inserting two period-2 squares at the two ends of Z_u . Statement 1 of Calculation 6 guarantees that these extra squares really are tiles of Δ_u .

Lemma 5.9 *There is a piecewise homothety h_s which carries Z_u^* to Z_s and respects the tilings Δ_u and Δ_s .*

Proof: By Statement 2 of Calculation 6, and rotational symmetry, the piecewise similarity

$$h_s = f_s \circ \omega_s \quad (23)$$

maps Z_u^* to Z_s . Thanks to Statement 1 of Calculation 6, the tile τ_u and its rotated image are really tiles of Δ_u . Thanks to Calculation 5, the map h_s maps the tiling $Z_u^* \cap \Delta_u$ to the tiling $Z_s \cap \Delta_s$. ♠

Lemma 5.10 *h_s conjugates $f_u|_{Z_u^*}$ to $f_s|_{Z_s}$.*

Proof: Choose some point $r_1 \in Z_u^*$. Let $p_1 = h_s(r_1) \in Z_s$. Let p_n be the first return of the forward f_s -orbit of p_1 to Z_s . So, p_2, \dots, p_{n-1} do not belong to Z_s . Define

$$q_j = f_s^{-1}(p_j), \quad j = 1, n. \quad (24)$$

By Statement 2 of Calculation 6, we have $q_n \in \omega_s(Z_u^*)$. Define

$$r_n = \omega_s^{-1}(q_n). \quad (25)$$

By Calculation 5, the point r_n lies in the forward f_u -orbit of r_1 . To finish our proof, we just have to show that r_n is the first return of this orbit to Z_u^* . If this is false, then there is some earlier point $r_k \in Z_u^*$. But then $h_s(r_k) = q_m \in Z_s$ for some $m = 2, \dots, (n-1)$. This is a contradiction. ♠

Lemma 5.11 *Any nontrivial f_s -orbit, except those contained in $\tau_s \cup \iota(\tau_s)$, intersects Z_s .*

Proof: Consider first the orbit of a point $p \in W_s$. Let $q = \omega_s^{-1}(p)$. Since the Main Theorem is true for the parameter u , the orbit of q intersects Z_u^* . But then, by Calculation 5, the orbit of q intersects $\omega_s(Z_u^*) = f_s^{-1}(Z_s)$. But then $f_s(q) \in Z_s$.

It remains to consider the orbit of a point $p \in X_s - Z_s - W_s$. If $p \in \tau_s \cup \iota(\tau_s)$, there is nothing to prove. Otherwise, Statement 3 of Calculation 6 finishes the proof. ♠

5.4 The Second Modular Symmetry

Now we turn our attention to the proof of Lemma 5.2. We re-use some of the notation from the other case. Define

$$T = \frac{3x-2}{2x-1}, \quad \omega_s(x, y) = (2s-1)(x, y) \pm (2s-2). \quad (26)$$

T here is the inverse of the one in Equation 20. We take $s \in [3/4, 1)$, so that $u = T(s) \in [1/2, 1)$. The domain of ω_s is the set Y_u from the Main Theorem. The (+) option for ω_s is taken when $x < 0$ and the (−) option is taken then $x > 0$. We set $W_s = \omega_s(Y_u)$.

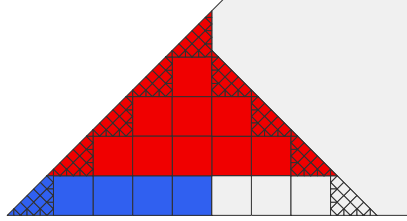


Figure 5.3: Half of W_s^0 for $s = 28/31$.

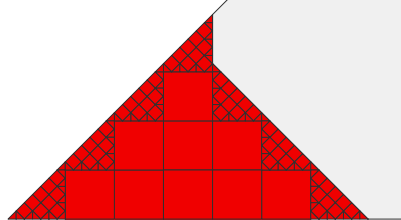


Figure 5.4: $\Delta_u \cap X_u^0$ for $u = T(28/31) = 22/25$.

The rest of the definitions are done exactly as in the previous section. The main difference here is that the tile τ_s and τ_u belong to Z_s and Z_u respectively. As above, δ_s is the vector which spans the diagonal of τ_s , pointing from the bottom left vertex to the top right vertex. Calculation 7 is the calculation parallel to Calculation 5.

Lemma 5.12 (Calculation 7) *Let $s \in [3/4, 1)$ and $u = T(s)$. Then ω_s conjugates $f_u|Y_u$ to $f_s|W_s$. Moreover, Z_s is a clean set.*

Calculation 8 is the calculation parallel to Calculation 6. Notice that there are some differences. Item 1 of Calculation 6 refers to τ_u . We will discuss the reason for this difference below. Item 2 of Calculation 8 refers to the modified set

$$(Z_s^0)^* = Z_s^0 - \tau_s. \quad (27)$$

We have to chop off the tile τ_s to make the statement true. Also, f_s appears in Item 2 of Calculation 8 whereas f_s^{-1} appears in Item 2 of Calculation 6. Item 3 is a slightly different statement, but the new statement works the same way in the proof of Lemma 5.11.

Lemma 5.13 (Calculation 8) *Let $s \in [3/4, 1)$. Then*

1. τ_s is a tile of Δ_s , having period 2.
2. $f_s(p) = p + \delta_s$ for all $p \in (Z_s^0)^*$.
3. $f_s(X_s - Z_s - W_s) \subset Z_s^*$.

5.5 Proof of Lemma 5.2

Let T be the map from Equation 26.

Lemma 5.14 *Let $s \in (3/4, 1)$ be any point. Then there is some positive k such that $T^k(s) \in (1/2, 3/4)$.*

Proof: Same proof as Lemma 5.7. ♠

The rest of the proof of Lemma 5.2 is like what we did for Lemma 5.1, but there are some small differences. First of all, this time we know that τ_s is a tile of Z_s , so all the nontrivial orbits intersect Z_s .

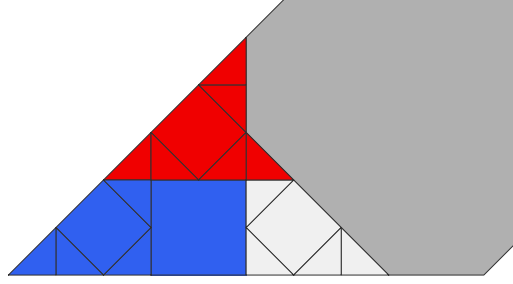


Figure 5.5: Half of W_s for $s = 4/5$.

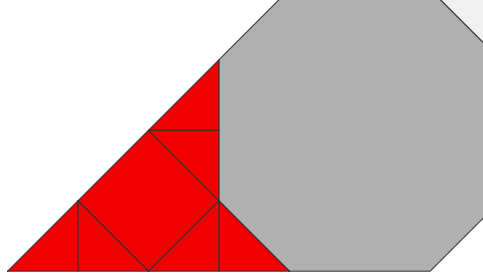


Figure 5.6: $\Delta_u \cap X_u^0$ for $u = 2/3$.

When $s \in [3/4, 5/6)$ and $u \in [1/2, 3/4)$ the tile τ_u does not exist. Figures 5.5 and 5.6 show the example of $s = 4/5$ and $u = 2/3$. However, we define

$$Z_s^* = (Z_s^0)^* \cup \iota((Z_s^0)^*) = Z_s - \tau_s - \iota(\tau_s). \quad (28)$$

and we use the pair (Z_s^*, Z_u) in place of the pair (Z_s, Z_u^*) . Making these changes, Lemmas 5.9, 5.10, and 5.11 go through without a problem.

6 Properties of the Tiling

6.1 The Rational Case

Even though we mainly care about the irrational case of Theorem 1.4, we find it convenient to prove the analogous result for the rational case. When $s = 1/2n$ we define

$$\phi_s(x, y) = \left(\frac{x}{2n}, \frac{y}{2n} \right). \quad (29)$$

This is a new definition, because the Main Theorem does not apply for $s = 1/2n$. When $s = 0$, we slightly abuse notation and define O_s to be (simultaneously) each of the 4 isosceles triangles having vertices $(0, 0)$ and $(\pm 1, \pm 1)$.

Lemma 6.1 *When $s \in (0, 1)$ is rational, a polygon arises in Δ_s if and only if it is translation equivalent to $T_n(O_{s_n})$ for some n .*

Proof: Our proof goes by induction on the value of n such that $T^n(s) = 0$.

Consider the base case. This corresponds to $s = 1/2n$, $n = 1, 2, 3, \dots$. For $s = 1/2$, we check that Δ_s consists of $O_{1/2}$ and each of the 4 triangles O_0 scaled down by a factor of 2. When $a = 1/2n$, we apply the Insertion Lemma and verify that the 4 triangles in $\Delta_{1/2n}$ have sizes consistent with the statement that they are translates of $T_0(O_0)$.

The general case follows from induction. Let $s = s_0$. By the Main Theorem, a tile appears in Δ_{s_0} if and only if it is either $O_{s_0} = T_0(O_{s_0})$ or if it is translation equivalent to a tile of the form

$$\phi_{s_0}(\sigma),$$

where σ is a tile of Δ_{s_1} . By induction, σ is translation equivalent to the tile

$$\phi_{s_1} \circ \dots \circ \phi_k(O_k),$$

for some k . Hence, τ is translation equivalent to the tile

$$\phi_{s_0} \circ \dots \circ \phi_k(O_k).$$

Conversely, all such tiles appear in Δ_{s_0} , by the same induction argument. ♠

6.2 The Irrational Case

Now we prove Theorem 1.4.

Let s be some irrational parameter. First of all, the argument in Lemma 6.1 applies *verbatim* to show that the a translate of the tile

$$T_k(O_u), \quad u = R^k(s)$$

does indeed appear in Δ_s . The argument is simply induction on k , combined with the Main Theorem.

We need to prove the converse, showing that these are the only tiles that appear in Δ_s when s is irrational. Let $\{{}_n s\}$ be a sequence of rationals converging to s .

P be a tile of Δ_s . By Lemma 3.5, we can find a tile ${}_n P$ of $\Delta_{{}_n s}$ such that ${}_n P \rightarrow P$ as $n \rightarrow \infty$. By Lemma 6.1, there is an integer k_n such that ${}_n P$ is translation equivalent to some tile of the form

$${}_n T_{k_n}(O_{u_n}), \quad u_n = R^{k_n}({}_n s).$$

Here ${}_n T_{0,n} T_{1,n} T_{2,n} \dots$ are the maps which arise in Lemma 6.1 relative to the parameter ${}_n s$.

Now, the scale factor of ${}_n T_k$ tends to 0 with k , and ${}_n P$ has uniformly large diameter. Therefore, the integer k_n is uniformly bounded from above. So, passing to a subsequence, we can assume that ${}_n k$ is independent of n . That is, P_n is a translation of

$${}_n T_k(O_{u_n}), \quad u_n = R^k({}_n s). \tag{30}$$

But

- ${}_n T_k \rightarrow T_k$,
- $u_n \rightarrow u = R^k(s)$,
- $O_{u_n} \rightarrow O_u$.

Hence P is a translate of $T_k(O_u)$.

The rest of this chapter is devoted to proving Theorem 1.1.

6.3 Existence of Square Tiles

Here we prove Statement 1 of Theorem 1.1. We will suppose that $s \neq \sqrt{2}/2$ and show that Δ_s has a square tile. We will first suppose that s is irrational.

Lemma 6.2 *Suppose that s and $t = R(s)$ lie in $(0, 1)$. If Δ_t has a non-central square tile, then so does Δ_s .*

Proof: By the Main Theorem, Δ_s has a similar copy of every non-central tile of Δ_t , and these similar copies are themselves non-central. ♠

Lemma 6.3 *Suppose that s is irrational. If $R^n(s) < 1/2$ for some even n , then Δ_s has a square tile.*

Proof: We choose n to be as small as possible. If $n = 0$ then $s < 1/2$ and the central tile of Δ_s is square. Suppose $n \geq 2$. Let $t = R^{n-2}(s)$ and $u = R^{n-1}(s)$ and $v = R^n(s)$. We know that $v < 1/2$. If $u > 1/2$ then $t < 1/2$, contradicting the minimality of n . So, $u < 1/2$. But then we apply the Main Theorem to the pair $(u, R(u))$ and conclude that some non-central tile of Δ_u is a square. Now we apply Lemma 6.2 repeatedly to conclude that Δ_s has a non-central square tile. ♠

Lemma 6.4 *Suppose that s is irrational. If $R^n(s) < 1/4$ for some odd n , then Δ_s has a square tile.*

Proof: If $n = 0$ then Δ_s has a central square tile. So, assume that $n > 0$. Let $t = R^{n-1}(s)$ and $u = R^n(s)$. Since $u < 1/4$, the tiling Δ_u has at least 3 central tiles, one of which is contained in the set $Y_t \subset \Delta_u$. But then $Z_t \subset \Delta_t$ contains a non-central square tile. Repeated applications of Lemma 6.2 finish the proof. ♠

Lemma 6.5 *Suppose that s is irrational and Δ_s has no square tiles. Then $s = \sqrt{2}/2$.*

Proof: We know that $R^n(s) > 1/2$ for every even n and $R^n(s) \in (1/4, 1/2)$ for every odd n . If $R^n(s) \in (1/3, 1/2)$ for some odd n , then $R^{n+1}(s) < 1/2$, because R maps $(1/3, 1/2)$ onto $(0, 1/2)$. Hence $R^n(s) \in (1/4, 1/3)$ for all odd n .

For $x \in (1/4, 1/3)$ we have the formula

$$R(x) = \frac{1}{2x} - 1 \quad (31)$$

Hence, if $x > 1/2$ and $R(x) \in (1/4, 1/3)$ we have

$$R^2(x) = \frac{1-2x}{-2+x} = Mx, \quad M = \begin{bmatrix} -\sqrt{2} & 1/\sqrt{2} \\ \sqrt{2} & -\sqrt{2} \end{bmatrix}. \quad (32)$$

Here M acts as a linear fractional transformation. Iterating, we have

$$R^{2n}(s) = M^n(s). \quad (33)$$

The map M , acting as a linear fractional transformation, fixes $\pm\sqrt{2}/2$ and is expanding in a neighborhood of $\sqrt{2}/2$. We conclude that there is some n such that $M^n(s) < 0$ unless $s = \sqrt{2}/2$. Since we never have $N^n(s) < 0$ we must have $s = \sqrt{2}/2$. ♠

Lemma 6.6 *If s is rational, the Δ_s has a square tile.*

Proof: The proof is the same as in the irrational case, except we have to worry about what happens if $R^n(s) \in \{1/4, 1/3, 1/2\}$ for some odd n . If $R^n(s) = 1/4$ for some odd n , then the same argument as in Lemma 6.4 applies. The point is that $\Delta_{1/4}$ still has 3 central square tiles.

If $R^n(s) = 1/2$ for some odd n , then $R^{n-1}(s) < 1/2$. But then the argument in Lemma 6.5 applies to the even iterate $R^{n-1}(s)$.

If $R^n(s) = 1/3$ for some odd n , then $R^{n+1}(s) = 1/2$. But then the argument in Lemma 6.5 applies to the even iterate $R^{n+1}(s)$. because $\Delta_{1/2}$ still has a central square tile. ♠

Putting together the last several lemmas, we finish the proof that Δ_s has a square tile as long as $s \neq \sqrt{2}/2$.

6.4 The Case of Squares

Here we prove Statement 2 of Theorem 1.1. We compare the map R with the *Gauss map*

$$\gamma(s) = 1/s - \text{floor}(1/s) \quad (34)$$

Lemma 6.7 *Let $s = [0, a_1, a_2, a_3, \dots]$ be the continued fraction expansion of s . Suppose that a_1 is even. Then $s, R(s) < 1/2$ and $R^2(s) = \gamma^2(s)$.*

Proof: Let $x = 1/s$. We write

$$x = a_1 + \frac{1}{a_2 + 1/y}.$$

The continued fraction expansion of $1/y$ is $[0, a_3, a_4, \dots]$. Hence $1/y = \gamma^2(s)$. Note, in particular, that $1/y < 1$. We need to show that $R^2(s) = 1/y$.

Since $a_1 > 1$, we have $s < 1/2$. Hence

$$R(s) = 1/(2s) - \text{floor}(1/(2s)) = x/2 - \text{floor}(x/2).$$

We have

$$x/2 = (a_1/2) + \frac{1}{2a_2 + 2/y}. \quad (35)$$

Hence

$$R(s) = \frac{1}{2a_2 + 2/y} < 1/2.$$

Since $R(s) < 1/2$ we have

$$R^2(s) = (a_2 + 1/y) - \text{floor}(a_2 + 1/y) = 1/y,$$

as desired. ♠

Let $[a_0, a_1, a_2, a_3, \dots]$ be the continued fraction expansion for s . We call s *oddly even* if s is irrational and a_k is even for all odd k . When $s \in (0, 1)$ we have $a_0 = 0$.

Lemma 6.8 *Let $s \in (0, 1)$ be irrational. Then s is oddly even if and only if $R^k(s) \in (0, 1/2)$ for all k .*

Proof: Suppose that s is oddly even. By the previous result, s and $R(s)$ lie in $(0, 1/2)$ and $R^2(s)$ is again oddly even. Hence $R^2(s)$ and $R^3(s)$ lie in $(0, 1/2)$ and $R^4(s)$ is oddly even. And so on.

Conversely, suppose that s is not oddly even. Applying Lemma 6.7 finitely many times if necessary, we reduce to the case where the first term in the continued fraction expansion of s is odd. If $s > 1/2$ we are done. Otherwise, s lies in one of the intervals $(1/3, 1/2)$, $(1/5, 1/4)$, $(1/7, 1/6)$, ..., and R maps each of these intervals onto $(1/2, 1)$. So $R(s) > 1/2$ in this case. Hence, if $R^k(s) \in (0, 1/2)$ for all k , then s is oddly even. ♠

Lemma 6.8 combines with Theorem 1.4 to prove Statement 2 of Theorem 1.1 in case $s \in (0, 1)$. But the case $s > 1$ now follows from the Inversion Lemma and from the fact that the map $x \rightarrow 1/(2x)$ preserves the set of oddly even numbers.

6.5 The Density of Shapes

Now we prove Statement 3 of Theorem 1.1. This result follows immediate from Theorem 1.4 and from the following lemma.

Lemma 6.9 *For almost all $s \in (0, 1)$, the orbit $\{R^n(s)\}$ is dense in $(0, 1)$.*

We will prove Lemma 6.9 through a series of smaller lemmas. We start with a classic result. See [BKS] for instance.

Lemma 6.10 *Almost every orbit of the Gauss map is dense in $(0, 1)$.*

This result has a well known geometric consequence. Let Σ_0 denote the trice-punctured sphere. Let $T_1(\Sigma)$ denote the unit tangent bundle of Σ . A geodesic in Σ_0 has a natural *lift* to the unit tangent bundle: One just keeps track of the points on the geodesic as well as their unit tangent vectors. We say that a geodesic on Σ_0 *emanates* from a cusp of Σ if one end of the geodesic is asymptotic with a cusp. The lift of such a geodesic to \mathbf{H}^2 has one endpoint on a parabolic fixed point of the surface fundamental group. There is a natural measure on the set of cusps emanating from one of the cusps of Σ_0 .

Corollary 6.11 *Almost every geodesic ray emanating from a cusp of Σ_0 lifts to a dense subset of $T_1(\Sigma_0)$.*

Proof: Let α be a geodesic emanating from a cusp of Σ_0 . By symmetry, it suffices to consider the case when some lift $\tilde{\alpha}$ of α is the vertical geodesic connecting ∞ to some $r \in (0, 1)$. The position of any given segment of $\tilde{\alpha}$ is determined, to arbitrary precision, by finite portions of the orbit of r under the Gauss map. If α is chosen so that this orbit is dense, then we can approximate any finite geodesic segment on Σ_0 , up to an arbitrarily small error, using a portion of α . ♠

Now let Σ be a finite normal covering surface of Σ_0 . That is, $\Sigma_0 = \Sigma/G$, where G is some finite group acting on Σ . There is again a natural measure on the set of geodesics emanating from a cusp of Σ .

Corollary 6.12 *Almost every geodesic ray emanating from the cusp of Σ lifts to a dense subset of $T_1(\Sigma)$.*

Proof: Let α be a geodesic emanating from our cusp of Σ . Let $\bar{\alpha}$ be the projection of α to Σ_0 . Almost every choice of α leads to $\bar{\alpha}$ having a dense lift in $T_1(\Sigma_0)$. But then the G -orbit of the lift of α is dense in $T_1(\Sigma)$. Let C be the closure of the lift of α in $T_1(\Sigma)$. We know that $G(C) = T_1(\Sigma)$. At the same time, we know that $\bar{\alpha}$ approximates, with arbitrary precision, any closed loop in Σ_0 . From this we see that in fact C is G -invariant. Hence $C = T_1(\Sigma)$, as desired. ♠

Let T be the $(2, 4, \infty)$ hyperbolic triangle generating our group Γ . One of the edges of T is contained in the geodesic circle C fixed pointwise by the map $z \rightarrow 1/(2\bar{z})$. We color C red. We color the other two edges blue. We then lift this coloring to the universal covering \mathbf{H}^2 . This gives us a pattern of geodesics that is invariant under the $(2, 4, \infty)$ triangle group. Among other colored geodesics in \mathbf{H}^2 , we have the red circle, and the blue lines connecting ∞ to half-integers.

Lemma 6.13 *Almost every geodesic emanating from the cusp of the $(2, 4, \infty)$ triangle has a billiard trajectory which hits the red edge in a dense set of points.*

Proof: We think of T as the $(2, 4, \infty)$ orbifold. There is a surface Σ (a 4-times punctured sphere) which covers T in the sense of orbifolds, and which also covers Σ_0 , the thrice punctured sphere. Say that a geodesic on Σ is good

if it emanates from a cusp of Σ and lifts to a dense set in $T_1(\Sigma)$. Almost every geodesic on T , emanating from the cusp of T , has a preimage which is a good geodesic. Hence, almost every geodesic emanating from the cusp of T has dense image in the unit tangent bundle of T . But such a geodesic would intersect each edge of T in a dense set of points. ♠

To prove that $\{R^n(s)\}$ is dense for almost every choice of $s \in (0, 1)$, it suffices to prove that $\{R^n(s)\}$ is dense for almost every choice of $s \in (0, 1/2)$. It is also useful to first consider the alternate map $R_1 : (0, 1/2) \rightarrow (0, 1/2)$, defined as follows:

- $R_1(s) = R(s)$ if $R(s) < 1/2$.
- $R_1(s) = 1 - R(s)$ if $R(s) > 1/2$.

One can describe R_1 like this. Starting with s_0 , we first reflect in the red circle C to produce the point s_1 . There is some nearest vertical blue line which separates s_1 from 0. We reflect in this blue line to produce s_2 . We now repeat these reflections in blue lines until we arrive at a point in $(0, 1/2)$, and this point is $R_1(s)$.

Each $s \in (0, 1/2)$ corresponds to a geodesic g_s of T , which emanates from the cusp. The recipe is that the lift of g_s to \mathbf{H}^2 is the geodesic connecting s to ∞ . From the description of R_1 above, we see that we can recover the action of R_1 by looking at the billiard path of g_s . The orbit $\{R^1(s)\}$ is dense provided that g_s intersects the red edge in a dense set. By Lemma 6.13, this happens for almost all $s \in (0, 1/2)$.

Knowing that $\{R_1^n(s)\}$ is dense is not quite the same as knowing the $\{R^n(s)\}$ is dense. However, there is a decomposition of the red edge of T into intervals $I_1, J_2, I_3, J_4, \dots$ such that an intersection point of g_s with I_j corresponds to a value s_k where $R_1(s_k) = R(s_k)$ and an intersection point of g_s with J_j corresponds to a value of s_k where $R_1(s_k) = 1 - R(s_k)$. In terms of billiards, the I intervals are such that g_s hits an even number of blue edges after hitting some I -interval.

The upshot of this interval decomposition is that, since g_s intersects both the I -intervals and the J -intervals densely, the orbit $\{R^n(s)\}$ is also dense.

7 Covering Results

7.1 An Area Estimate

Recall that X_s^0 is the portion of X_s to the left of the central tiles. Define

$$\lambda(s) = \frac{\text{Area}(\Delta_s \cap X_s^0)}{\text{Area}(X_s^0)}. \quad (36)$$

Lemma 7.1 (Area) *The function $\lambda(s)$ is uniformly bounded away from 0, for all $s \in (0, 1)$.*

Proof: By the Insertion Lemma, it suffices to take $s \in [1/4, 1)$. The case $s = 1/4$ is trivial, so we consider $s \in (1/4, 1)$. When s is bounded away from $1/2$ and 1 , the size of the largest square in X_s^0 is bounded away from 0 . (Figure 7.1 below shows a picture of the case when s is very near $1/4$, the other potential place to worry about.)

As $s \rightarrow 1$, the size of τ_s tends to 0 . However, the inductive argument given to prove Lemma 5.1 shows that the union of squares isometric to τ forms the following pattern. There is a bottom row of $2k + 1$ squares, then a row of $2k - 1$ squares, then a row of $2k - 3$ squares, and so on, all the way down to a single top square. When $s > 1$, the number k is such that $T^k(s) \in (5/4, 3/2)$. When $s < 1$, the number k is such that $T^k(s) \in (3/4, 5/6)$.

Technically, the argument we gave above establishes the existence of the left half of the picture (and the central column.) Combining the Inversion Lemma and the Bilateral Lemma, we see that the reflection ρ in the vertical line through the top vertex of X_s^0 maps the right half of $\Delta_s \cap X_s^0$ into the left half. This lets us deduce that the right half of X_s^0 has the same pattern of squares as the left half.

As $s \rightarrow 1$, the bottom row is more and more nearly filled up with squares isometric to τ . Hence, the “triangular pile” of squares fills more and more of X_s^0 as $s \rightarrow 1$. Indeed, $\lambda(s) \rightarrow 1$ as $s \rightarrow 1$.

When $s \rightarrow 1/2$, we can again apply the Inversion Lemma to instead consider the case $s \rightarrow 1$, which we have already treated. ♠

Remark: The Area Lemma is really what is responsible for our result that $\widehat{\Lambda}_s$ always has measure 0 .

7.2 A Length Estimate

Say that a *special edge* is an edge of X_s^0 which is contained either in the bottom edge or the left edge of X_s . Let b_s and ℓ_s be the bottom and left edges of X_s^0 respectively. We will first focus on ℓ_s . When the dependence on the parameter is clear, we will set $\ell = \ell_s$ and $b = b_s$. Given a special edge E of X_s^0 , define

$$\lambda(E, s) = \frac{\text{length}(E \cap \Delta_s)}{\text{length}(E)} \quad (37)$$

This equation needs some interpretation because Δ_s , being the union of open tiles, is technically disjoint from E . What we are talking about here is the portion of E contained in edges of tiles of Δ_s .

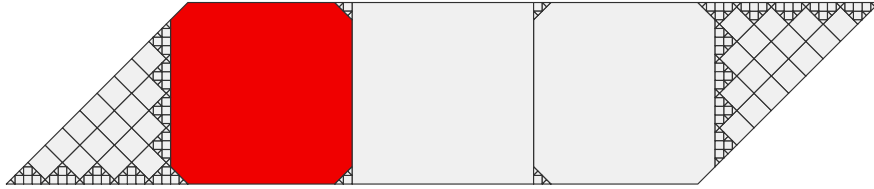


Figure 7.1 Δ_s for $s = 21/80$.

The area estimate given above has an analogue for lengths, but the result is more subtle. Figure 6.1 indicates some of the subtlety. Figure 7.1 shows the tiling for a parameter very near $1/4$. The edge ℓ is very nearly covered by the edges of square tiles, whereas the right half of b is nearly covered by the edge of a single tile and the left half meets the tiles in a jagged¹ kind of way. This “jagged edge” phenomenon is what makes our length estimate more subtle than the area estimate.

Lemma 7.2 (Length) *Let $s \in (0, 1)$. Then $\lambda(\ell, s)$ and $\lambda(b, s)$ are uniformly bounded away from 0 as long as $1/(2s) \bmod 1$ lies in a compact subset of $(0, 1)$.*

We will prove the Length Lemma through a series of smaller lemmas.

Lemma 7.3 *There is a uniform lower bound on $\lambda(\ell, s)$ for $s \in [1/4, 2/3]$.*

¹Technically, in the rational case, the special edges are completely covered by tile edges, but Figure 7.1 is supposed to suggest the kind of complicated phenomena which can arise in the irrational case.

Proof: Our analysis for the case of area gives us a uniform lower bound for (b_s, s) when $s \in [3/4, 3/2]$. By the Inversion Lemma, we get the same result for (ℓ_s, s) when $s \in [1/3, 2/3]$. So, we just have to worry about $s \in [1/4, 1/3]$.

When $s \in [1/4, 1/3]$ we have $t = R(s) > 1/2$. Let O_t be the trivial octagonal tile of Δ_t . By Statement 3 of the Main Theorem, ϕ_s extends to O_t and $\phi_s(O_t)$ has an edge in ℓ_s . As long as t is bounded away from 1, which corresponds to s being bounded away from $1/4$, there is a lower bound to the length of $\phi_s(O_t) \cap \lambda_s$. Again, we interpret O_t as a closed tile for this statement.

Consider what happens when $s \rightarrow 1/4$ from above. In this case $t \rightarrow 1$ from below. We check that Z_s nearly covers all of ℓ_s . All that is missing is a small portion of the very top of ℓ_s , coming from $\phi_s(O_t)$. See Figure 7.1. So, by the Main Theorem, and our analysis in the Area Lemma, $\lambda(\ell_s, s) \rightarrow 1$ as $s \rightarrow 1/4$ from above. ♠

Lemma 7.4 *$\lambda(\ell, s)$ is uniformly bounded away from 0 on any compact subset of $[2/3, 1)$.*

Proof: When $s = 2/3$, there is a large square diamond whose edge lies in ℓ_s . This tile is stable, as one can see from the arithmetic graph, so $\lambda(\ell, s)$ uniformly bounded away from 0 in a neighborhood of $2/3$. As long as t is bounded away from 0, the tile τ_t of Δ_t sharing a vertical edge with the trivial tile has an edge in β_s whose length is bounded away from 0. So, by the Main Theorem, we get a uniform lower bound on $\lambda(\ell_s, s)$ for $s \in (2/3, 1)$ as long as s stays away from 1. ♠

Combining the the results above, we see that $\lambda(\ell, s)$ is uniformly bounded away from 0 when $s \in (0, 1)$ is uniformly bounded away from 1. This result certainly implies the result for ℓ_s claimed in the Length Lemma. Now we turn our attention to the edge b_s .

Lemma 7.5 *There is a uniform lower bound on $\lambda(b, s)$ when s lies in a compact subset of $(1/2, 1)$.*

Proof: We have a uniform lower bound on $\lambda(\ell, s)$ for s in a compact subset of $(1/2, 1)$. Now we apply the Inversion Lemma, which maps s to $1/2s$ and switches the roles of ℓ and b . ♠

Lemma 7.6 *There is a uniform lower bound on $\lambda(b, s)$ when s lies in a compact subset of $(1/4, 1/2)$.*

Proof: Let $t = R(s) < 1$. The left edge of Y_t is all of ℓ_t . When $s \in (1/4, 1/2)$, the scale factor of ϕ_s , from the Main Theorem, is bounded uniformly away from 0. Hence, the bottom edge of Z_s is uniformly large. As long as t is bounded away from 1, the trivial tile in Δ_t has edges which take up a uniformly large fraction of the top and bottom edges of X_t . By the Main Theorem, the corresponding tile in Δ_s has a uniformly large edge in b_s . ♠

The Length Lemma for b_s now follows from the Insertion Lemma and the preceding two results.

7.3 The Covering Lemma

Let s be some parameter, and let t be some other parameter. We say that a *similar copy* of X_t^0 is a set of the form $T(X_t^0)$ where T is a similarity. We say that $A = T(X_t^0)$ *fits nicely* over X_s if

$$T^{-1}(\widehat{\Lambda}_s \cap A) \subset \widehat{\Lambda}_t. \quad (38)$$

We don't require that A is actually a subset of X_s^0 .

Say that a *nice covering* of X_s^0 is a covering of the form

$$X_s^0 \subset A_1 \cup \dots \cup A_m \cup B_1 \cup \dots \cup B_n, \quad (39)$$

where each A_i is a similar copy of X_t^0 which fits nicely over X_s^0 and each B_j is a periodic tile of Δ_s .

Lemma 7.7 (Covering) *Let $t = R(s)$. The set X_s^0 has a nice covering by similar copies of X_t^0 . All the similarities associated to the pieces in the cover have the form $I \circ \phi_s$, where I is an isometry and ϕ_s is as in the Main Theorem.*

We will prove this result through a series of smaller lemmas.

Lemma 7.8 *The Covering Lemma holds for $s \in (1/4, 1/3)$.*

Proof: Let A_s and B_s be the hexagon and triangle from the Bilateral Lemma. For $s \in (1/4, 1/3)$ we have $R(s) \in (1/2, 1)$. For these values, a calculation shows that $B_s \subset Z_s$. The largest tile in Z_s is an octagon, τ , the image of the central tile in Δ_t under ϕ_s . Figure 7.4 below shows the typical example of $s = 3/10$.

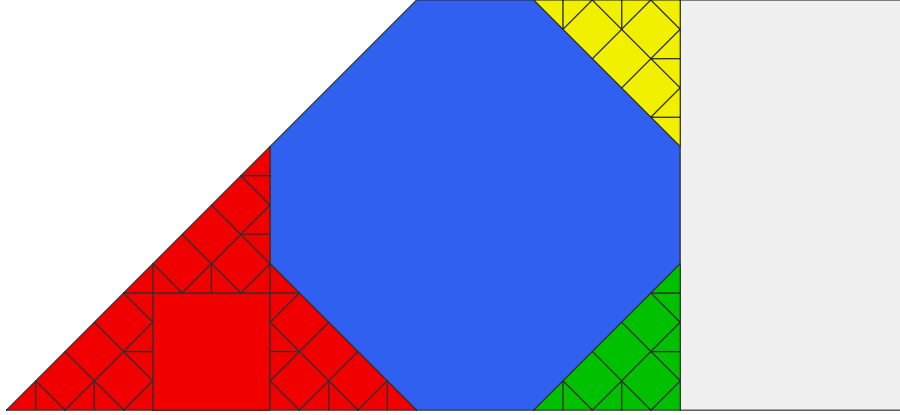


Figure 7.2 X_s (red) and τ (blue) and $X_s^0 - Z_s - \tau$ (yellow, green)

Let ρ_1 be the reflection in the line D_s from the Bilateral Lemma. The tiles in the collection $\rho_1(\Delta_s \cap Z_s) \cap X_s$ are again tiles of Δ_s by the Bilateral Lemma, and $\rho_1(Z_s) \cap X_s$ is precisely the region of X_s^0 lying above τ . This is the yellow region in Figure 7.2. Hence $\rho_2(Z_s)$ fits nicely over Δ_s .

Let ρ_2 be reflection in the line H_s from the Bilateral Lemma. By the Bilateral Lemma, $\rho_2 \circ \rho_1(Z_s)$ fits nicely over Δ_s . The intersection $\rho_2 \circ \rho_1(Z_s) \cap X_s$ is precisely the region of X_s^0 lying below and to the right of τ . This is the green region in Figure 7.2.

To finish the proof, we note that $Z_s = \phi_s(X_t^0)$. The point is that there is just one central tile in Δ_t . So, all the sets we are using have the form $I \circ \rho_s(X_t^0)$, where I is an isometry. ♠

Corollary 7.9 *The Covering Lemma holds for $s \in (3/2, 2)$.*

Proof: For s in this range, we have $R(s) = s - 1$. The result now follows from the Inversion Lemma. ♠

Lemma 7.10 *The Covering Lemma holds for $s \in (1/3, 2/5)$.*

Proof: Figure 7.5 shows a typical case, for the parameter $s = 19/50$.

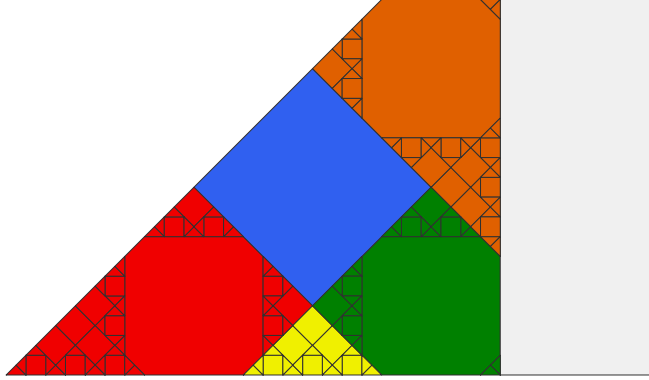


Figure 7.3 Z_s (red) and A_s (green, blue, orange) and B_s (red, yellow)

For $s \in (1/3, 2/5)$, the set Z_s covers the left half of the triangle B_s from the Bilateral Lemma, and also $Z_s \subset B_s$. Let ρ_1 be reflection in the vertical line of symmetry of B_s . By the Bilateral Lemma, the set $\rho_1(Z_s)$ fits nicely over Δ_s . The two pieces Z_s and $\rho_1(Z_s)$ cover B_s .

Let ρ_2 be reflection in the line D_s from the Bilateral Lemma. The pieces $\rho_2(Z_s)$ and $\rho_2 \circ \rho_1(Z_s)$ fit nicely over Δ_s . This is the orange region in Figure 7.3.

Aside from the blue tile τ , the only region not yet covered is the green region, and this is covered by $\rho_3 \circ \rho_2(Z_s)$, where ρ_2 is reflection in the x -axis, H . This last-mentioned piece also fits nicely over Δ_s .

To finish the proof, we note again that $Z_s = \phi_s(X_t^0)$. The point, again, is that there is just one central tile in Δ_t . So, all the sets we are using have the form $I \circ \rho_s(X_t^0)$, where I is an isometry. ♠

Corollary 7.11 *The Covering Lemma holds for $s \in (5/4, 3/2)$. Moreover, none of the similar copies of X_t^0 crosses the bottom edge of X_s^0 .*

Proof: This follows from the Inversion Lemma, and from the fact that the covering we constructed in Lemma 7.10 is such that no similar copy crosses the left edge of X_s^0 . ♠

Lemma 7.12 *The Covering Lemma holds for $s \in (1, 3/2)$.*

Proof: We give the same kind of inductive proof we used in the proof of Lemma 5.1. We already know the result holds for $s \in (5/4, 3/2)$. Given $s \in (1, 5/4)$ we let $u = T(s)$, where T is the map in Equation 20. We will show that the truth of the lemma for u implies the truth of the lemma for s . In all cases, we will use the fact that no tile in the covering crosses the bottom edge of the relevant region.

Let $t = R(s)$ and $v = R(u)$. Suppose that X_u^0 has a nice covering by similar copies of X_v^0 , with the additional property that no piece crosses the bottom edge of X_u^0 . Using the map $\omega_s : Y_u \rightarrow W_s$ from the proof of Lemma 5.1, we get a nice covering of W_s by finitely many tiles of Δ_s and finitely many similar copies of X_t^0 . We also have the piece Z_s .

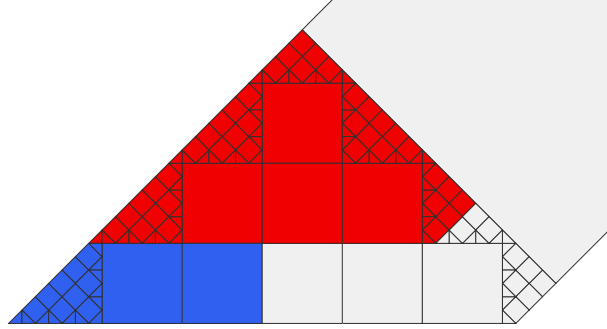


Figure 7.4: Half of W_s for $s = 22/19$.

For convenience, we repeat Figure 5.1 here. The union $Z_s \cup W_s$ covers the entire left half of X_s^0 , namely the half which lies to the left of the vertical line through the top vertex of X_s^0 . Moreover, as in the proof of Lemma 5.1, we note that reflection in this vertical line maps the left right half of the tiling into the left half. Thus, we can extend our covering to all of X_s^0 using this reflection. Some of the pieces slop over into the central tile of Δ_s , but this does not bother us.

As in the proof of Lemma 5.1, this lemma now follows from induction on the number k needed so that $T^k(s) \in (5/4, 3/2)$. ♠

Corollary 7.13 *The Covering Lemma holds for $s \in (0, 1/2)$.*

Proof: Combining the previous results, we see that the Covering Lemma holds for all $s \in (1, 2)$. By the Inversion Lemma, the Covering Lemma holds for all $s \in (1/4, 1/2)$. But then, by repeated applications of the Insertion Lemma, the Covering Lemma holds for all $s \in (0, 1/2)$. ♠

Remark: We have ignored the parameter $1/4$. The Covering Lemma is vacuous here, because $R(1/4) = 0$.

Lemma 7.14 *The Covering Lemma Holds for $s \in (1/2, 3/4)$.*

Proof: This case is similar to the case treated in Lemmas 7.8. Figure 7.5 shows the rather typical case of $s = 7/10$.

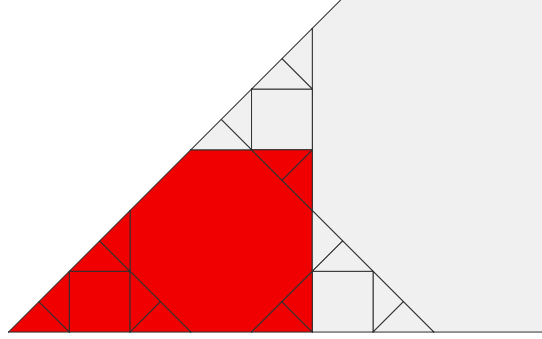


Figure 7.5: Δ_s (white, red) and Z_s (red) for $s = 7/10$.

Using reflections in the lines V_s and D_s from the Bilateral Lemma, we produce two isometric copies of Z_s which nicely fit over Δ_s . ♠

Lemma 7.15 *The Covering Lemma Holds for $s \in (3/4, 5/6)$.*

Proof: The proof is similar to the case for $s \in (1/2, 3/4)$. Figure 7.6 shows a typical example. ♠

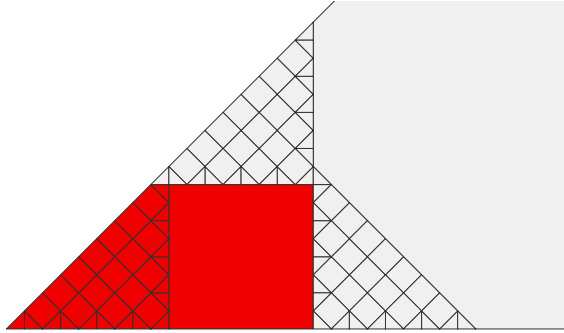


Figure 7.6: $\Delta)s$ (white, red) and Z_s (red) for $s = 13/17$.

Lemma 7.16 *The Covering Lemma Holds for $s \in (5/6, 1)$.*

Proof: The proof here relates to the proof of Lemma 5.2 in the same way that the proof of Lemma 7.12 relates to the proof of Lemma 5.1. We omit the details. ♠

8 Properties of the Limit Set

8.1 Area Zero

Here we show that $\widehat{\Lambda}_s$ has zero area. It suffices to prove this for the left half of $\widehat{\Lambda}_s$, which we denote by S_s .

Lemma 8.1 *Let s be irrational. For any $\epsilon > 0$, the set X_s^0 has a nice covering by similar copies of X_t^0 , all having diameter at most ϵ .*

Proof: The nice fitting property is hereditary. If a similar copy $T_u(X_u^0)$ fits nicely over X_t^0 and a similar copy $T_t(X_t^0)$ fits nicely over X_s^0 , then the similar copy $T_t \circ T_u(X_u)$ fits nicely over X_s^0 . The boundary-adapted property is also hereditary. We let $s_n = R^n(s)$ and note that, by induction, X_s^0 has a nice and boundary adapted covering by similar copies of X_t^0 where $t = s_n$. The scale factor of the similarities involved is the product of the scales factors of ϕ_{s_i} , taken over $i = 0, \dots, (n-1)$. At least every other time, $s_i < 1/2$ and the corresponding scale factor is less than $\sqrt{2}/2$, so the total scale factor is less than $2^{-n/4}$. We can make this less than ϵ/D by taking n large enough. Here $D < 2$ is the maximum diameter of any set X_u^0 , taken over all $u \in (0, 1)$. ♠

Say that a *near disk* is a compact set D which is contained in a disk of radius $10r$ and contains a disk of radius r . For every s , the set X_s^0 is a near disk. Let μ denote the 2-dimensional Lebesgue measure. The following is an immediate consequence of the Lebesgue Density Theorem.

Lemma 8.2 *Suppose that $S \subset \mathbf{R}^2$ is a bounded measurable set of positive Lebesgue measure. Then almost every point $p \in S$ has the following property. If $\{D_n\}$ is a sequence of near disks containing p , having diameter shrinking to 0, then $\mu(D_n \cap S)/\mu(S) \rightarrow 1$, as $n \rightarrow \infty$.*

Suppose now that S_s has positive measure. We can find a point $p \in S_s$ satisfying the conclusion of Lemma 8.2. By Corollary 8.1 we can find a sequence $\{D_n\}$ of near disks such that $p \in D_n$ for all n , and the diameter of D_n tends to 0, and D_n is a similar copy of X_u^0 for some $u = u_n$. The Area Lemma now tells us that $\mu(S_s \cap D_n) < \lambda(1 - \epsilon)(D_n)$ for some universal constant $\epsilon > 0$. This contradicts Lemma 8.2. Hence Λ_s has zero area.

8.2 Characterization of the Limit Set

Now that we know $\widehat{\Lambda}_s$ has area zero, we can give a nicer characterization of the limit set.

Lemma 8.3 *A point belongs to $\widehat{\Lambda}_s$ if and only if every open neighborhood of the point contains infinitely many periodic tiles of Δ_s .*

Proof: Certainly, $\widehat{\Lambda}_s$ contains all such points. For the converse, suppose that $p \in \widehat{\Lambda}_s$. There exists a sequence of points $q_n \rightarrow p$ with the following property $f^1(q_n), \dots, f^n(q_n)$ are all defined and distinct. Since $\widehat{\Lambda}_s$ has measure 0, and the set of points with undefined orbits has measure 0, the set of periodic points has full measure. So, we can take a new sequence $\{q'_n\}$ of periodic points converging to p , and we can make $|q_n - q'_n|$ as small as we like. Making these distances sufficiently small, we guarantee that q'_n has periodic at least n . But then every neighborhood of p intersects infinitely many periodic tiles.

♠

8.3 Projections of the Limit Set

Let $s \in (0, 1)$ be irrational and let π denote projection onto the x -axis. We will show that $\pi(\widehat{\Lambda}_s)$ contains a line segment. Following this, we will deal with projections onto lines parallel to the other 8th roots of unity. We suppress the parameter s . Since $\widehat{\Lambda}$ is a closed set, it suffices to prove that $\pi(\Lambda)$ contains a dense subset of a line segment.

There are countably many vertical lines which contain vertices of tiles in Δ . We ignore such lines. Let L be a vertical line which contains both a point on the bottom edge b of X and a point on the left edge ℓ of X . Assume that L does not contain a tile vertex. We will prove that L contains a point of $\widehat{\Lambda}$. From this it follows that $\pi(\ell) \subset \pi(\widehat{\Lambda})$, which proves what we want.

Suppose L does not intersect $\widehat{\Lambda}$. Then L only intersects finitely many tiles, τ_1, \dots, τ_n . We order these tiles according to when L enters them as we move upwards along L . Note that L must leave τ_i and enter τ_{i+1} at the same point. Otherwise, the segment of L lying between these two tiles would be the accumulation point of infinitely many tiles. For the same reason, the bottom edge of τ_1 must lie in b and the top edge of τ_n must lie in ℓ .

Since L leaves τ_i and enters τ_{i+1} at the same point, τ_i and τ_{i+1} must share an edge, and this shared edge contains a point of L . In particular, if L leaves τ_i through a horizontal edge, then L enters τ_{i+1} through a horizontal edge.

Since L is a vertical line, and the tiles of Δ are semi-regular octagons with sides parallel to the 8th roots of unity, we get the following result: L enters τ_i through a horizontal edge if and only if L leaves τ_i through a horizontal edge.

We know that L enters τ_1 through a horizontal edge. Using the properties above, we see that L leaves τ_n through a horizontal edge. But the top edge of τ_n , which is contained in ℓ , is not horizontal. This is a contradiction. Hence L does intersect $\widehat{\Lambda}$.

Remark: When s is rational, our argument breaks down because of the existence of triangular tiles.

Now we deal with projection into a line parallel to a different 8th root of unity. Let ω be an 8th root of unity. Unless $\omega = \pm i$, we can find lines perpendicular to ω which intersect both a horizontal and a diagonal edge of X . Once we have such lines, the argument we gave for $\omega = \pm 1$ works in this new context.

We just have to worry about the case $\omega = \pm i$. In this case, we observe that some edge of the trivial tile in Δ is vertical. Thus, there are horizontal lines connecting ℓ to this vertical edge. Now we run the same argument again, interchanging the roles played by the horizontal and vertical directions.

8.4 Finite Unions of Lines

Let s be irrational. Let S_s denote the left half of $\widehat{\Lambda}_s$. We will assume that there exists an irrational parameter s such that S_s is contained in a finite union of lines, and we will derive a contradiction.

Say that an *essential cover* of S_s is a finite union of lines which covers all but finitely many points of S_s . Let $c(s)$ denote the cardinality of an essential cover of S_s having the fewest number of lines. We call s a *minimal failure* if $c(s)$ achieves the minimum possible value of the function ² $c : (0, 1) \rightarrow \mathbf{N}$. We call a cover realizing $c(s)$ a *minimal essential cover*. For the rest of our proof we assume that s is a minimal failure.

²We define $c(t) = \infty$ if S_t has no essential cover.

Referring to the Main Theorem, we can pull back essential covers by ϕ_s . Suppose that L is a line intersecting Z_s^0 in a segment. Then we define $\phi_s^{-1}(L)$ to be the line extending the segment $\phi_s^{-1}(L \cap Z_s^0)$. If L does not intersect Z_s^0 in a line segment we define $\phi_s^{-1}(L)$ to be the empty set.

Let $t = R(s)$. By the Main Theorem,

$$\phi_s(S_t) \subset S_s \cap Z_s^0. \quad (40)$$

for this reason, t is also a minimal failure, and the pullback of a minimal essential cover of S_s is a minimal essential cover of S_t .

Lemma 8.4 *Every line of a minimal essential cover of S_s contains v_s , the bottom left vertex of X_s .*

Proof: Let $d(s, L)$ denote the distance from v_s to a line L of an essential minimal cover. Let $d(s)$ denote the maximum of $d(s, L)$, taken over all lines of L which appear in some essential minimal cover of S_s . Suppose that $d(s) > 0$. Since ϕ_s is a contraction, we have $d(s) < d(t)$. Also, setting $u = R(t)$, we have

$$d(s) < d(u)/\sqrt{2}. \quad (41)$$

This is true because at least one of the maps ϕ_s or ϕ_t contracts distances by at least a factor of $\sqrt{2}$.

Equation 41 is not possible for all choices of s . Note that X_s has diameter at most $1 + \sqrt{2}$. So, $d(s)$ is uniformly bounded. Hence, we can choose s so as to maximize $d(s)$, amongst all minimal counterexamples, up to a factor of (say) 9/10. But then $d(u)$ exceeds the maximum. This is a contradiction. The only way out is that $d(s) = 0$. ♠

Lemma 8.5 *Let A_s denote the hexagon from the Bilateral Lemma. Only finitely many points of S_s lie in the $A_s - \partial X_s$.*

Proof: Let S'_s denote the subset of S_s contained in the interior of A_s . Let U_s denote a minimal essential cover. Let ρ denote reflection in the x -axis, as in the Bilateral Lemma. $\rho(S'_s) = S'_s$. But then $S'_s \subset U_s \cap \rho(U_s)$. This is just a finite set of points, because all lines in U_s contain the vertex v_s and none of the lines in $\rho(U_s)$ contains v_s . Hence S'_s is a finite set.

Consider points of S_s lying on the edge of A_s that does not lie in ∂X_s . If this edge contained infinitely many points of S_s then U_s would have infinitely many lines. The point is that this edge of A_s does not contain the vertex v_s . ♠

Lemma 8.6 *Let B_s denote the triangle from the Bilateral Lemma. Only finitely many points of S_s lie in the $B_s - \partial X_s$.*

Proof: Same argument as above. ♠

Now we know that the interior of X_s contains only finitely many points of S_s .

Let ℓ_+ (respectively ℓ_-) denote the subset of the interior of ℓ lying above (respectively below) $(-1, 0)$, a common vertex of A_s and B_s . Let ρ be reflection in the x -axis. By the Bilateral Lemma,

$$\rho(S_s \cap \ell_+) \subset S_s \cap \text{interior}(X_s). \quad (42)$$

Hence $S_s \cap \ell_+$ is finite. A similar argument shows that $S_s \cap \ell_-$ is finite. Hence $S_s \cap \ell$ is finite.

But then S_s is contained in the top and bottom (horizontal) edges of X_s , except for finitely many points. But then the projection of S_s onto the y -axis does not contain a segment. This contradicts Statement 2 of Theorem 1.2. Hence a minimal failure cannot exist. This proves Statement 3 of Theorem 1.2.

8.5 Intersection with the Bad Set

Here we will show that $\widehat{\Lambda}_s - \Lambda_s$ has length 0 for almost every parameter s . What we will actually prove is that $\widehat{\Lambda}_s - \Lambda_s$ has length zero provided that the sequence

$$\left\{ \frac{1}{2R^n(s)} \mod 1 \right\}$$

has an accumulation point in $(0, 1)$. Almost every choice of s satisfies this criterion. Suppose now that $s \in (0, 1)$ is a parameter which satisfies the condition above.

Lemma 8.7 *Let s be irrational. For any $\epsilon > 0$, some open neighborhood of the special segments of X^0 has a nice covering by open subsets of similar copies of X_t^0 , all having diameter at most ϵ . Moreover, t can be chosen so that $1/(2t) \bmod 1$ is uniformly bounded away from 0 and 1.*

Proof: We simply restrict the covers produced in the Covering Lemma to neighborhoods of the special segments. This gives us everything in the lemma except the last statement. The last statement comes from the hypotheses on s . ♠

Lemma 8.8 $\widehat{\Lambda}_s \cap \partial X_s$ has length 0.

Proof: Referring to the Length Lemma from the previous chapter, it suffices to show that Λ_s intersects the special segments in sets of measure 0. The proof of this lemma is exactly like what we did for S_s , except that we use the Lebesgue Density Theorem for length instead of for area, and we use Lemma 8.7 in place of Corollary 8.1. ♠

Let $B_s \subset X_s$ denote the set of points where some iterate of f_s is undefined. Let B_s^+ (respectively B_s^-) denote the set of points where some positive (respectively negative) iterate of f is undefined. We will show that $\widehat{\Lambda} \cap B_s^+$ has length 0. The case of $\widehat{\Lambda}_s \cap B_s^-$ is quite similar.

Lemma 8.9 *Let $s > 1/2$. If $\widehat{\Lambda}_s \cap B_s^+$ has positive length, then $\Lambda_s \cap \partial X_s$ has positive length.*

Proof: We suppress the parameter s . Suppose that $\widehat{\Lambda} \cap B^+$ has positive length.

Recall that $X' = F_1 \cup F_2$ and $f' : X' \rightarrow X'$ is such that $f = (f')^2$. It is easier to work with f' because the discontinuity set is simpler. Let $S'_n \subset X'$ denote the set of points where one of the first n iterates of f' is not defined.

We have

$$B_+ \subset \bigcup_{n=1}^{\infty} S'_n \quad (43)$$

The set on the right is countable. So, if $\widehat{\Lambda} \cap B_+$ has positive length, there is some n such that $\widehat{\Lambda} \cup S'_n$ has positive length. We also have the equation

$$f'(S'_n - S'_1) \subset S'_{n-1}. \quad (44)$$

Using this equation, together with the fact that f' is a piecewise isometry, we see by induction that $\widehat{\Lambda} \cap S'_1$ has positive length.

By symmetry, the $\pi/2$ rotation carries F_1 to F_2 and $\widehat{\Lambda} \cap F_1$ to $\widehat{\Lambda} \cap F_2$ and $S'_1 \cap F_1$ to $S'_1 \cap F_2$. Hence, if $\widehat{\Lambda}$ has positive length intersection with S'_1 , then $\widehat{\Lambda}$ also has positive length intersection with $S'_1 \cap F_1$. (Recall that $X = F_1$.)

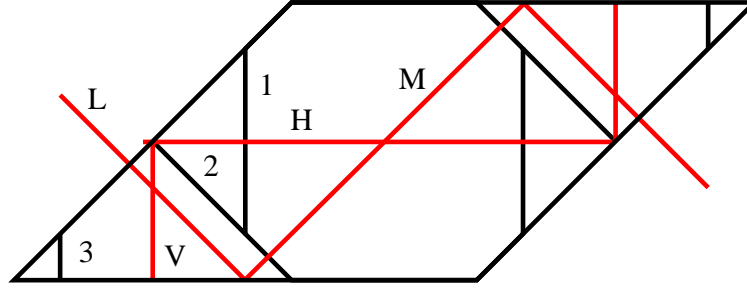


Figure 8.1: The set $S'_1 \cap X$ in black, and symmetry lines in red.

The red lines labelled H, V, L in Figure 8.1 are lines of symmetry from Bilateral Lemma I and Bilateral Lemma II. The fact that line M is a line of symmetry follows from the Inversion Lemma and the fact that L_t is a line of symmetry for A_t when $t = 1/2s$.

Let R_L denote reflection in line L , etc. We now have 3 cases.

1. Suppose $\widehat{\Lambda}$ intersects the segment labelled 1 in a set of positive length. We apply R_L . Lemma 8.3 and the Bilateral Lemma II combine to say that $\widehat{\Lambda} \cap \partial X$ has positive length.
2. Suppose $\widehat{\Lambda}$ intersects the line labelled 2 in a set of positive length. On at least one side of line 2 there are tiles of Δ_s which accumulate on line 2 in a set of positive length. Depending on which side has this property we either apply R_H or R_V . Lemma 8.3 and Bilateral Lemma I combine to say that $\widehat{\Lambda} \cap \partial X$ has positive length.
3. Suppose $\widehat{\Lambda}$ intersects the line labelled 3 in a set of positive length. This is the same argument as in Case 2, except we use one of the reflections $R_L \circ R_V$ or $R_M \circ R_V$.

If $\widehat{\Lambda}$ intersects S'_1 on the right hand side of the picture in a set of positive length, then we use the rotational symmetry to reduce to the cases above. ♠

Combining the previous result with Lemma 8.8, we see that $\widehat{\Lambda}_s \cap B_s^+$ has zero length when $s > 1/2$. Now consider the case $t < 1/2$. Suppose that $\widehat{\Lambda}_t \cap B_t^+$ has positive length. Let $s = 1 - t$ so that $t = R(s)$. By the Main Theorem, $\widehat{\Lambda}_s \cap B_s^+$ has positive length. But then, by the previous result, $\widehat{\Lambda}_s \cap \partial X_s$ has positive length. Lemma 8.8 rules this out.

8.6 Hyperbolic Symmetry

In this section, we prove Theorem 1.5. Let $i = \sqrt{-1}$, as usual. Let Γ' denote the group of maps of $\mathbf{C} \cup \infty$ generated by the following maps.

1. $z \rightarrow \bar{z}$.
2. $z \rightarrow -z$.
3. $z \rightarrow z - 1$.
4. $z \rightarrow 1/(2z)$.

Let $\Gamma \subset \Gamma'$ be the index 2 subgroup which preserves \mathbf{H}^2 .

Lemma 8.10 *If s and t lie in the same Γ' orbit, then (X_s, f_s) and (X_t, f_t) are locally equivalent.*

Proof: Local equivalence is an equivalence relation, so we just have to check this result on the generators of Γ . Note that local equivalence is an empty condition for rational parameters. So, we only work with irrational parameters.

Complex conjugation fixes \mathbf{R} pointwise. So, for this generator there is nothing to prove.

If $t = -s$ then the two systems are identical, by definition.

If $t = 1/2s$, then the two systems are conjugate, by the Inversion Lemma.

The one nontrivial case is when $t = s - 1$. There are several cases to consider. By symmetry, it suffices to consider the case when $s > 0$. There are several cases to consider. When $s > 2$, the result follows from the Insertion Lemma.

Suppose that $s \in (1, 2)$. By the Covering Lemma, X_s^0 is nicely covered by similar copies of X_t^0 . Moreover, in our construction, at least one of these similar copies, namely Z_s , lies entirely in X_s^0 . The local equivalence follows immediately in this case. To make this work, we need to throw out points on the finitely many lines extending the sides of the similar copies of X_t^0 .

Suppose that $s \in (1/2, 1)$ and $t' = s - 1$. Then $t' < 0$ and we can switch to the parameter $t = -t' = 1 - s$. Now we apply the Covering Lemma again, just as in the previous case.

Finally, suppose that $s \in (0, 1/2)$. Again, we consider $t = 1 - s \in (1/2, 1)$. Switching the roles of s and t we reduce to the previous case. ♠

It just remains to recognize Γ .

- Γ contains the element $\rho_1(z) = -\bar{z}$. This is the reflection in the geodesic joining 0 to ∞ .
- Γ contains the element $\rho_2(z) = \overline{1 - z}$. This is the reflection in the geodesic ray joining $1/2 + i/2$ to ∞ .
- Γ contains the element $\rho_3(z) = 1/(2\bar{z})$. This is a reflection in the geodesic joining $i/\sqrt{2}$ to $1/2 + i/2$.

In short, Γ contains ρ_j for $j = 1, 2, 3$, and these elements generate the $(2, 4, \infty)$ triangle group generated by reflections in the sides of the triangle with vertices $i/\sqrt{2}$, and $1/2 + i/2$, and ∞ . We omit the proof that these elements generate Γ , since what we have done already gives a proof of Theorem 1.5.

9 The Eight Calculations

9.1 The Fiber Bundle Picture

Our strategy is to reduce all our calculations to statements about convex lattice polyhedra. In this section, we explain the main idea behind this reduction. For the most part, we only need to make our calculations for parameters $a \in [1/4, 2]$, and so this interval will make a frequent appearance in the discussion.

In our standard normalization, X_s be the parallelogram with vertices

$$(\epsilon_1 + \epsilon_2 s, \epsilon_2 s), \quad \epsilon_1, \epsilon_2 \in \{-1, 1\}. \quad (45)$$

We define

$$\mathcal{X} = \{(x, y, s) \mid (s, y) \in X_s\} \subset \mathbf{R}^2 \times [1/4, 2] \quad (46)$$

The space \mathcal{X} is both a convex lattice polyhedron and a fiber bundle over $[1/4, 2]$ such that the fiber above s is the parallelogram X_s . See §10.1 for the list of vertices of \mathcal{X} . The maps $f_s : X_s \rightarrow X_s$ piece together to give a fiber-preserving map $F : \mathcal{X} \rightarrow \mathcal{X}$.

Lemma 9.1 *The map F is a piecewise affine map.*

Proof: Consider some point $p \in X_s$. There is some vector

$$V_s = (A + Bs, C + Ds)$$

Here A, B, C, D are integers. such that $f_s(p) = p + V_s$. If we perturb both V and s , the integers A, B, C, D do not change. So, in a neighborhood of p in \mathcal{X} , the map F has the form

$$(F(x, y, s) = (x + Bs, y + Ds, s) + (A, C, 0).$$

This is a locally affine map of \mathbf{R}^3 . ♠

Let $\mathcal{X}(S)$ be the subset of our fiber bundle lying over a set $S \subset [1/4, 2]$. Given the nature of the map, we find it useful to split our fiber bundle into 3 pieces, namely

$$\mathcal{X} = \mathcal{X}[1/4, 1/2] \cup \mathcal{X}[1/2, 1] \cup \mathcal{X}[1, 2]. \quad (47)$$

A *maximal domain* of $\mathcal{X}(S)$ is a maximal subset on which F is entirely defined and continuous. The map F acts as an affine map on each maximal subset. In §9.3 we explain how we verify the following experimentally discovered facts.

- $\mathcal{X}[1/4, 1/2]$ is partitioned into 19 maximal domains, each of which is a convex rational polytope. The vertices in the partition of \mathcal{X} are of the form $(a/q, b/q, p/q)$ where $a, b, p, q \in \mathbf{Z}$ and

$$(p, q) \in \{(1, 4), (2, 7), (3, 10), (1, 3), (1, 2)\}.$$

These polyhedra are permuted by the map $\iota_1(x, y, s) = (-x, -y, s)$.

- $\mathcal{X}[1/2, 1]$ is partitioned into 13 maximal domains, each of which is a convex rational polytope. The vertices in the partition of $\mathcal{X}[1/2, 1]$ are of the form $(a/q, b/q, p/q)$ where $a, b, p, q \in \mathbf{Z}$ and

$$(p, q) \in \{(1, 2), (2, 3), (3, 4), (1, 1)\}.$$

These polyhedra are permuted by ι_1 .

- The 19 polyhedra in the partition of $\mathcal{X}[1, 2]$ are all images of the polyhedra in the partition of $\mathcal{X}[1/4, 1/2]$ under the map $\iota_2 \circ F$, where

$$\iota_2(x, y, s) \rightarrow ((x + y)/2s, (x - y)/2s, 1/2s).$$

These polyhedra are permuted by ι_1 .

In §10.3 we will explain the action of the map F on each polyhedron. We scale all the polyhedra by a factor of $420 = 10 \times 7 \times 4$ so that we can make all our calculations using integer arithmetic. One can think of this rescaling as a way of clearing all denominators in advance of the calculations.

We will list the 420-scaled polyhedra in §10.2. For now, call them

$$\alpha_0, \dots, \alpha_{18}, \beta_0, \dots, \beta_{12}, \gamma_0, \dots, \gamma_{18}.$$

We have labeled so that list these so that

$$\alpha_i \subset \mathcal{X}[105, 210], \quad \beta_i \subset \mathcal{X}[210, 420], \quad \gamma_i \subset \mathcal{X}[420, 840]. \quad (48)$$

$\mathcal{X}[105, 210]$ is our name for the 420-scaled version of $\mathcal{X}[1/4, 1/2]$, etc. When we want to discuss these polyhedra all at once, we call them P_0, \dots, P_{50} .

9.2 Computational Methods

Here we describe the main features of our calculations. As we mentioned above, all our calculations boil down to calculations involving convex lattice polytopes.

Operations on Vectors: The only operations we perform on vectors are vector addition and subtraction, the dot and cross product, scaling a vector by an integer, and dividing a vector by $d \in \mathbf{Z}$ provided d divides all the coordinates. These operations in turn only use plus, minus, and times, and integer division.

Avoiding Computer Error: We represent integers as *longs*, a 64 bit integer data type. One can represent any integer strictly between -2^{63} and 2^{63} . (The extra bit gives the sign of the number.) There are two possible sources of error: overflow error and division errors.

We subject all our calculations to an overflow checker, to make sure that the computer never attempts a basic operation (plus, minus, times) in with either the inputs or the output is out of range. To give an example, if we want to take the cross product $V_1 \times V_2$, we first check that all entries in V_1 and V_2 are less than 2^{30} in size. This guarantees that all intermediate answers, as well as the final answer, will be in the legal range for longs.

We also check our division operations. Before we compute n/d , we make sure that $n \equiv 0 \pmod{d}$. The java operation $n\%d$ does this. Once we know that $n\%d = 0$, we know that the computer correctly computes the integer n/d .

No Collinearities: Given a polyhedron P , let P_1, \dots, P_n denote the vertices. We first check that

$$(P_k - P_i) \times (P_j - P_i) \neq 0, \quad \forall i < j < k \in \{1, \dots, n\}. \quad (49)$$

This guarantees that no three points in our vertex list of P are collinear. We found the polyhedra of interest to us in an experimental way, and initially they had many such collinearities. We detected collinearities by the failure of Equation 49, and then removed all the redundant points.

Face Lists: For each of our polyhedra P , we find and then store the list of faces of the polyhedron. To do this, we consider each subset $S = \{S_1, \dots, S_m\}$

having at least 3 members. We check for three things.

1. S lies in a single plane. We compute a normal $N = (S_2 - S_1) \times (S_3 - S_1)$ and then check that $N \cdot S_i$ is independent of i . Assuming this holds, let $D = N \cdot S_i$.
2. S lies on ∂P . To check this, we compute the normal N as above, and then check that either $\max N \cdot P_i \leq D$ or $\min N \cdot P_i \geq D$.
3. We check that S is maximal with respect to sets satisfying the first two properties.

Improved Normals: We noticed computationally that all of the normals to all of the polyhedron faces can be scaled so that they have the following form: At least two of the three coordinates lie in $\{-1, 0, 1\}$ and the third coordinate lies in $\{-8, \dots, 8\}$. When we use the normals in practice, we make this scaling. This is one more safeguard against overflow error.

No Face Redundancies: Once we have the face list, we check that each vertex of each polyhedron lies in exactly 3 faces. In particular, all the vertices of our polyhedra are genuine vertices.

Containment Algorithm: Suppose we want to check if a vector V lies in a polyhedron P . For each face S of P , we let N be the (scaled) normal to S . we set $D = N \cdot S_0$, and then we verify the following.

- If $\max N \cdot P_i \leq D$ then $V \cdot N \leq D$.
- If $\min N \cdot P_i \geq D$ then $V \cdot N \geq D$.

If this always holds then V lies on the same side of S as does P , for all faces S . In this case, we know that $V \in P$. If we want to check that $V \in \text{interior}(P)$, we make the same tests, except that we require strict inequalities.

Disjointness Algorithm: Let $\mathbf{Z}_{10} = \{-10, \dots, 10\}$. To prove that two polyhedra P and Q have disjoint interiors, we produce (after doing a search) an integer vector $W \in \mathbf{Z}_{10}^3$ such that

$$\max W \cdot P_i \leq \min W \cdot Q_j. \quad (50)$$

Volumes: For many of the lattice polytopes P we consider, we compute $6 \text{volume}(P) \in \mathbb{Z}$. To compute this volume, we decompose P into prisms by choosing a vertex of $v \in P$ and then computing

$$\sum_{f \in P} 6 \text{volume}([v, f]). \quad (51)$$

The sum is taken over all faces f of P and $[v, f]$ denotes the prism obtained by taking the convex hull of $v \cup f$. We compute the volumes of these prisms by taking various triple products of the vectors involved.

9.3 Verifying the Partition

Now we explain how we verify that the polyhedra we mention in §9.1 (and list in §10.2) really are correct. Let $\mathcal{R}\mathcal{X}$ denote the polytope obtained from \mathcal{X} by rotating 90 degrees. We have $F = (F')^2$, where F' is the original PET which swaps \mathcal{X} and $\mathcal{R}\mathcal{X}$.

Pairwise Disjointness: Using the Disjointness Algorithm, we check that P_i and P_j have disjoint interiors for all $i \neq j \in \{0, \dots, 50\}$. We check the same thing for $F(P_i)$ and $F(P_j)$.

Containment: Using the Containment Algorithm, we check that

- $P_i \subset \mathcal{X}$ for $i = 0, \dots, 50$.
- $F(P_i) \subset \mathcal{X}$ for $i = 0, \dots, 50$.
- $F'(P_i) \subset \mathcal{R}\mathcal{X}$ for $i = 0, \dots, 50$.

We also see, by inspection, that F has a different action on P_i and P_j whenever P_i and P_j share a (non-horizontal) face. These checks show that each P_i is a maximal domain for the action of F

Filling: It remains to check we check that \mathcal{X} is partitioned into P_0, \dots, P_{50} . We check that

$$\sum_{i=0}^{50} \text{volume}(P_i) = \text{volume}(\mathcal{X}). \quad (52)$$

The same equation shows that \mathcal{X} is also partitioned into $F(P_0), \dots, F(P_{50})$.

9.4 Calculation 1

Let $H = F^{-1}$, and let \mathcal{H} be the partition of $\mathcal{X}[1/4, 1]$ by the polyhedra $F(P_0), \dots, F(P_{31})$. Then \mathcal{H} is the partition by maximal domains for F^{-1} . We rename the members of \mathcal{H} as H_0, \dots, H_{31} .

We have the partition

$$\mathcal{X}[1/4, 1] = \mathcal{A}[1/4, 1] \cup \mathcal{B}[1/4, 1] \cup \mathcal{C}[1/4, 1] \quad (53)$$

Here \mathcal{A} is such that the fiber of \mathcal{A} over s is the hexagon A_s . The polyhedron \mathcal{B} has the same definition relative to the triangle β_s . The polyhedron \mathcal{C} is obtained from \mathcal{B} by reflecting in the line $x = y = 0$.

The map μ from Calculation 1 acts on each of \mathcal{A} and \mathcal{B} and \mathcal{C} as a reflection. We verify that each polyhedron α_i and β_i is a subset of one of these 3 big pieces. Thus, μ acts on each polyhedron as a reflection. The new partition

$$\mathcal{X}[1/4, 1] = \bigcup_{i=0}^{18} \mu(\alpha_i) \cup \bigcup_{i=0}^{12} \mu(\beta_i) \quad (54)$$

is the partition for the map

$$G = \mu \circ f \circ \mu^{-1}. \quad (55)$$

We call this partition \mathcal{G} , and we rename its members G_0, \dots, G_{31} .

So, in summary \mathcal{G} is the partition for G and \mathcal{H} is the partition for H . Next, we find a list of 48 pairs i, j so that

$$\text{interior}(G_i) \cap \text{interior}(H_j) \neq \emptyset$$

only if (i, j) lies on our list. More precisely, we use the Separation Algorithm to show that all other pairs have disjoint interiors.

Finally, we consider the grid

$$\Gamma = \{(20i, 20k, 105 + 10k) \mid i = -42, \dots, 42, \ j = -21, \dots, 21, \ k = 0, \dots, 31\}. \quad (56)$$

We check the identity $G = H$ on each point of Γ and we also check that at least one point of Γ is contained in each intersection $G_i \cap H_j$ for each of our 48 pairs. This suffices to establish the identity on all of $\mathcal{X}[1/4, 1]$.

9.5 Calculation 2

Calculation 2 follows the same scheme as Calculation 1. Here we just explain the differences in the calculation.

- We set $H = F$ and $G = \nu F^{-1}\nu$.
- \mathcal{H} is the partition consisting of $\alpha_0, \dots, \alpha_{18}$.
- $\mathcal{X}[1/4, 1/2]$ is partitioned into 5 smaller polyhedra, coming from P_s , Q_s , the central tile, $\iota(P_s)$ and $\iota(Q_s)$. the map ν acts as a reflection on each piece. For $i = 0, \dots, 18$, the polyhedron $F(\alpha_i)$ is contained in one of the 5 pieces, so that ν acts isometrically on $F(\alpha_i)$.
- \mathcal{G} be the partition of $\mathcal{X}[1/4, 1/2]$ by the polyhedra

$$\nu \circ F(\alpha_0), \dots, \nu \circ F(\alpha_{18}).$$

- We find a list of 27 pairs (i, j) such that G_i and H_j do not have disjoint interiors.

The rest of the calculation is the same.

9.6 Calculation 3

Let $s \in [5/4, 2]$ and let $t = s - 1 \in [1/4, 1]$. We want to show that ϕ_s conjugates $f_t|Y_t$ to $f_s|Z_s$ and that every orbit of f_s intersects Z_s , except the following orbits.

- Those in the trivial tile $(\alpha_0 \cup \beta_0)_s$ of Δ_s .
- Those in the set

$$\tau_s = \phi_s\left((\alpha_0 \cup \beta_0)_t\right).$$

Once we are done, we will know that τ_s is in fact a tile of Δ_s , and that τ_s has period 2.

For this section we set $\mathcal{X} = \mathcal{X}[5/4, 2]$. Let \mathcal{Y} denote the subset of \mathcal{X} whose fiber over s is the set Y_s . Define \mathcal{Z} in a similar way. The maps $\phi_s : Y_t \rightarrow Z_s$ piece together to give an isometry $\phi : \mathcal{Y} \rightarrow \mathcal{Z}$. The map is given by

$$\phi(x, y, z) = (x \pm 1, y \pm 1, z - 1) \tag{57}$$

Whether we add or subtract 1 to the first two coordinates depends on whether the point (x, y, z) lies in the left half of \mathcal{Y} or in the right half.

For what we describe next, we always refer to open polyhedra, and our equalities are meant to hold up to sets of codimension 1, namely the boundaries of our polyhedra.

We have

$$\mathcal{Y} = \alpha_1 \cup \dots \cup \alpha_{18} \cup \beta_1 \cup \dots \cup \beta_{12}. \quad (58)$$

For each $i = 1, \dots, 18$ we check computationally that there is some $k = k_i$ with the following three properties.

1. The first $k_i + 1$ iterates of F^{-1} are defined on $\phi \circ F(\alpha_i)$. This amounts to checking that

$$P_{ij} = F^{-i} \circ \phi \circ F(\alpha_i) \quad (59)$$

is contained in some α_a or β_b for suitable indices a and b , and for all $i = 0, \dots, k_i$.

- 2.

$$P_{ij} \cap \mathcal{Z} = \emptyset, \quad j = 1, \dots, k_i. \quad (60)$$

Equation 60 shows that

$$F|_{P_{i0}} = F^{k_i}$$

That is, on P_{i0} , the map F returns to \mathcal{Z} as F^{k_i} . To establish Equation 60, we use the Separation Algorithm so show that

$$P_{ij} \cap \phi(\alpha_a) = \emptyset, \quad P_{ij} \cap \phi(\beta_b) = \emptyset$$

for all $a = 1, \dots, 18$ and $b = 1, \dots, 12$, and all relevant indices i and j . This suffices because \mathcal{Z} is partitioned into the polyhedra

$$\mathcal{Z} = \phi(\alpha_\infty) \cup \dots \cup \phi(\alpha_{\infty\forall}) \cup \phi(\beta_\infty) \cup \dots \cup \phi(\beta_{\infty\epsilon}).$$

3. $P_{i,k_i+1} = \phi(\alpha_i)$.

We make all the same calculations for $\beta_1, \dots, \beta_{12}$, finding an integer ℓ_i which works for β_i . We define Q_{ij} with respect to β_i just as we defined P_{ij} with respect to α_i .

Our calculations above show that ϕ conjugates $F|_{\mathcal{Y}}$ to $F|_{\mathcal{Z}}$. Also, by construction, the boundary of \mathcal{Z} is contained in the union of the boundaries of the polyhedra $\phi(\alpha_i) \cup \phi(\beta_j)$. Hence, Z_s is a clean set for all $s \in [5/4, 2]$.

We still want to see that all orbits except those of period 1 and 2 actually intersect \mathcal{Z} . We check the following.

1. F is entirely defined on $\phi(\alpha_0)$ and has order 2.
2. Both $\phi(\alpha_0)$ and $F \circ \phi(\alpha_0)$ are disjoint from \mathcal{Z} . We use the same trick with the Separation Algorithm to do this.

We claim that the open polyhedra in the following union are pairwise disjoint.

$$\bigcup_{i=1}^{18} \bigcup_{j=0}^{k_i} P_{ij} \cup \bigcup_{i=1}^{12} \bigcup_{j=0}^{\ell_i} Q_{ij} \cup \bigcup_{j=0}^1 F^j \circ \phi(\alpha_0) \cup \bigcup_{j=0}^1 F^j \circ \phi(\beta_0) \cup \alpha_0 \cup \beta_0. \quad (61)$$

Suppose, for instance, that P_{ab} and P_{cd} were not disjoint. Then $P_{a,b+e}$ and $P_{c,d+f}$ would not be disjoint for $e > 0$ and $f > 0$ such that $b+e = k_a + 1$ and $c+f = k_b + 1$. But we know that these last polyhedra are disjoint because they respectively equal the disjoint polyhedra $\phi(\alpha_a)$ and $\phi(\alpha_c)$. Similar arguments work for the other cases.

Similar to Equation 52, we compute the sum of the volumes of the polyhedra in Equation 61 and see that it coincides with the volume of \mathcal{X} . Thus, \mathcal{X} is partitioned into the polyhedra in Equation 61. This fact implies the all orbits except those of period 1 and 2 actually intersect \mathcal{Z} .

Finally, we see by process of elimination that τ_s really is a tile of Δ_s . All other points not in the interior of τ_s either have undefined orbits, or lie in the trivial tile, or have orbits which intersect \mathcal{Z} . Thus f_s cannot be defined on any point of the boundary of τ_s . Since f_s is defined, and has period 2, on the interior of τ_s , we see that τ_s is a tile of Δ_s having period 2.

9.7 Calculation 4

Calculation 4 follows the same scheme as Calculation 3. Here we will describe the differences between the two calculations.

- We consider the behavior of polyhedra on the interval $s \in [1/2, 3/4]$ rather than on $[5/4, 1]$. Here $t = 1 - s \in [1/4, 1/2]$.
- The map ϕ is not an isometry here, but rather a volume preserving affine map. The formula is

$$\phi(x, y, z) = (x \pm (1 - 2z), y \pm (1 - 2z), 1 - z). \quad (62)$$

The choice of plus or minus again depends on whether (x, y, z) lies in the left of the right half of \mathcal{Y} .

- \mathcal{Y} is partitioned into the tiles $\alpha_1, \dots, \alpha_{18}$. The B -tiles are not needed here.
- The tiles τ and $\iota(\tau)$ already belong to \mathcal{Z} . The work in Calculation 3 shows that τ_s and ι_s are indeed period 2 tiles of Δ_s . This time, τ and $\iota(\tau)$ are amongst the images of $\alpha_1, \dots, \alpha_{18}$ under ϕ .
- Using the notation from the previous section, the partition in Equation 61 becomes

$$\bigcup_{i=1}^{18} \bigcup_{j=0}^{k_i} P_{ij} \cup \alpha_0 \quad (63)$$

The rest of the calculation is the same.

9.8 Calculation 5

Calculation 5 follows the same scheme as Calculation 3, except that we don't need to keep track of the volumes. Let T and ω be as in Calculation 5. Let $s \in (1, 4/3]$ and let $t = T(s) \in (1, 2]$.

We define \mathcal{W} and \mathcal{Y} as the global versions of W_s and Y_u , as in Calculation 3. We are interested in $\mathcal{Y}[1, 2]$ and $\mathcal{W}[1, 4/3]$. Similar to Calculation 3, we have a global map $\omega : \mathcal{Y} \rightarrow \mathcal{W}$. We have the formula

$$\omega(x, y, z) = (\omega_s(x, y), s), \quad s = T^{-1}(z). \quad (64)$$

We want to see that ω conjugates $F|_{\mathcal{Y}}$ to $F|_{\mathcal{W}}$.

We have

$$\mathcal{Y} = \gamma_1 \cup \dots \cup \gamma_{18}. \quad (65)$$

By the same methods used in Calculation 3, we check, for each $i = 1, \dots, 18$, that there is some $k = k_i$ with the following three properties.

1. The first $k_i + 1$ iterates of F^{-1} are defined on $\omega \circ F(\gamma_i)$. Define

$$P_{ij} = F^{-i} \circ \omega \circ F(\gamma_i) \quad (66)$$

- 2.

$$P_{ij} \cap \mathcal{W} = \emptyset, \quad j = 1, \dots, k_i. \quad (67)$$

3. $P_{i, k_i+1} = \omega(\alpha_i)$.

These facts imply that ω conjugates $F|\mathcal{Y}$ to $F|\mathcal{W}$.

Finally, the set Z_s is clean for each s for the following reasons.

- The top edge of Z_s^0 and the bottom edge of $\iota(Z_s^0)$ are contained in the union of slices of the sets $\omega \circ F(\partial\gamma_i)$.
- The vertical edges of Z_s are contained in the set $\partial\tau_s \cup \iota(\partial\tau_s)$.
- The remaining edges of Z_s lie in the ∂X_s .

9.9 Calculation 6

As we mentioned in §5, Calculation 6 practically amounts to inspecting the partition. For Statement 1, we let τ be the polyhedron which restricts to τ_s for $s \in [1, 3/2]$. We list this polyhedron in §10.1. We check that F is entirely defined on (the interior of) τ and that $F^2(\tau) = \tau$.

For each polyhedron P , let P_s denote the intersection of P with the horizontal plane of height s .

For Statement 2, let \mathcal{Z} be the polyhedron which restricts to Z_s^0 for $s \in [1, 5/4]$. We compute that

$$\mathcal{Z} \subset F(\gamma_{13}). \quad (68)$$

We also try a single point $(x, y, s) \in F(\gamma_{13})$ and check that $f_s^{-1}(p) = p + \delta_s$. Since $F(\gamma_{13})$ is a domain of continuity for F^{-1} , the same result holds for all points in $F(\gamma_{13})$, including all the points in \mathcal{Z} . This proves Statement 2.

For Statement 3, let \mathcal{K} be the union of two polyhedra which intersect the fiber X_s in $X_s - Z_s - W_s$, for $s = (1, 5/4]$. We see by inspection that

$$\mathcal{K} = F(\gamma_2) \cup F(\gamma_8) \cup F(\gamma_{11}) \cup F(\gamma_{17}); \quad \gamma_j \subset \mathcal{Z}, \quad j = 2, 8, 11, 17. \quad (69)$$

This proves Statement 3.

Remark: We could have made an explicit computation to establish Equation 69, but this is something that is obvious from a glance at just 2 planar pictures. We just have to check Equation 69 at the parameters $s = 1$ and $s = 3/2$ because every polyhedron P in sight, when restricted to the fibers above $[1, 5/4]$, is the convex hull of $P_1 \cup P_{5/4}$.

9.10 Calculation 7

Calculation 7 follows the same scheme as Calculation 5. Here are the differences.

- Here we are interested in $\mathcal{Y}[1/2, 1]$ and $\mathcal{W}[3/4, 1]$.
- Here we use the formula from 26 to define the map ω in Equation 64.
- Here we have

$$\mathcal{Y} = \beta_1 \cup \dots \cup \beta_{12}. \quad (70)$$

The rest of the calculation is the same.

9.11 Calculation 8

Calculation 8 works essentially the same as Calculation 6. For Statement 1, we let τ be the polyhedron which restricts to τ_s for $s \in [3/4, 1]$. We list this polyhedron in §10.1. We check that F is entirely defined on (the interior of) τ and that $F^2(\tau) = \tau$.

For Statement 2, we let \mathcal{Z}^* be the polyhedron which intersects X_s in $(Z_s^0)^*$ for $s \in [3/4, 1]$. We compute that

$$\mathcal{Z}^* \subset \beta_7 \quad (71)$$

and we finish the proof of Statement 2 just as in Calculation 6.

For Statement 3, we define \mathcal{K} as in Calculation 6 and we see by inspection that

$$\mathcal{K} = \beta_2 \cup \beta_6 \cup \beta_8 \cup \beta_{12}, \quad F(\beta_j) \subset \mathcal{Z}, \quad j = 2, 6, 8, 12. \quad (72)$$

This proves Statement 3.

10 The Raw Data

10.1 Auxilliary Polyhedra

Here we list the coordinates of the auxilliary polyhedra which arise in our calculations. All our polyhedra are scaled by a factor of 420.

Here is $\mathcal{X}[1/4, 2]$.

$$\begin{bmatrix} -525 \\ -105 \\ 105 \end{bmatrix} \begin{bmatrix} 315 \\ -105 \\ 105 \end{bmatrix} \begin{bmatrix} -315 \\ 105 \\ 105 \end{bmatrix} \begin{bmatrix} 525 \\ 105 \\ 105 \end{bmatrix} \begin{bmatrix} -1260 \\ -840 \\ 840 \end{bmatrix} \begin{bmatrix} -420 \\ -840 \\ 840 \end{bmatrix} \begin{bmatrix} 420 \\ 840 \\ 840 \end{bmatrix} \begin{bmatrix} 1260 \\ 840 \\ 840 \end{bmatrix}$$

Here is $\mathcal{A}[1/4, 1]$. This set intersects the fiber X_s in the hexagon A_s , for $s \in [1/4, 1]$.

$$\begin{bmatrix} 315 \\ 105 \\ 105 \end{bmatrix} \begin{bmatrix} -315 \\ 105 \\ 105 \end{bmatrix} \begin{bmatrix} -315 \\ -105 \\ 105 \end{bmatrix} \begin{bmatrix} 315 \\ -105 \\ 105 \end{bmatrix} \begin{bmatrix} 420 \\ 0 \\ 105 \end{bmatrix} \begin{bmatrix} -420 \\ 0 \\ 105 \end{bmatrix} \begin{bmatrix} 0 \\ 420 \\ 420 \end{bmatrix} \begin{bmatrix} 420 \\ 0 \\ 420 \end{bmatrix} \begin{bmatrix} -420 \\ 0 \\ 420 \end{bmatrix} \begin{bmatrix} 0 \\ -420 \\ 420 \end{bmatrix}$$

Here is $\mathcal{B}[1/4, 1]$. This set intersects the fiber X_s in the triangle β_s , for $s \in [1/4, 1]$.

$$\begin{bmatrix} -315 \\ -105 \\ 105 \end{bmatrix} \begin{bmatrix} -420 \\ 0 \\ 105 \end{bmatrix} \begin{bmatrix} -525 \\ -105 \\ 105 \end{bmatrix} \begin{bmatrix} -840 \\ -420 \\ 420 \end{bmatrix} \begin{bmatrix} -420 \\ 0 \\ 420 \end{bmatrix} \begin{bmatrix} 0 \\ -420 \\ 420 \end{bmatrix}$$

Here is $\mathcal{P}[1/4, 1/2]$. This set intersects the fiber X_s in the pentagon P_s , for $s \in [1/4, 1/2]$.

$$\begin{bmatrix} -315 \\ -105 \\ 105 \end{bmatrix} \begin{bmatrix} -105 \\ -105 \\ 105 \end{bmatrix} \begin{bmatrix} -105 \\ 105 \\ 105 \end{bmatrix} \begin{bmatrix} -315 \\ 105 \\ 105 \end{bmatrix} \begin{bmatrix} -630 \\ -210 \\ 210 \end{bmatrix} \begin{bmatrix} -210 \\ -210 \\ 210 \end{bmatrix} \begin{bmatrix} -210 \\ 210 \\ 210 \end{bmatrix}$$

Here is $\mathcal{Q}[1/4, 1/2]$. This set intersects the fiber X_s in the triangle Q_s , for $s \in [1/4, 1/2]$.

$$\begin{bmatrix} -525 \\ -105 \\ 105 \end{bmatrix} \begin{bmatrix} -315 \\ -105 \\ 105 \end{bmatrix} \begin{bmatrix} -315 \\ 105 \\ 105 \end{bmatrix} \begin{bmatrix} -630 \\ -210 \\ 210 \end{bmatrix}$$

Here is the period 2 tile $\tau[1, 5/4]$ from Calculation 6.

$$\begin{bmatrix} -525 \\ -315 \\ 315 \end{bmatrix} \begin{bmatrix} -315 \\ -315 \\ 315 \end{bmatrix} \begin{bmatrix} -315 \\ -105 \\ 315 \end{bmatrix} \begin{bmatrix} -525 \\ -105 \\ 315 \end{bmatrix} \begin{bmatrix} -420 \\ -420 \\ 420 \end{bmatrix}$$

Here is the period 2 tile $\tau[3/4, 1]$ from Calculation 8.

$$\begin{bmatrix} -420 \\ -420 \\ 420 \end{bmatrix} \begin{bmatrix} -210 \\ -630 \\ 630 \end{bmatrix} \begin{bmatrix} -210 \\ -210 \\ 630 \end{bmatrix} \begin{bmatrix} -630 \\ -210 \\ 630 \end{bmatrix} \begin{bmatrix} -630 \\ -630 \\ 630 \end{bmatrix}$$

Here is the domain $\mathcal{Z}[1, 5/4]$ from Calculation 6.

$$\begin{bmatrix} -420 \\ -420 \\ 420 \end{bmatrix} \begin{bmatrix} -840 \\ -420 \\ 420 \end{bmatrix} \begin{bmatrix} -945 \\ -525 \\ 525 \end{bmatrix} \begin{bmatrix} -525 \\ -525 \\ 525 \end{bmatrix} \begin{bmatrix} -525 \\ -315 \\ 525 \end{bmatrix} \begin{bmatrix} -735 \\ -315 \\ 525 \end{bmatrix}$$

Here is the domain $\mathcal{Z}[3/4, 1]$ from Calculation 8.

$$\begin{bmatrix} -420 \\ -420 \\ 420 \end{bmatrix} \begin{bmatrix} -840 \\ -420 \\ 420 \end{bmatrix} \begin{bmatrix} -945 \\ -525 \\ 525 \end{bmatrix} \begin{bmatrix} -525 \\ -525 \\ 525 \end{bmatrix} \begin{bmatrix} -525 \\ -315 \\ 525 \end{bmatrix} \begin{bmatrix} -735 \\ -315 \\ 525 \end{bmatrix}$$

10.2 The Polyhedra in the Partition

Define

$$\iota_1(x, y, s) = (-x, -y, s), \quad \iota_2(x, y, s) = \left(\frac{x+y}{2s}, \frac{x-y}{2s}, \frac{1}{2s} \right). \quad (73)$$

The partition of $\mathcal{X}[1/4, 1/2]$ consists of the 19 polyhedra

$$\alpha_0, \alpha_1, \dots, \alpha_9, \iota_1(\alpha_1), \dots, \iota_1(\alpha_9). \quad (74)$$

The partition of $\mathcal{X}[1/2, 1]$ consists of the 13 polyhedra

$$\beta_0, \beta_1, \dots, \beta_6, \iota_1(\beta_1), \dots, \iota_1(\beta_6). \quad (75)$$

The partition of $\mathcal{X}[1, 2]$ consists of the 19 polyhedra

$$\iota_2 \circ F(\alpha_i), \quad i = 0, \dots, 18. \quad (76)$$

Here $\alpha_0, \dots, \alpha_{18}$ are the polyhedra from Equation 74.

As we mentioned in the last chapter, we scale each polyhedron by a factor of 420 so that all the entries are integers. Here are the polyhedra.

$$A_0 = \begin{bmatrix} 105 \\ 105 \\ 105 \end{bmatrix} \begin{bmatrix} -105 \\ 105 \\ 105 \end{bmatrix} \begin{bmatrix} -105 \\ -105 \\ 105 \end{bmatrix} \begin{bmatrix} 105 \\ -105 \\ 105 \end{bmatrix} \begin{bmatrix} 210 \\ 210 \\ 210 \end{bmatrix} \begin{bmatrix} -210 \\ 210 \\ 210 \end{bmatrix} \begin{bmatrix} -210 \\ -210 \\ 210 \end{bmatrix} \begin{bmatrix} 210 \\ -210 \\ 210 \end{bmatrix}$$

$$A_1 = \begin{bmatrix} 420 \\ 0 \\ 105 \end{bmatrix} \begin{bmatrix} 525 \\ 105 \\ 105 \end{bmatrix} \begin{bmatrix} 315 \\ 105 \\ 105 \end{bmatrix} \begin{bmatrix} 280 \\ 140 \\ 140 \end{bmatrix}$$

$$A_2 = \begin{bmatrix} 105 \\ 105 \\ 105 \end{bmatrix} \begin{bmatrix} 280 \\ 140 \\ 140 \end{bmatrix} \begin{bmatrix} 140 \\ 140 \\ 140 \end{bmatrix} \begin{bmatrix} 210 \\ -210 \\ 210 \end{bmatrix}$$

$$A_3 = \begin{bmatrix} 280 \\ 140 \\ 140 \end{bmatrix} \begin{bmatrix} 140 \\ 140 \\ 140 \end{bmatrix} \begin{bmatrix} 210 \\ 210 \\ 210 \end{bmatrix} \begin{bmatrix} 210 \\ -210 \\ 210 \end{bmatrix} \begin{bmatrix} 420 \\ 0 \\ 210 \end{bmatrix}$$

$$A_4 = \begin{bmatrix} 525 \\ 105 \\ 105 \end{bmatrix} \begin{bmatrix} 420 \\ 0 \\ 140 \end{bmatrix} \begin{bmatrix} 420 \\ 0 \\ 210 \end{bmatrix} \begin{bmatrix} 630 \\ 210 \\ 210 \end{bmatrix} \begin{bmatrix} 210 \\ 210 \\ 210 \end{bmatrix}$$

$$A_5 = \begin{bmatrix} 315 \\ -105 \\ 105 \end{bmatrix} \begin{bmatrix} 420 \\ 0 \\ 105 \end{bmatrix} \begin{bmatrix} 315 \\ 105 \\ 105 \end{bmatrix} \begin{bmatrix} 420 \\ 0 \\ 120 \end{bmatrix} \begin{bmatrix} 378 \\ -42 \\ 126 \end{bmatrix}$$

$$A_6 = \begin{bmatrix} 420 \\ 0 \\ 120 \end{bmatrix} \begin{bmatrix} 462 \\ 42 \\ 126 \end{bmatrix} \begin{bmatrix} 420 \\ 0 \\ 140 \end{bmatrix} \begin{bmatrix} 420 \\ 140 \\ 140 \end{bmatrix} \begin{bmatrix} 280 \\ 140 \\ 140 \end{bmatrix} \begin{bmatrix} 210 \\ 210 \\ 210 \end{bmatrix}$$

$$A_7 = \begin{bmatrix} 315 \\ 105 \\ 105 \end{bmatrix} \begin{bmatrix} 420 \\ 0 \\ 120 \end{bmatrix} \begin{bmatrix} 378 \\ -42 \\ 126 \end{bmatrix} \begin{bmatrix} 420 \\ 0 \\ 140 \end{bmatrix}$$

$$A_8 = \begin{bmatrix} 315 \\ -105 \\ 105 \end{bmatrix} \begin{bmatrix} 315 \\ 105 \\ 105 \end{bmatrix} \begin{bmatrix} 105 \\ 105 \\ 105 \end{bmatrix} \begin{bmatrix} 105 \\ -105 \\ 105 \end{bmatrix} \begin{bmatrix} 420 \\ 0 \\ 140 \end{bmatrix} \begin{bmatrix} 280 \\ 140 \\ 140 \end{bmatrix} \begin{bmatrix} 210 \\ -210 \\ 210 \end{bmatrix} \begin{bmatrix} 420 \\ 0 \\ 210 \end{bmatrix}$$

$$\begin{aligned}
A9 &= \begin{bmatrix} 420 \\ 0 \\ 105 \end{bmatrix} \begin{bmatrix} 525 \\ 105 \\ 105 \end{bmatrix} \begin{bmatrix} 420 \\ 0 \\ 120 \end{bmatrix} \begin{bmatrix} 462 \\ 42 \\ 126 \end{bmatrix} \begin{bmatrix} 420 \\ 140 \\ 140 \end{bmatrix} \begin{bmatrix} 280 \\ 140 \\ 140 \end{bmatrix} \\
B0 &= \begin{bmatrix} 105 \\ 105 \\ 105 \end{bmatrix} \begin{bmatrix} -105 \\ 105 \\ 105 \end{bmatrix} \begin{bmatrix} -105 \\ -105 \\ 105 \end{bmatrix} \begin{bmatrix} 105 \\ -105 \\ 105 \end{bmatrix} \begin{bmatrix} 210 \\ 210 \\ 210 \end{bmatrix} \begin{bmatrix} -210 \\ 210 \\ 210 \end{bmatrix} \begin{bmatrix} -210 \\ -210 \\ 210 \end{bmatrix} \begin{bmatrix} 210 \\ -210 \\ 210 \end{bmatrix} \\
B1 &= \begin{bmatrix} 420 \\ 0 \\ 105 \end{bmatrix} \begin{bmatrix} 525 \\ 105 \\ 105 \end{bmatrix} \begin{bmatrix} 315 \\ 105 \\ 105 \end{bmatrix} \begin{bmatrix} 280 \\ 140 \\ 140 \end{bmatrix} \\
B2 &= \begin{bmatrix} 105 \\ 105 \\ 105 \end{bmatrix} \begin{bmatrix} 280 \\ 140 \\ 140 \end{bmatrix} \begin{bmatrix} 140 \\ 140 \\ 140 \end{bmatrix} \begin{bmatrix} 210 \\ -210 \\ 210 \end{bmatrix} \\
B3 &= \begin{bmatrix} 280 \\ 140 \\ 140 \end{bmatrix} \begin{bmatrix} 140 \\ 140 \\ 140 \end{bmatrix} \begin{bmatrix} 210 \\ 210 \\ 210 \end{bmatrix} \begin{bmatrix} 210 \\ -210 \\ 210 \end{bmatrix} \begin{bmatrix} 420 \\ 0 \\ 210 \end{bmatrix} \\
B4 &= \begin{bmatrix} 525 \\ 105 \\ 105 \end{bmatrix} \begin{bmatrix} 420 \\ 0 \\ 140 \end{bmatrix} \begin{bmatrix} 420 \\ 0 \\ 210 \end{bmatrix} \begin{bmatrix} 630 \\ 210 \\ 210 \end{bmatrix} \begin{bmatrix} 210 \\ 210 \\ 210 \end{bmatrix} \\
B5 &= \begin{bmatrix} 315 \\ -105 \\ 105 \end{bmatrix} \begin{bmatrix} 420 \\ 0 \\ 105 \end{bmatrix} \begin{bmatrix} 315 \\ 105 \\ 105 \end{bmatrix} \begin{bmatrix} 420 \\ 0 \\ 120 \end{bmatrix} \begin{bmatrix} 378 \\ -42 \\ 126 \end{bmatrix} \\
B6 &= \begin{bmatrix} 420 \\ 0 \\ 120 \end{bmatrix} \begin{bmatrix} 462 \\ 42 \\ 126 \end{bmatrix} \begin{bmatrix} 420 \\ 0 \\ 140 \end{bmatrix} \begin{bmatrix} 420 \\ 140 \\ 140 \end{bmatrix} \begin{bmatrix} 280 \\ 140 \\ 140 \end{bmatrix} \begin{bmatrix} 210 \\ 210 \\ 210 \end{bmatrix}
\end{aligned}$$

10.3 The Action of the Map

In this section we explain the action of the map on each of the polyhedra listed above. To each polyhedron we associate a 4-tuple of integers. The list $V = (u_1, v_1, u_2, v_2)$ tells us that

$$F_V \begin{bmatrix} x \\ y \\ s \end{bmatrix} = \begin{bmatrix} 1 & 0 & 2v_1 - 2v_2 \\ 0 & 1 & 2v_1 + 2v_2 \\ 0 & 0 & 1 \end{bmatrix} \begin{bmatrix} x \\ y \\ s \end{bmatrix} + \begin{bmatrix} -2u_1 \\ 2u_2 \\ 0 \end{bmatrix}. \quad (77)$$

Remark; Equation 77 gives the equation for the action on the unscaled polyhedra. When we acts on the scaled polyhedra listed above, we need to scale the translation part of the map by 420. That is, $-2u_1$ and $2u_2$ need to be replaced by $-840u_1$ and $840u_2$.

The polyhedra α_0 and β_0 correspond to the trivial tiles. The vectors associated to these are $a_0 = b_0 = (0, 0, 0, 0)$. Below we will list the vectors $a_1, \dots, a_9, b_1, \dots, b_6$. We have the relations

$$a_{9+i} = -a_i, \quad b_{6+i} = -b_i. \quad (78)$$

The vector c_i associated to $\iota_2 \circ F(\alpha_i)$ is given by the following rule:

$$a_i = (u_1, v_1, u_2, v_2) \implies c_i = (-v_2, -u_2, -v_1, -u_1). \quad (79)$$

Recall that the map F is really the composition $(F')^2$, where F' maps the bundle $\mathcal{X}[1/4, 2]$ to the polyhedron obtained by rotating $\mathcal{X}[1/4, 2]$ by 90 degrees about the z -axis. To get the action of F' we simply replace each vector $V = a_1, a_2, \dots$ by V' , where

$$V = (u_1, v_1, u_2, v_2) \implies V' = (u_1, v_1, 0, 0). \quad (80)$$

Here are the vectors.

$$\begin{aligned} a_1 &= (1, 2, 0, -2), & a_2 &= (0, -1, -1, -2) & a_3 &= (0, -1, -1, -1). \\ a_4 &= (1, 1, 0, -1), & a_5 &= (0, -2, -1, -2) & a_6 &= (1, 2, 1, 1). \\ a_7 &= (0, -2, -1, -1), & a_8 &= (0, -1, 0, 1) & a_9 &= (1, 2, 1, 2). \\ b_1 &= (1, 0, -1, -1), & b_2 &= (1, 1, 0, -1) & b_3 &= (1, 1, 1, 0). \\ b_4 &= (0, -1, -1, 0), & b_5 &= (0, -1, -1, -1) & b_6 &= (1, 1, 1, 1). \end{aligned}$$

11 References

- [AG] A. Goetz and G. Poggiaspalla, *Rotations by $\pi/7$* , Nonlinearity **17** (2004) no. 5 1787-1802
- [AKT] R. Adler, B. Kitchens, and C. Tresser, *Dynamics of non-ergodic piecewise affine maps of the torus*, Ergodic Theory Dyn. Syst **21** (2001) no. 4 959-999
- [BKS] T. Bedford, M. Keane, and C. Series, eds., *Ergodic Theory, Symbolic Dynamics, and Hyperbolic Spaces*, Oxford University Press, Oxford (1991).
- [B] J. Buzzi, *Piecewise isometries have zero topological entropy (English summary)* Ergodic Theory and Dynamical Systems **21** (2001) no. 5 pp 1371-1377
- [GH1] E Gutkin and N. Haydn, *Topological entropy of generalized polygon exchanges*, Bull. Amer. Math. Soc., **32** (1995) no. 1., pp 50-56
- [GH2] E Gutkin and N. Haydn, *Topological entropy polygon exchange transformations and polygonal billiards*, Ergodic Theory and Dynamical Systems **17** (1997) no. 4., pp 849-867
- [H] H. Haller, *Rectangle Exchange Transformations*, Monatsh Math. **91** (1985) 215-232
- [Hoo] W. Patrick Hooper, *Renormalization of Polygon Exchange Maps arising from Corner Percolation* Invent. Math. 2012.
- [LKV] J. H. Lowenstein, K. L. Koupsov, F. Vivaldi, *Recursive Tiling and Geometry of piecewise rotations by $\pi/7$* , nonlinearity **17** (2004) no. 2. [Low] J. H. Lowenstein, *Aperiodic orbits of piecewise rational rotations of convex polygons with recursive tiling*, Dyn. Syst. **22** (2007) no. 1 25-63
- [R] G. Rauzy, *Exchanges d'intervalles et transformations induites*, Acta. Arith. **34** 315-328 (1979)
- [S0] R.E. Schwartz *The Octagonal PET II: Topology of the Limit Sets*,

preprint (2012)

[S1] R.E. Schwartz *Outer Billiards, Quarter Turn Compositions, and Polytope Exchange Transformations*, preprint (2011)

[S2] R. E. Schwartz, *Outer Billiards on Kites*, Annals of Math Studies **171**, Princeton University Press (2009)

[S3] R. E. Schwartz, *Outer Billiards on the Penrose Kite: Compactification and Renormalization*, Journal of Modern Dynamics, 2012.

[T] S. Tabachnikov, *Billiards*, Société Mathématique de France, “Panoramas et Synthèses” 1, 1995

[VL] F. Vivaldi and J. H. Lowenstein, —it Arithmetical properties of a family of irrational piecewise rotations, *Nonlinearity* **19**:1069–1097 (2007).

[Y] J.-C. Yoccoz, *Continued Fraction Algorithms for Interval Exchange Maps: An Introduction*, Frontiers in Number Theory, Physics, and Geometry Vol 1, P. Cartier, B. Julia, P. Moussa, P. Vanhove (editors) Springer-Verlag 4030437 (2006)

[Z] A. Zorich, *Flat Surfaces*, Frontiers in Number Theory, Physics, and Geometry Vol 1, P. Cartier, B. Julia, P. Moussa, P. Vanhove (editors) Springer-Verlag 4030437 (2006)

The Octagonal PET I: Renormalization and Hyperbolic Symmetry

Richard Evan Schwartz *

December 5, 2018

Abstract

This paper is a sequel to [S0]. In [S0], we introduced a family of polytope exchange transformations acting on parallelotopes in \mathbf{R}^{2n} , for $n = 1, 2, 3, \dots$. In the case $n = 1$, we have a 1-parameter family of 2-dimensional examples. In this case, we showed that the 2-dimensional family is completely renormalizable and that the $(2, 4, \infty)$ hyperbolic reflection triangle group acts (by linear fractional transformations) as the renormalization group on the moduli space. These results have a number of geometric corollaries for the system.

1 Introduction

1.1 Background

A *polytope exchange transformation* (or PET) is defined by a polytope X which has been partitioned in two ways into smaller polytopes:

$$X = \bigcup_{i=1}^m A_i = \bigcup_{i=1}^m B_i.$$

For each i there is some vector V_i such that $B_i = A_i + V_i$. That is, some translation carries A_i to B_i . One then defines a map $f : X \rightarrow X$ by the formula $f(x) = x + V_i$ for all $x \in \text{int}(A_i)$. It is understood that f is not

* Supported by N.S.F. Research Grant DMS-0072607

defined for points in the boundaries of the small polytopes. The inverse map is defined by $f^{-1}(y) = y - V_i$ for all $y \in \text{int}(B_i)$.

The simplest examples of PETs are 1-dimensional systems, known as *interval exchange transformations* (or IETs). These systems have been extensively studied in the past 30 years, and there are close connections between IETs and other areas of mathematics such as Teichmüller theory. See, for instance, [Y] and [Z] and the many references mentioned therein.

The *Rauzy renormalization* [R] gives a satisfying renormalization theory for the family of IETs all having the same number of intervals in the partition. The idea is that one starts with an n -interval IET, and then considers the first return map to a specially chosen sub-interval. This first return map turns out to give another n -interval IET. This mechanism sheds a lot of light on IETs. Some examples of polygon exchange maps have been studied in [AG], [AKT], [H], [Hoo], [LKV], [Low], [S2], [S3], and [T]. Some definitive theoretical work concerning the (zero) entropy of such systems is done in [GH1], [GH2], and [B].

Often, renormalization phenomena are found in these systems: The first return to some subset is conjugate to the original system, and this allows for a detailed understanding of the system. In [S1] and [Hoo], a renormalizable family of polygon exchange maps is constructed. In this setting, like in Rauzy renormalization, the first return map to a subset of one system is conjugate to the first return map of another system in the family. The family in [Hoo] is 2-dimensional and the family in [S1] is 1-dimensional.

In [S1] we introduced a class of PETs which we called *double lattice PETs*. See §2 for a definition. These PETs are defined in terms of a pair of Euclidean lattices, and in each dimension there is a large space of them. We originally found (some of) the double lattice PETs as compactifications of polygonal outer billiards systems, but it seems reasonable to study these objects for their own sake. One motivation for studying these objects is to search for good examples of renormalization schemes for families of higher dimensional PETs.

In this paper we introduce a family of double lattice PETs in every even dimension. In dimension $2n$, the objects are indexed by $GL_n(\mathbf{R})$. In the two-dimensional setting, there is a 1-parameter family. In this paper we will study the 1-parameter family of 2-dimensional examples in detail, showing that it has a complete renormalization scheme. The $(2, 4, \infty)$ reflection triangle group acts on the parameter space, and points in the same orbit have closely related dynamics - e.g., their limit sets have the same Hausdorff dimension.

1.2 The Planar Construction

We will describe the $2n$ -dimensional examples systematically in §2.2. Here we explain the 2-dimensional case in a visual way. Our construction depends on a parameter $s \in (0, \infty)$. Usually, but not always, we take $s \in (0, 1)$. Below we suppress s from most of our notation.

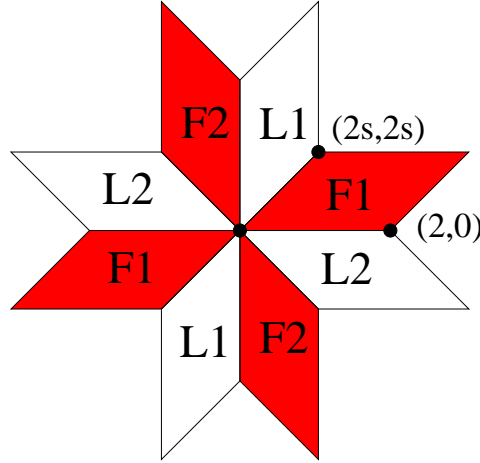


Figure 1.1: The scheme for the PET.

The 8 parallelograms in Figure 1.1 are the orbit of a single parallelogram P under a dihedral group of order 8. Two of the sides of P are determined by the vectors $(2, 0)$ and $(2s, 2s)$. For $j = 1, 2$, let F_j denote the parallelogram centered at the origin and translation equivalent to the ones in the picture labeled F_j . Let L_j denote the lattice generated by the sides of the parallelograms labeled L_j . (Either one generates the same lattice.)

In §2 we will check the easy fact that F_i is a fundamental domain for L_j , for all $i, j \in \{1, 2\}$. We define a system (X', f') , with $X' = F_1 \cup F_2$, and $f' : X' \rightarrow X'$, as follows. Given $p \in F_j$ we let

$$f'(p) = p + V_p \in F_{3-j}, \quad V_p \in L_{3-j}. \quad (1)$$

The choice of V_p is almost always unique, on account of F_{3-j} being a fundamental domain for L_{3-j} . When the choice is not unique, we leave f' undefined. When $p \in F_1 \cap F_2$ we have $V_p = 0 \in L_1 \cap L_2$. We will show in §2 that (X', f') is a PET.

We prefer the map $f = (f')^2$, which preserves both F_1 and F_2 . We set $X = F_1$. Our system is $f : X \rightarrow X$, which we denote by (X, f) .

1.3 The Tiling and the Limit Set

We define a *periodic tile* for (X, f) as a maximal convex polygon on which f and its iterates are completely defined and periodic. So, every point in a periodic tile has the same period and every periodic point is contained in a nontrivial periodic tile. We call the union Δ of the periodic tiles the *tiling*.

We define the *aperiodic set* Λ to be the set of aperiodic points of f . The aperiodic set is a subset of a somewhat more natural set which we call the *limit set* and denote by $\hat{\Lambda}$. The set $\hat{\Lambda}$ is the set of weakly aperiodic points. We call a point $p \in X$ *weakly aperiodic* if there is a sequence $\{q_n\}$ converging to p with the following property. The first iterates of f are defined on q_n and the points $f^k(q_n)$ for $k = 1, \dots, n$ are distinct. When Δ is dense (and it turns out that this always happens for our system) we can say alternately that $\hat{\Lambda}$ consists of those points p such that every neighborhood of p intersects infinitely many tiles of Δ . See Lemma 8.3. One advantage $\hat{\Lambda}$ has over Λ is that $\hat{\Lambda}$ is compact.

Figures 1.2 and 1.3 show (approximations of) Δ and $\hat{\Lambda}$ for two quadratic irrational parameters. In Figure 1.2, the picture is the same (locally) as what one sees for outer billiards on the regular octagon. In Figure 1.3, $\hat{\Lambda}$ is the union of two curves (though we do not give a proof in this paper). Isometric copies of these curves arise in Pat Hooper's system [Hoo]. Hooper and I plan to explore this "coincidence" later.

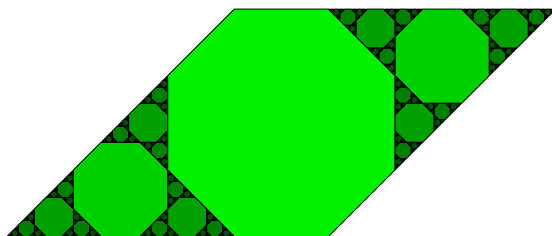


Figure 1.2: The tiling associated to $s = \sqrt{2}/2$

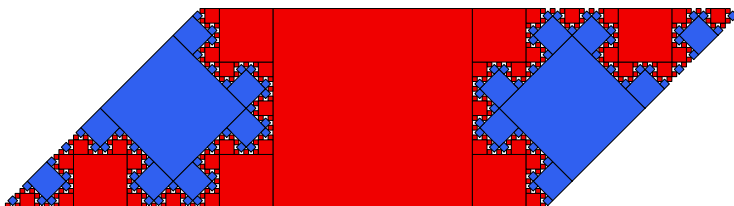


Figure 1.3: The tiling associated to $s = \sqrt{3}/2 - 1/2$.

Here are some results about the tiling.

Theorem 1.1 *When s is rational, Δ_s is a finite union of squares, semi-regular octagons, and right-angled isosceles triangles. When s is irrational, Δ_s is an infinite union of squares and semi-regular octagons. Moreover, the following is true.*

1. Δ_s has at least one square unless $s = \sqrt{2}/2$.
2. Δ_s has only squares if and only if the continued fraction expansion of s has the form $[a_0, a_1, a_2, a_3, \dots]$ where a_k is even for all odd k .
3. Δ_s has infinitely many squares and a dense set of shapes of semi-regular octagons, for almost all s .

A *semi-regular octagon* is an octagon with 8-fold dihedral symmetry. Theorem 1.1 is a corollary of a more precise statement about Δ_s , Theorem 1.4 below. We defer the statement of Theorem 1.4 because it requires a build-up of terminology.

Here are some results about the limit set and the aperiodic set. We only care about the irrational case. These sets are empty when s is rational. See Lemma 2.4.

Theorem 1.2 *Suppose s is irrational.*

1. $\widehat{\Lambda}_s$ has zero area.
2. The projection of $\widehat{\Lambda}_s$ onto a line parallel to any 8th root of unity contains a line segment. Hence $\widehat{\Lambda}_s$ has Hausdorff dimension at least 1.
3. $\widehat{\Lambda}_s$ is not contained in a finite union of lines.
4. $\widehat{\Lambda}_s - \Lambda_s$ has zero length for almost all s . Hence Λ_s has Hausdorff dimension at least 1 for almost all s .

Remark: In §8.5 we prove a more precise result about when $\widehat{\Lambda}_s - \Lambda_s$ has zero length.

The results above are consequences of the renormalization properties of the family $\{(X_s, f_s) \mid s \in (0, 1)\}$. We explain this next.

1.4 Renormalization

We define the *renormalization map* $R : (0, 1) \rightarrow [0, 1)$ as follows.

- $R(x) = 1 - x$ if $x > 1/2$
- $R(x) = 1/(2x) - \text{floor}(1/(2x))$ if $x < 1/2$.

R relates to the $(2, 4, \infty)$ reflection triangle much in the way that the classical Gauss map relates to the modular group.

Define

$$Y = F_1 - F_2 = X - F_2 \subset X. \quad (2)$$

For any subset $S \subset X$, let $f|S$ denote the first return map to S , assuming that this map is defined. When we use this notation, it means implicitly that the map is actually defined, at least away from a finite union of line segments. We call S *clean* if no point on ∂S has a well defined orbit. This means, in particular, that no tile of Δ crosses over ∂S .

Theorem 1.3 (Main) *Suppose $s \in (0, 1)$ and $t = R(s) \in (0, 1)$. There is a clean set $Z_s \subset X_s$ such that $f_t|Y_t$ is conjugate to $f_s^{-1}|Z_s$ by a map ϕ_s .*

1. ϕ_s commutes with reflection in the origin and maps the acute vertices of X_t to the acute vertices of X_s .
2. When $s < 1/2$, the restriction of ϕ_s to each component of Y_t is an orientation reversing similarity, with scale factor $s\sqrt{2}$.
3. When $s < 1/2$, either half of ϕ_s extends to the trivial tile of Δ_t and maps it to a tile in Δ_s .
4. When $s < 1/2$, the only nontrivial orbits which miss Z_s are contained in the ϕ_s -images of the trivial tile of Δ_t . These orbits have period 2.
5. When $s > 1/2$ the restriction of ϕ_s to each component of Y_s is a translation.
6. When $s > 1/2$, all nontrivial orbits intersect Z_s .

The Main Theorem is an example of a result where a picture says a thousand words. Figures 1.4 and 1.5 show the Main Theorem in action for $s < 1/2$. Figures 1.6 and 1.7 show the Main Theorem in action for $s > 1/2$.

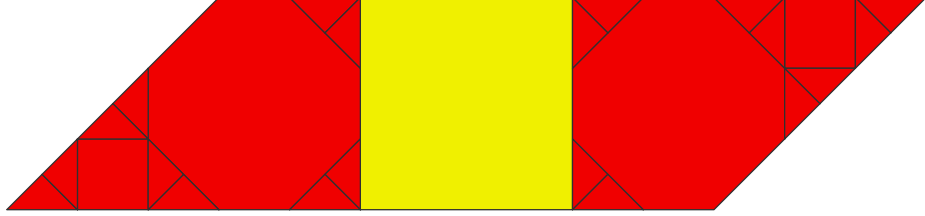


Figure 1.4: Y_t in red for $t = 3/10 = R(5/13)$.

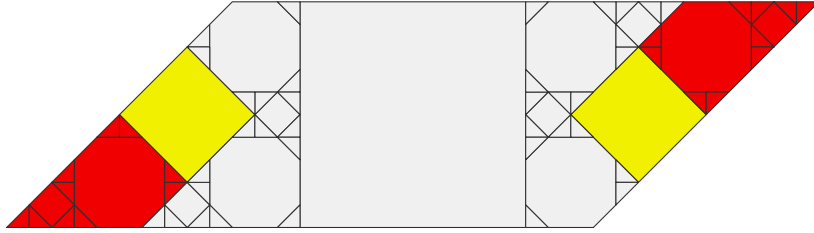


Figure 1.5: Z_s in red $s = 5/13$.

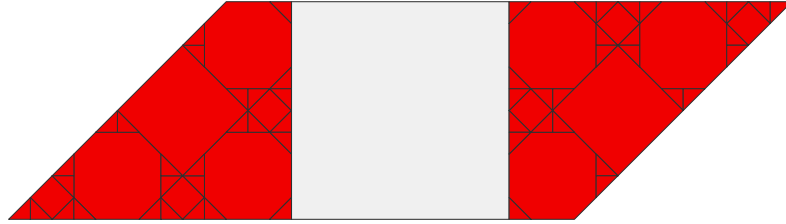


Figure 1.6: Y_t in red for $t = R(8/13) = 5/13$.

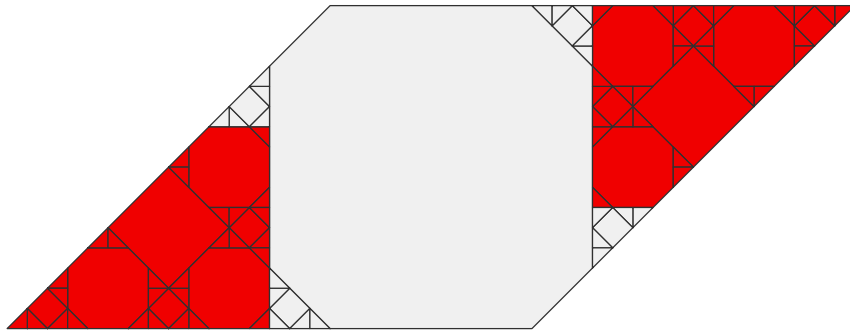


Figure 1.7: Z_s in red for $s = 8/13$.

Now we explain the result behind Theorem 1.1. When $s > 1/2$, the intersection

$$O_s = (F_1)_s \cap (F_2)_s \quad (3)$$

is the semi-regular octagon with vertices

$$(\pm s, \pm(1-s)), \quad (\pm(1-s), \pm s). \quad (4)$$

When $s < 1/2$, the intersection O_s is the square with vertices $(\pm s, \pm s)$.

Suppose we fix some irrational $s = s_0 \in (0, 1)$. Let $s_n = R^n(s)$. Let T_0 be the identity map and, referring to the Main Theorem, let T_n be the linear part of the composition

$$\phi_{s_0} \circ \dots \circ \phi_{s_{n-1}}. \quad (5)$$

The map T_n is a similarity whose exact nature can be computed using the information given in the Main Theorem.

Theorem 1.4 *When $s \in (0, 1)$ is irrational, a polygon arises in Δ_s if and only if it is translation equivalent to $T_n(O_{s_n})$ for some $n = 0, 1, 2, \dots$*

Remark: When s is rational, we get a very similar result, except that Δ_s also contains some right-angled isosceles triangles. See Lemma 6.1.

1.5 Hyperbolic Symmetry

Let $\mathbf{H}^2 \subset \mathbf{C}$ denote the upper half plane model of the hyperbolic plane. Let Γ denote the $(2, 4, \infty)$ reflection triangle group, generated by reflections in the sides of the hyperbolic triangle with vertices

$$\frac{i}{\sqrt{2}}, \quad \frac{1}{2} + \frac{i}{2}, \quad \infty. \quad (6)$$

We extend our parameter range so that our system is defined for all $s \in \mathbf{R}$. The systems at s and $-s$ are identical. Γ acts on the parameter set by linear fractional transformations.

We call the two systems (X_s, f_s) and (X_t, f_t) *locally equivalent* if the following is true. There is a finite union L of lines such that, for each point $p_s \in \widehat{\Lambda}_s - L$, there is a point $p_t \in \widehat{\Lambda}_t$, together with open neighborhoods U_s and U_t of p_s and p_t respectively, such that $\Delta_s \cap U_s$ is equivalent to $\Delta_t \cap U_t$ by a similarity. We also require the same statement to be true with the roles of s and t reversed.

Local equivalence is strong: For instance, the limit sets of locally equivalent systems have the same Hausdorff dimension.

Theorem 1.5 *Suppose s and t are in the same orbit of Γ . Then (X_s, f_s) and (X_t, f_t) are locally equivalent. In particular, the Hausdorff dimension of the limit set, as a function of the parameter, is a Γ -invariant function.*

Remarks:

- (i) Γ is contained with index 4 in the group generated by reflections in the ideal triangle with vertices $0, 1, \infty$. Using this fact, together with a classic result about continued fractions, we will show that the forward orbit $\{R^n(s)\}$ is dense in $(0, 1)$ for almost all $s \in (0, 1)$.
- (ii) The need to exempt a finite union of lines in the definition of local equivalence seems partly to be an artifact of our proof, but in general one needs to disregard some points to make everything work.
- (iii) Given the ergodic nature of the action of Γ , we can say that there is some number δ_0 such that $\dim(\widehat{\Lambda}_s) = \delta_0$ for almost all s . However, we don't know the value of δ_0 .

1.6 Further Results and Claims

This paper now has a sequel [S0]. Here is the main result of that paper.

Theorem 1.6 *Let $s \in (0, 1)$ be irrational.*

1. $\widehat{\Lambda}_s$ is a disjoint union of two arcs if and only if Δ_s contains only squares.
(This happens if and only if $R^n(s) < 1/2$ for all n .)
2. $\widehat{\Lambda}_s$ is a finite forest if and only if Δ_s contains finitely many octagons.
(This happens if and only if $R^n(s) > 1/2$ for finitely many n .)
3. $\widehat{\Lambda}_s$ is a Cantor set if and only if Δ_s contains infinitely many octagons.
(This happens if and only if $R^n(s) > 1/2$ for infinitely many n .)

It turns out that our system here is intimately related to outer billiards on semi-regular octagons. Recall that O_s is the octagon from Equation 4.

Claim 2: *For any $s \in (1/2, 1)$, the limit set and periodic tiling produced by outer billiards on O_s are locally isometric to $\widehat{\Lambda}_s$ and Δ_s , respectively, except at finitely many points.*

This claim is amply supported by computer evidence, and I basically know how to prove it. I hope to prove this claim in a sequel paper.

1.7 Organization

This paper is organized as follows. In §2 we will define our PETs in every even dimension and give some basic information about them.

In §3 we prove some basic results about our PETs, most of which have to do with the stability of orbits under the perturbation of the parameter.

In §4 we prove some symmetry results about our PETs, modulo 2 computer calculations.

In §5 we prove the Main Theorem, modulo 6 more computer calculations.

In §6 we prove Theorem 1.4 and Theorem 1.1.

In §7 we deduce some length and area estimates for the limit set.

In §8 we prove Theorem 1.5 and Theorem 1.2.

In §9 we will do the 8 calculations left over from §4-5. These are exact integer arithmetic calculations.

In §10 we list the raw data needed for the calculations done in §9.

1.8 OctaPET

This paper has a companion java program, called *OctaPET*. I discovered practically everything in the paper while developing and using this program. Also, the calculations mentioned in §9 are all done using OctaPET. I encourage you to use OctaPET while reading the paper. OctaPET relates to this paper much like a song relates to musical notes written on a page. You can download OctaPET from

<http://www.math.brown.edu/~res/Java/OCTAPET.tar>

This is a tarred directory, which untars to a directory called OctaPET. This directory contains a java program which you can compile and then run.

1.9 Acknowledgements

I would like to thank Nicolas Bedaride, Pat Hooper, Injee Jeong, John Smillie, and Sergei Tabachnikov for interesting conversations about topics related to this work. Some of this work was carried out at ICERM in Summer 2012, and some was carried out during my sabbatical in 2012-13. This sabbatical was funded from many sources. I would like to thank the National Science Foundation, All Souls College, Oxford, the Oxford Maths Institute, the Simons Foundation, the Leverhulme Trust, and Brown University for their support during this time period.

2 The Examples

2.1 Double Lattice PETs

Generalizing the construction made in the introduction, we will define what we mean by a double lattice PET. The input to an n -dimensional double lattice PET is a quadruple (L_1, L_2, F_1, F_2) , where

- L_1 and L_2 are lattices in \mathbf{R}^n .
- F_1 and F_2 are parallelotopes.
- F_i is a fundamental domain for L_j for all $i, j \in \{1, 2\}$.

Given (F_1, F_2, L_1, L_2) we have a PET defined on $X' = F_1 \cup F_2$ as follows. For each $x \in F_i$ we define (if possible) $f'(x) = x + V_x$, where $V_x \in F_{3-i}$ is the unique vector such that $x + V_x \in F_{3-i}$. It may happen that V_x is not uniquely defined. In these cases, we leave f undefined. Note that $V_x = 0 \in L_1 \cap L_2$ when $x \in F_1 \cap F_2$, so that our definition is not ambiguous for such points.

Lemma 2.1 (X', f') is a PET.

Proof: First, we check that f is invertible. The inverse map $(f')^{-1}$ is defined just as f' is defined, but with the roles of L_1 and L_2 reversed: For each $x \in F_i$ we define (if possible) $f'(x) = x + W_x$, where $W_x \in F_i$ is the unique vector such that $x + W_x \in F_{3-i}$.

The set X' is partitioned as follows. Let $U \subset X'$ denote the set of points for which the assignment $p \rightarrow V_p$ is defined. The set $X' - U$ is contained in a finite union of hyperplanes. Let $U' \subset X'$ denote the complement of these hyperplanes. Then U' is a finite union of convex polytopes which partitions X' .

The assignment $p \rightarrow V_p$ is constant on each component of U' . Hence $V' = f'(U')$ is also a finite union of polytopes. But construction, the polytopes in V' have disjoint interior, and their union has full measure. Hence V' is a second partition of X' . The two partitions U' and V' determine f in the manner of a PET. ♠

As in the introduction, it is convenient to set $f = (f')^2$ and $X = F_1$. Then (X, f) is also a PET, and the domain of f is the parallelotope X .

2.2 Basic Construction

In this section we construct examples of double lattice PETs in every even dimension. To describe the examples in a natural way, it is useful to work in \mathbf{C}^n , complex n -space. Note, however, that when it comes time to do calculations in the case of interest, \mathbf{C} , we will revert to working in \mathbf{R}^2 .

Let J denote multiplication by i . Consider the following totally real subspaces

$$H = \{(z_1, \dots, z_n) \mid \Im(z_j) = 0 \ \forall j\} \quad D = \{(z_1, \dots, z_n) \mid \Im(z_j) = \Re(z_j) \ \forall j\}. \quad (7)$$

H and D respectively are the fixed point sets of the reflections

$$R_H(z_1, \dots, z_n) = (\bar{z}_1, \dots, \bar{z}_n) \quad R_D(z_1, \dots, z_n) = (i\bar{z}_1, \dots, i\bar{z}_n). \quad (8)$$

Clearly $J = R_D \circ R_H$.

Let $\{H_1, \dots, H_n\}$ and $\{D_1, \dots, D_n\}$ be any \mathbf{R} -bases for H and D respectively. Let F_1 be the parallelogram centered at the origin, whose sides are spanned by the vectors $\{H_1, \dots, H_n, D_1, \dots, D_n\}$. We let $F_2 = J(F_1)$. Since $J^2 = -I$, and F_j is centrally symmetric, we have $J(F_2) = F_1$.

We let L_1 be the lattice spanned by the vectors

$$H_1, \dots, H_n, R_H(D_1), \dots, R_H(D_n).$$

We let L_2 be the lattice spanned by the vectors

$$D_1, \dots, D_n, R_D(H_1), \dots, R_D(H_n).$$

Lemma 2.2 $J(L_1) = L_2$ and $J(L_2) = L_1$.

Proof: Since $J^2 = -\text{Identity}$, we have $J^2(L_j) = L_j$ for $j = 1, 2$. So, it suffices to prove that $J(L_1) = L_2$. We have

$$J(H_j) = R_D R_H(H_j) = R_D(H_j) \in L_2,$$

$$J(R_H(D_j)) = R_D R_H R_H(D_j) = R_D(D_j) = D_j \in L_2.$$

This does it. ♠

In the next result we will use the notation of \mathbf{C}^n but we point out in advance that our argument only uses the \mathbf{R} -structure of \mathbf{C}^n .

Lemma 2.3 F_1 is a fundamental domain for both L_1 and L_2 .

Proof: The proof works the same way for both L_1 and L_2 . So, we will just prove that F_1 is a fundamental domain for L_1 . Let L'_1 denote the lattice generated by the sides of F_1 . A \mathbf{Z} -basis for L'_1 is $\{H_1, \dots, H_n, D_1, \dots, D_n\}$. Let $L''_1 \subset L_1 \cap L'_1$ be the \mathbf{Z} -span of $\{H_1, \dots, H_n\}$.

Note that L_1 and L'_1 have the same co-volume, by symmetry. But the volume of F_1 coincides with the co-volume of L'_1 . Hence, the volume of F_1 coincides with the co-volume of L_1 . To finish the proof we just have to show the following: For any $p \in \mathbf{C}^n$ there is some vector $V \in L_1$ such that $p + V \in F_1$.

Let $\pi : \mathbf{C}^n \rightarrow H^\perp$ be orthogonal projection. The kernel of π is exactly H . Moreover, $\pi(F_1)$ is a fundamental domain for $\pi(L'_1)$ in H^\perp . However $\pi(L_1) = \pi(L'_1)$. So, $\pi(F_1)$ is a fundamental domain for $\pi(L_1)$ as well. Since $\pi(L_1)$ is a fundamental domain for $\pi(F_1)$, there is some $V_1 \in L_1$ such that the translate H' of H , through $p + V_1$, intersects F_1 .

Since F_1 is a parallelotope which intersects H in a parallelotope, the intersection $H' \cap F_1$ is isometric to $H \cap F_1$, and hence is a fundamental domain for L''_1 . Hence, there is some $V_2 \in L''_1$ such that $p + V_1 + V_2 \in F_1$. But $V = V_1 + V_2 \in L_1$. So, $p + V \in F_1$. This proves what we want. ♠

Since J swaps F_1 with F_2 and also swaps L_1 with L_2 , the preceding lemma shows that F_i is a fundamental domain for L_j for all $i, j \in \{1, 2\}$. Now we know that the quadruple (F_1, F_2, L_1, L_2) defines a double lattice PET. We imagine that these higher dimensional examples are interesting, but so far the 2-dimensional case is hard enough for us.

Remark: In our examples, both F_1 and F_2 are centered at the origin. One can define a PET without this property, but some computer experimentation suggests that the character of the PET is much different when F_1 and F_2 are not centered at the origin. In the 2-dimensional example, which is the only one we've looked at, these "exotic" examples all have limit sets which contain open sets. That is, there are aperiodic orbits which are dense in open sets. Indeed, in the 2 dimensional example, this seems to happen for every placement of F_1 and F_2 except for the case when they have a common center (which we might as well take as the origin.)

2.3 The Moduli Space

We keep the notation from the previous section. Let $M \in GL_n(\mathbf{R})$ denote any invertible real $n \times n$ matrix. Note that M commutes with both R_H and R_D . In particular $M(H) = H$ and $M(D) = D$. The system (F_1, F_2, L_1, L_2) is conjugate to the system $(M(F_1), M(F_2), M(L_1), M(L_2))$. So, up to conjugacy, we might as well consider systems in which $\{H_1, \dots, H_n\}$ is the standard basis for \mathbf{R}^n .

We can specify one of our PETs by giving a lattice $\mathbf{s} \subset D$. In case $n = 1$, the lattice \mathbf{s} is 1 dimensional and generated by its shortest vector $s + is$. Identifying \mathbf{C} with \mathbf{R}^2 , this shortest vector becomes (s, s) . For later convenience, we scale everything by a factor of 2, and this gives us the same collection of objects as discussed in connection with Figure 1.1.

We can always take $s \in (0, 1)$ because the case $s > 1$ can be reduced to the case $s \in (0, 1)$ by interchanging the roles of D and H . More precisely, the two parameters s and $s' = 1/(2s)$ give rise to conjugate systems. We will formalize this idea in §4, in the Inversion Lemma. Technically, we could take $s \in (0, \sqrt{2}/2)$, but this further restriction is not convenient to us.

Fixing n , let \mathcal{F} denote the set of PETs which arise from our construction in \mathbf{C}^n . It seems worth pointing out that \mathcal{F} contains a natural collection of rational points. These correspond to taking \mathbf{s} as a sub-lattice of $(\mathbf{Q}[i])^n$. We call such systems rational. In case $n = 1$, this just amounts to taking $s \in \mathbf{Q}$. Here is an easy observation.

Lemma 2.4 *For any rational system, all the orbits are periodic.*

Proof: Let $G = (\mathbf{Z}[i])^n$ be the usual lattice of Gaussian integers. We can conjugate a rational system by a dilation so that $L_1, L_2 \subset G$ and also the vertices of F_1 and F_2 belong to G .

Letting (X, f) denote the associated PET, we observe that all the points in an orbit of f differ from each other by vectors of G . Moreover, such orbits are bounded. Hence, they are finite. ♠

Consider the 2-dimensional case, setting $s = p/q$. In this case, we can dilate so that $H_1 = q$ and $H_2 = p + ip$. Then F_1 and F_2 have volume $(pq)^2$. In this case, the maximum period of any point in the system is $(pq)^2$.

3 Stability and Limiting Considerations

3.1 Intersection of the Lattices

For the rest of the paper, we will consider the case $n = 1$ discussed in the previous chapter. We will work in \mathbf{R}^2 . Our main goals in this chapter are the Stability Lemma and the Convergence Lemma, stated below.

Lemma 3.1 *If s is irrational, then $L_1 \cap L_2 = 0$.*

Proof: L_1 is the \mathbf{Z} -span of $(2, 0)$ and $(2s, -2s)$. and L_2 is the \mathbf{Z} -span of $(0, 2)$ and $(2s, 2s)$. If this lemma is false, then we can find an equation of the form

$$(A + Bs, Bs) = (D, C + D). \quad (9)$$

for integers A, B, C, D . This forces

$$s = \frac{A}{D - B} = \frac{-C}{B + D}, \quad (10)$$

which is only possible if s is rational. ♠

We say that (X, f) is *sharp* if, for any vector V , the sets

$$\{p \mid f(p) = p + V\} \quad (11)$$

are open and convex. The issue is that such a set, if nonempty, might be a finite union of open convex polygons. The systems (X_s, f_s) are not sharp for $s = 1/n$ and $n = 2, 3, 4, \dots$

Lemma 3.2 *Suppose that $s \in [1/4, 1]$. Then (X_s, f_s) is sharp unless $s = 1/n$ for $n = 1, 2, 3, 4$.*

Proof: we first observe that (X_s, f_s) has the following property for all s . Suppose we specify a pair of vectors $(V_1, V_2) \in L_1 \times L_2$. Then the set of points

$$S(V_1, V_2) = \{p \in F_1 \mid p + V_2 \in F_2, p + V_1 + V_2 \in F_1\}$$

is always convex: It is the intersection of 3 parallelograms. So, if (X_s, f_s) is not sharp, then we can find vectors $(V_1, V_2) \in L_1 \times L_2$ and $(V'_1, V'_2) \in L_1 \times L_2$ such that

- $S(V_1, V_2)$ and $S(V'_1, V'_2)$ are both nonempty,
- $V_1 + V_2 = V'_1 + V'_2$
- $(V_1, V_2) \neq (V'_1, V'_2)$.

In this situation, we get a relation like the one in Equation 9.

Both L_1 and L_2 have a standard basis. Let $\{v_{j1}, v_{j2}\}$ be the standard basis for L_j . For instance $v_{11} = (2, 0)$ and $v_{12} = (2s, -2s)$. Since $s \geq 1/4$, the vectors V_j and V'_j must be fairly short. Specifically, we have

$$V_1 = av_{11} + bv_{12}, \quad |a| \leq 1 \quad |b| \leq 2. \quad (12)$$

Similar bounds hold for the other vectors. This means that the relation in Equation 9 satisfies

$$\max(|A|, |C|) \leq 2, \quad \min(|B + D|, |B - D|) \leq 4.$$

But then Equation 10 forces $s = p/q$ where $q \leq 4$. This leaves only the cases $s = 1/n$ for $n = 1, 2, 3, 4$. ♠

Let $p \in X$ be a periodic point of period n . We define the *displacement list* of p to be the list of vectors V_1, \dots, V_n so that

$$f^k(p) = p + \sum_{i=1}^k V_i, \quad k = 1, \dots, n. \quad (13)$$

Corollary 3.3 *Suppose $s \in [1/4, 1]$ and s does not have the form $1/n$ for $n = 1, 2, 3, 4$. Then the set of periodic points in X_s having the same period and displacement list is a single tile of Δ_s .*

.

Proof: We check the result by hand for $s = 1/n$, $n = 1, 2, 3, 4$. For the remaining parameters, the system is sharp, and the set in question is the intersection of n convex polygons. ♠

Remark: In Corollary 4.5, we promote Lemma 3.2 and Corollary 3.3 to results about all $s \in (0, 1)$.

3.2 The Arithmetic Graph

Suppose that $p_0 \in X$ is some point on which the orbit of f is well defined. Call this orbit $\{p_i\}$. There are unique vectors $V_i \in L_1$ and $W_i \in L_2$ such that

$$f'(p_i) = p_i + V_i, \quad f'(p_i + V_i) = p_i + V_i + W_i = p_{i+1}.$$

We call the sequence $\{(V_i, W_i)\}$ the *symbolic encoding* of the orbit. We define the *arithmetic graph* to be the polygon whose i th vertex is $V_0 + \dots + V_i$. We define the *conjugate arithmetic graph* to be the polygon whose i th vertex is $W_0 + \dots + W_i$.

Remark: The displacement list is determined from the arithmetic graph, but the reverse is not *a priori* true. One way to interpret Corollary 3.3 (and the more general Corollary 4.5) is that, unless $s = 1/n$, we can determine the graph from the displacement list.

We hope to explain the structure of the arithmetic graphs associated to systems such as these in a later paper. In this paper, we are mainly interested in using the graph to detect when an orbit is stable under perturbation of the parameter.

Lemma 3.4 (Stability) *If s is irrational and p is a periodic point of f , then both the arithmetic graph of p is a closed polygon.*

When the orbit is periodic, of period n , we have

$$\sum_{i=1}^n (V_i + W_i) = 0. \tag{14}$$

We can re-write this as

$$\sum_{i=1}^n V_i = - \sum_{i=1}^n W_i.$$

But then the common sum belongs to $L_1 \cap L_2$. When s is irrational, Lemma 3.1 then tells us that

$$\sum_{i=1}^n V_i = 0, \quad \sum_{i=1}^n W_i = 0. \tag{15}$$

These two equations are equivalent to the lemma. ♠

3.3 Convergence Properties

We say that a sequence of (solid) polygons P_n converges to a (solid) polygon P_∞ if the sequence converges in the *Hausdorff metric* on the set of compact sets. Concretely, for every $\epsilon > 0$ there should be an N such that $n > N$ implies that every point of P_n is within ϵ of P_∞ and *vice versa*. In the next lemma, we write $\Delta_\infty = \Delta_{s_\infty}$ and $\Delta_n = \Delta_{s_n}$ for ease of notation.

Lemma 3.5 (Approximation) *Let $s_\infty \in (0, 1)$ be irrational, and let $\{s_n\}$ be a sequence of rationals converging to s_∞ . Let P_∞ be a tile of Δ_∞ . Then for all large n there is a tile P_n of Δ_n such that $\{P_n\}$ converges to P_∞ .*

Proof: For any object A that depends on a parameter, we let $A(n)$ denote the object corresponding to the parameter s_n .

Let $p \in P_\infty$ be a periodic point of period N . Let $\{(V_i(\infty), W_i(\infty))\}$ be the symbolic encoding of the orbit. The lattice $L_j(n)$ converges to the lattice $L_j(\infty)$. So, we can uniquely choose vectors $V_i(n) \in L_1(n)$ and $W_i(n) \in L_2(n)$ which converge respectively to $V_i(\infty)$ and $W_i(\infty)$.

By the Stability Lemma, $\sum_{i=1}^N V_i(\infty) = 0$. Hence $\sum_{i=1}^N V_i(n) \rightarrow 0$ as $n \rightarrow \infty$. But, independent of n , there is some ϵ so that the ϵ balls centered on lattice points of $L_1(n)$ are disjoint. This shows that $\sum_{i=1}^N V_i(n) = 0$ for large n . The same argument works with W in place of V . For n large, the symbolic encoding of p starts out

$$V_1(n), W_1(n), \dots, V_N(n), W_N(n).$$

But then p is a periodic point of period N for n large, and the above list is the whole symbolic encoding. In short, p is a periodic point of the same period relative to f_n as it is relative to f_∞ . Let P_n denote the periodic tile containing p .

The size of n required for this continuity argument depends only on the distance from p to ∂P_∞ . For this reason, P_∞ is contained in the ϵ neighborhood of P_n for n sufficiently large. On the other hand, if q lies just outside P_∞ , the symbolic encoding of q relative to f_∞ differs from the symbolic encoding of p relative to f_∞ . But then, by continuity, the same goes for large n in place of ∞ . This shows that P_n is contained in an arbitrarily small neighborhood of P_∞ , once n is sufficiently large.

Putting everything together, we see that $\{P_n\}$ converges to P_∞ , as desired. ♠

4 Symmetry

4.1 Rotational Symmetry

In this chapter we discuss the symmetry of the system (X_s, f_s) . We begin with an obvious result. Define

$$\iota(x, y) = (-x, -y) \quad (16)$$

Note that $\iota(X) = X$ for every parameter.

Lemma 4.1 (Rotation) *ι and f_s commute for all $s \in (0, 1)$.*

Proof: ι preserves F_1, F_2, L_1 , and L_2 . For this reason ι commutes with f . ♠

The subsets of Δ_s and Λ_s lying to the right of the central tiles are reflected images of the subsets of Δ_s and Λ_s lying to the left of the central tiles. For this reason, we will usually consider the picture just on the left hand side.

4.2 Inversion Symmetry

As we have already remarked, we usually take the parameter s to lie in $(0, 1)$ but we can define all the objects for any $s \in (0, \infty)$.

Lemma 4.2 (Inversion) *(X_t, f_t) and (X_s, f_s) are conjugate if $t = 1/2s$.*

Proof: An easy calculation shows that there is a similarity $\phi : R_t \rightarrow R_s$ which maps the horizontal (respectively diagonal) side of R_t to the diagonal (respectively horizontal) side of R_s .

We denote F_1 , at the parameter s , by F_1^s . We make similar notations for the other parameters. We already know that $\phi(F_1^t) = F_1^s$. Let J be rotation by $\pi/2$ clockwise. The map ϕ conjugates J to J^{-1} . For this reason, we have $\phi(F_j^t) = F_j^s$ and $\phi(L_j^t) = L_j^s$ for $j = 1, 2$. This does it. ♠

Lemma 4.2 is really the source of the renormalization map R . However, Lemma 4.2 does not directly apply to our situation. Let's consider the situation in some detail. Let $\rho(s) = 1/2s$. The map ρ is an involution of the parameter interval $[1/2, 1]$. However, the Main Theorem requires us to use the map $R(s) = 1 - s$ on this interval. When $s \in 1/2$ we have $R(s) = t_1$ and $\rho(s) = t_2$, where $t_1 = t_2 - k$, where k is the integer such that $t_2 - k \in (0, 1]$. However, it is not yet clear that the two systems at t_1 and t_2 are related.

4.3 Insertion Symmetry

When $s \in (1/2, 1)$, the intersection $F_1 \cap F_2$ is an octagon, which we call the *central tile*. When $s \leq 1/2$ or $s \geq 1$, the intersection $F_1 \cap F_2$ is a square. This square generates a grid in the plane, and finitely many squares in this grid lie in $X = F_1$. We call these squares the *central tiles*. See Figure 4.1.

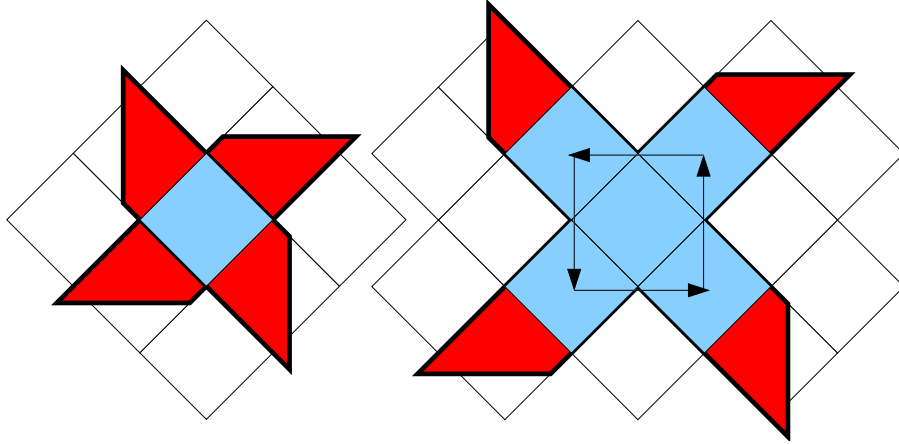


Figure 4.1: The central tiles (blue) for $s = 5/4$ and $t = 9/4$.

Let X^0 denote the portion of X which lies to the left of the central tiles. The set $\iota(X^0)$ is the portion of X which lies to the right of the central tiles. The union $X^0 \cup \iota(X)$ is an f -invariant set.

Lemma 4.3 (Insertion) *Suppose $s \geq 1$ and $t = s + 1$, or suppose $s \leq 1/2$ and $t = s/(2s + 1)$. The restriction of f_s to $X_s^0 \cup \iota(X_s^0)$ is conjugate to the restriction of f_t to $X_t^0 \cup \iota(X_t^0)$. The conjugacy is a piecewise similarity.*

Proof: The case when $s < 1/2$ is equivalent to the case $s > 1$ by the Inversion Lemma. So, we will take $s > 1$ and $t = s + 1$.

We consider how X_s and X_t sit relative to the grid of diamonds mentioned above. When $s, t > 1$, the squares in the grid are diagonals of length 2. Significantly, the diagonals of the diamonds are parallel to the vectors $(\pm 2, 0) \in L_1$ and $(0, \pm 2) \in L_2$. This is true independent of the parameters. There are two more diamonds contained in X_t than there are in X_s . On the central tile, the map f has the obvious action shown in Figure 4.1.

The sets X_s^0 and X_s^t have the same relative position relative to the diamond grid, and there is an obvious translation carrying the one set to the

other. This translation extends to give piecewise translation from the complement of the diamonds in X_s to the complement of the diamonds in X_t . Call points related by this piecewise translation *partners*

Let $p_s \in X_s^0$ and $p_t \in X_s^t$ be partners. Let λ_s and λ_t respectively be the vectors in $(L_2)_s$ and $(L_2)_t$ such that $p_s + \lambda_s \in (F_2)_s$ and $p_t + \lambda_t \in (F_2)_t$. We have either $\lambda_s = \lambda_t + (2, 0)$ or $\lambda_s = \lambda_t + (0, 2)$, depending on whether or not $p_s + \lambda_s$ and $p_t + \lambda_t$ lie in the top or bottom of $(F_2)_s$ and $(F_2)_t$ respectively. The answer (top/bottom) is the same for s as it is for t . In short, the two new points $p_s + \lambda_s$ and $p_t + \lambda_t$ are again partner points. Repeating this construction again, we see that $f_s(p_s)$ and $f_t(p_t)$ are partner points. This is what we wanted to prove. ♠

Remark: Informally, what Insertion Lemma says is that, for $s \geq 1$, the tiling Δ_{s+1} is obtained from the tiling Δ_s by inserting two new large diamonds.

Lemma 4.4 Δ_s consists entirely of squares and right-angled isosceles triangles when $s = 1, 2, 3, \dots$ and when $s = 1/2, 1/4, 1/6, \dots$

Proof: We check this for $n = 1$ just by a direct calculation. See Figure 4.2.

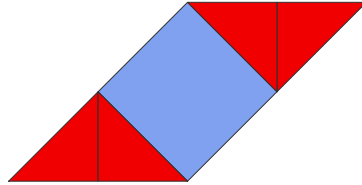


Figure 4.2: The tiling Δ_s for $s = 1$.

The cases $n = 2, 3, 4, \dots$ now follow from the Insertion Lemma. The cases $n = 1/2, 1/4, 1/6, \dots$ follow from the cases $n = 1, 2, 3, \dots$ and the Inversion Lemma. ♠

Combining the Insertion Lemma with Lemmas 3.2 and Corollary 3.3, we have

Corollary 4.5 *Let $s \in (0, 1)$. Suppose s does not have the form $1/n$ for $n = 1, 2, 3, \dots$. Then (X_s, f_s) is clean, and the set of periodic points in X_s having the same period and displacement list is a single tile of Δ_s .*

4.4 Bilateral Symmetry

In this section we always take $s \in (0, 1)$. We say that a line L is a *line of symmetry* for Δ_s if

$$\Delta_s \cap (X_s \cap \rho(X_s)) \quad (17)$$

is invariant under the reflection ρ in L . Note that X_s itself need not be invariant under L .

Figure 4.3 shows 3 lines. H is the line $y = 0$ and V is the line $x = -1$ and D_s is the line of slope -1 through the bottom vertex of the leftmost central square of Δ_s .

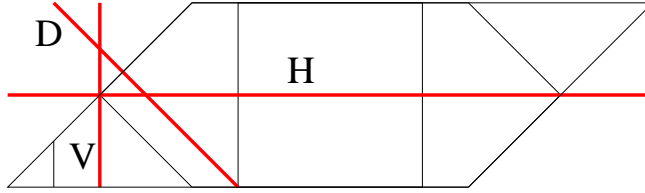


Figure 4.3 H and V and D_s for the parameter $s = 2/5$.

In this section we will prove (modulo 2 finite calculations) the following result.

Lemma 4.6 (Bilateral) *For all $s \in (0, 1)$, the lines H , V , and D_s are lines of symmetry of Δ_s .*

We will prove this result through a series of smaller lemmas.

Define

$$A = X \cap \rho_H(X), \quad B = X \cap \rho_V(X). \quad (18)$$

Here ρ_H is the reflection in H and ρ_V is the reflection in V . A is the green hexagon shown in Figure 4.4. The complement $X - A$ consists of two triangles, B and $\iota(B)$ as shown in Figure 4.4.

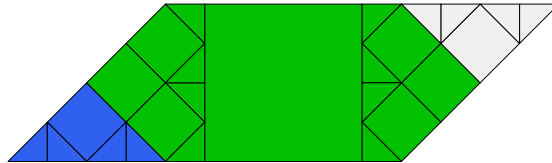


Figure 4.4 A_s (green) and B_s (blue) and $\iota(B_s)$ (white) for $s = 2/5$.

Each of the pieces A , B and $\iota(B)$ has a vertical line of bilateral symmetry. The reflections across these vertical lines gives rise to a piecewise isometry of X . We call this map μ . If $p \in A$ we define $\mu(p)$ to be reflection in the vertical line of symmetry for A , etc.

The Insertion Lemma allows us to turn many infinite-appearing calculations into finite calculations. The problem with trying to compute something for every parameter in $(0, 1)$ is that the number of domains of continuity for the map f_s tends to ∞ as $s \rightarrow 0$. However, if we restrict our attention to $s \in [1/4, 1)$, then there is a uniform bound on the number of regions of continuity. In this range, we can establish identities using a finite calculation. The picture for any parameter $s < 1/4$ is the same as some picture for $s' > 1/4$, up to the insertion of finitely many central tiles. In §9 we prove the following result by direct calculation.

Lemma 4.7 (Calculation 1) *If $s \in [1/4, 1]$ then $\mu_s \circ f_s \circ \mu_s = f_s^{-1}$ wherever both maps are defined.*

Combining this calculation with the Insertion Lemma, we have

Corollary 4.8 *Suppose $s \in (0, 1)$ then $\mu_s \circ f_s \circ \mu_s = f_s^{-1}$ wherever both maps are defined.*

Proof of Statements 1 and 2: Now we prove Statements 1 and 2 of the Bilateral Lemma. Using the rotational symmetry, it suffices to prove that $\Delta \cap A$ and $\Delta \cap B$ are invariant under the action of μ . We will consider the situation in the Hexagon A . The situation in the other regions has a similar treatment.

Let τ be a tile of Δ that is contained in A . All iterates of f are defined on the interior of τ . Let n be the order of f on the interior of τ . The first n iterates of $\mu f \mu$ are defined on an open set $\tau' = \tau - L$. Here L is a finite union of line segments. For each $p \in \tau'$, the period of $\mu f \mu$ on p is n . Since μ is everywhere defined in the interior of A , we see that f^{-1} is defined on all points of $\mu(\tau')$. But all the points in $\mu(\tau')$ have the same displacement list. Hence $\mu(\tau')$ is convex. This is only possible if $\tau' = \tau$. ♠

Define

$$P = X \cap \rho_D(X), \quad Q = X^0 - P. \quad (19)$$

When $s < 1/2$, the set P_s is a pentagon and Q_s is an isosceles triangle. When $s > 1/2$, the set P_s is a triangle and Q_s is empty. Figures 4.5 shows the case $s < 1/2$.

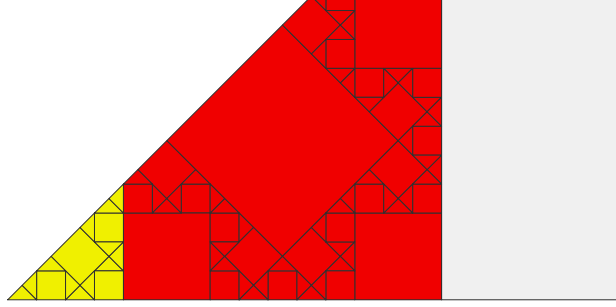


Figure 4.5: P_s (red) and Q_s (yellow) for $s = 11/30$.

X_s is partitioned into square central tiles and the additional tiles P_s , Q_s , $\iota(P_s)$ and $\iota(Q_s)$. (When $s > 1/2$, the tiles Q_s and $\iota(Q_s)$ do not exist.) Each tile in this partition has reflection symmetry, in a line of slope -1 . Let $\nu_s : X_s \rightarrow X_s$ be the piecewise isometry which does this reflection on each piece.

In §9 we prove the following result by direct calculation.

Lemma 4.9 (Calculation 2) *If $s \in [1/4, 1]$, then $\nu_s \circ f_s \circ \nu_s = f_s^{-1}$ wherever both maps are defined.*

Combining this calculation with the Insertion Lemma, we have

Corollary 4.10 *If $s \in (0, 1)$ then $\nu_s \circ f_s \circ \nu_s = f_s^{-1}$ wherever both maps are defined.*

Proof of Statement 3: Statement 3 of the Bilateral Lemma is deduced from Corollary 4.10 in the same way that Statements 1 and 2 are deduced from Corollary 4.8. ♠

5 Proof of the Main Theorem

5.1 Discussion and Overview

The Inversion Lemma and the Insertion Lemma go part of the way towards proving the Main Theorem. These two results say that the systems (X_s, f_s) and (X_t, f_t) are related, in the appropriate sense, for pairs $(s, 1/2s)$ and, assuming $s > 1$, for pairs $(s, s - 1)$. These results are not strong enough to establish the Main Theorem. For instance, when $s = 2/5$ we have $R(s) = 1/4$. We can say that the parameters $2/5$ and $5/4$ are related by Condition 1 above. However, Condition 2 does not apply to $(s, t) = (1/4, 5/4)$ because $s < 1$. Similarly, if $s = 3/4$ we have $R(s) = 1/4$. Here, neither condition applies.

The reader might wonder why we care about R in the first place. Perhaps we can prove all the corollaries to the Main Theorem just with the limited symmetries we have already established. The virtue of R is that, for every rational parameter p/q , one of the two iterates $R(p/q)$ or $R^2(p/q)$ has denominator smaller than q . Thus, the map R gives us an inductive mechanism for understanding our system at all rational values. Once we have a good understanding of what happens at rational values, we can take limits. We cannot do this much with just the two conditions listed above.

Referring to Theorem 1.5, the existence of Γ sheds light on what we have said above. The way we prove the Main Theorem, roughly speaking, is to verify certain facts on the generators of Γ , by computation or symmetry, and then use the group structure to extract global statements about the renormalization map R . What we are saying, in a sense, is that we haven't checked *enough* of Γ yet. What is missing is a statement about what happens for pairs $(s, s - 1)$ with $s \in (1, 2)$ and for pairs $(s, 1 - s)$ with $s \in (1/2, 1)$.

Here are the two results we prove in this chapter. The first is equivalent to the half of the Main Theorem corresponding to $s \in (0, 1/2)$.

Lemma 5.1 *Suppose $s \in (1, 2)$ and $t = s - 1$. Let $\phi_s : Y_t \rightarrow X_s$ be the map which is a translation on each half of Y_t and maps the acute vertices of Y_t to the acute vertices of X_s . Let $Z_s = \phi_s(Y_t)$. Then ϕ_s conjugates $f_t|_{Y_t}$ to $f_s|_{Z_s}$, and Z_s is a clean set. Either half of ϕ_s extends to the trivial tile of Δ_t and maps it to tiles τ_1 and τ_2 . The only nontrivial f_s -orbits which miss Z_s are contained in $\tau_1 \cup \tau_2$ and have period 2.*

Our other result is just a restatement of the half of the Main Theorem corresponding to $s \in (1/2, 1)$.

Lemma 5.2 *Suppose $s \in (1/2, 1)$ and $t = 1 - s$. Let $\phi_s : Y_t \rightarrow X_s$ be the map which is a translation on each half of Y_t and maps the acute vertices of Y_t to the acute vertices of X_s . Let $Z_s = \phi_s(Y_t)$. Then ϕ_s conjugates $f_t|_{Y_t}$ to $f_s^{-1}|_{Z_s}$, and Z_s is a clean set. All nontrivial f_s -orbits intersect Z_s .*

To be sure, let's deduce the Main Theorem from these results.

Proof of the Main theorem: Lemma 5.2 is just a restatement of the Main Theorem for $s \in (1/2, 1)$. Suppose that $s < 1/2$. By the Insertion Lemma, it suffices to consider the case when $s \in (1/4, 1/2)$. By the Inversion Lemma, the system (X_s, f_s) is conjugate to the system (X_t, f_t) , where $t = 1/2s$. Here $t \in (1, 2)$. But now Lemma 5.1 applies to the pair $(t, t - 1)$ and $t - 1 = R(s)$. When we combine the conjugacy given by the Inversion Lemma with the one given by Lemma 5.1, we get the statement of the Main Theorem. ♠

We would like to have conceptual proofs of Lemmas 5.1 and 5.2, but we do not. Instead, we will give computational proofs. The difficulty in giving a computational proof is that it seems to involve an infinite amount of calculation. Consider, for instance, what happens in Lemma 5.1 as $s \rightarrow 1$. In this case, the area of Y_t tends to 0. But then, the proportion of X_s taken up by Z_s tends to 0. But then the amount of time it takes for some orbits to return to X_s probably tends (and, in fact, does tend) to ∞ . This makes a direct computer verification difficult. A similar problem happens for Lemma 5.2 as $t \rightarrow 1$.

In §9 we will prove the following results by a direct and finite calculation.

Lemma 5.3 (Calculation 3) *Lemma 5.1 holds for all $t \in [5/4, 2]$.*

Lemma 5.4 (Calculation 4) *Lemma 5.2 holds for all $t \in [1/2, 3/4]$.*

The trick is to relate the system on the intervals $[1/2, 3/4]$ and $[5/4, 2]$ to the larger intervals $[1/2, 1)$ and $(1, 2]$. We will do this by establishing some auxilliary symmetry results. One can view these auxilliary results as statements about some of the other elements in the group Γ .

5.2 First Modular Symmetry

Define the maps

$$T(s) = \frac{s-2}{2s-3}, \quad \omega_s(x, y) = (3-2s)(x, y) \pm (2-2s, 0). \quad (20)$$

We take $s \in (1, 4/3]$, so that $u = T(s) \in (1, 2]$. The domain of ω_s is the set Y_u from the Main Theorem. The (+) option for ω_s is taken when $x < 0$ and the (-) option is taken then $x > 0$. We set $W_s = \omega_s(Y_u)$. A picture says a thousand words. In the picture W_s^0 is the left half of W_s and Y_u^0 is the left half of Y_u .

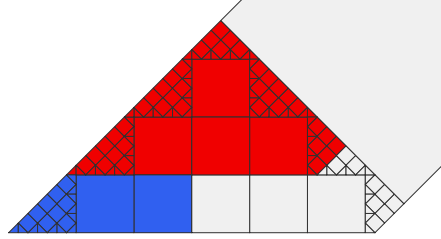


Figure 5.1: $\Delta_s \cap W_s^0$ (red) for $s = 22/19$.

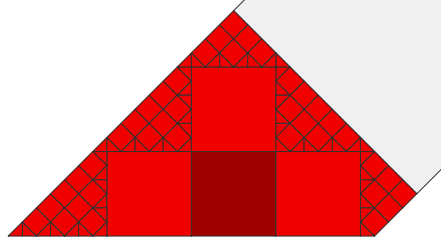


Figure 5.2: $\Delta_u \cap Y_u^0$ (red) for $u = T(22/19) = 16/13$.

Lemma 5.5 (Calculation 5) *Let $s \in (1, 4/3]$ and $u = T(s)$. Then ω_s conjugates $f_u|Y_u$ to $f_s|W_s$. Moreover, Z_s is a clean set.*

Remarks:

- (i) As a corollary, we see that ω_s maps $\Delta_u \cap Y_u^0$ to $\Delta_s \cap W_s^0$. This explains why the tilings in the red regions in Figures 5.1 and 5.2 look the same.
- (ii) We only need Calculation 5 for $s \in (1, 5/4]$, but it is more convenient to make the calculation on the larger interval.

The blue set in Figure 5.1 is isometric the left half of Y_{s-1} . We denote this set by Z_s^0 and we set $Z_s = Z_s^0 \cup \iota(Z_s)$. Here ι is reflection in the origin. We let τ denote the square whose left side coincides with the right side of Z_u^0 . The square τ_u is a darker red than the others in Figure 5.1. We define τ_s just as we defined τ_u , with s in place of u . Let δ_s be the vector which spans the diagonal of τ_s , pointing from the bottom left vertex to the top right vertex.

Lemma 5.6 (Calculation 6) *Let $s \in (1, 5/4]$, so that $u = T(s) \in (1, 3/2]$. Then*

1. τ_u is a tile of Δ_u , having period 2.
2. $f_s^{-1}(p) = p + \delta_s$ for all $p \in Z_s^0$.
3. $f_s^{-1}(X_s - Z_s - W_s) \subset Z_s \cup \tau_s \cup \iota(\tau_s)$.

We will establish these results in §9. Calculation 6 really just amounts to inspecting the partitions for f_u and f_s .

5.3 Proof of Lemma 5.1

Let T be the map from Equation 20.

Lemma 5.7 *Let $s \in (1, 5/4)$ be any point. Then there is some positive k such that $T^k(s) \in (5/4, 3/2)$.*

Proof: T is a parabolic linear fractional transformation fixing 1 and having the property that $T(5/4) = 3/2$. So, the iterates $T^j(s)$, $j = 1, 2, 3, \dots$ are increasing, but then cannot avoid the interval $(5/4, 3/2)$. ♠

Lemma 5.1 follows immediately from Lemma 5.7 and from the following result.

Lemma 5.8 *If Lemma 5.1 is true for some $u \in (1, 3/2)$, then Lemma 5.1 is also true for $s = T^{-1}(u)$.*

The rest of this section is devoted to proving Lemma 5.8. Let $s' = s - 1$ and $u' = u - 1$. A calculation shows that

$$s' = \frac{u'}{2u' + 1}. \quad (21)$$

In other words, s' and u' are related exactly as in the Insertion Lemma. So, the dynamics relative to s' is the same as the dynamics relative to u' , except that two more central squares are inserted for s' . These central squares have period 2. We need to establish the same relation between $f_u|_{Z_u}$ and $f_s|_{Z_s}$.

Define

$$Z_u^* = Z_u \cup \tau_u \cup \iota(\tau_u). \quad (22)$$

We are augmenting Z_u by inserting two period-2 squares at the two ends of Z_u . Statement 1 of Calculation 6 guarantees that these extra squares really are tiles of Δ_u .

Lemma 5.9 *There is a piecewise homothety h_s which carries Z_u^* to Z_s and respects the tilings Δ_u and Δ_s .*

Proof: By Statement 2 of Calculation 6, and rotational symmetry, the piecewise similarity

$$h_s = f_s \circ \omega_s \quad (23)$$

maps Z_u^* to Z_s . Thanks to Statement 1 of Calculation 6, the tile τ_u and its rotated image are really tiles of Δ_u . Thanks to Calculation 5, the map h_s maps the tiling $Z_u^* \cap \Delta_u$ to the tiling $Z_s \cap \Delta_s$. ♠

Lemma 5.10 *h_s conjugates $f_u|_{Z_u^*}$ to $f_s|_{Z_s}$.*

Proof: Choose some point $r_1 \in Z_u^*$. Let $p_1 = h_s(r_1) \in Z_s$. Let p_n be the first return of the forward f_s -orbit of p_1 to Z_s . So, p_2, \dots, p_{n-1} do not belong to Z_s . Define

$$q_j = f_s^{-1}(p_j), \quad j = 1, n. \quad (24)$$

By Statement 2 of Calculation 6, we have $q_n \in \omega_s(Z_u^*)$. Define

$$r_n = \omega_s^{-1}(q_n). \quad (25)$$

By Calculation 5, the point r_n lies in the forward f_u -orbit of r_1 . To finish our proof, we just have to show that r_n is the first return of this orbit to Z_u^* . If this is false, then there is some earlier point $r_k \in Z_u^*$. But then $h_s(r_k) = q_m \in Z_s$ for some $m = 2, \dots, (n-1)$. This is a contradiction. ♠

Lemma 5.11 *Any nontrivial f_s -orbit, except those contained in $\tau_s \cup \iota(\tau_s)$, intersects Z_s .*

Proof: Consider first the orbit of a point $p \in W_s$. Let $q = \omega_s^{-1}(p)$. Since the Main Theorem is true for the parameter u , the orbit of q intersects Z_u^* . But then, by Calculation 5, the orbit of q intersects $\omega_s(Z_u^*) = f_s^{-1}(Z_s)$. But then $f_s(q) \in Z_s$.

It remains to consider the orbit of a point $p \in X_s - Z_s - W_s$. If $p \in \tau_s \cup \iota(\tau_s)$, there is nothing to prove. Otherwise, Statement 3 of Calculation 6 finishes the proof. ♠

5.4 The Second Modular Symmetry

Now we turn our attention to the proof of Lemma 5.2. We re-use some of the notation from the other case. Define

$$T = \frac{3x-2}{2x-1}, \quad \omega_s(x, y) = (2s-1)(x, y) \pm (2s-2). \quad (26)$$

T here is the inverse of the one in Equation 20. We take $s \in [3/4, 1)$, so that $u = T(s) \in [1/2, 1)$. The domain of ω_s is the set Y_u from the Main Theorem. The (+) option for ω_s is taken when $x < 0$ and the (−) option is taken then $x > 0$. We set $W_s = \omega_s(Y_u)$.

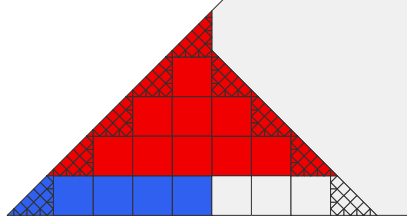


Figure 5.3: Half of W_s^0 for $s = 28/31$.

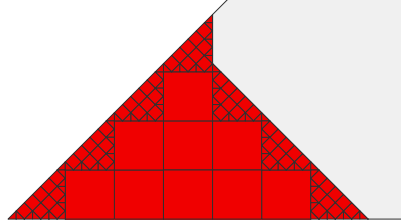


Figure 5.4: $\Delta_u \cap X_u^0$ for $u = T(28/31) = 22/25$.

The rest of the definitions are done exactly as in the previous section. The main difference here is that the tile τ_s and τ_u belong to Z_s and Z_u respectively. As above, δ_s is the vector which spans the diagonal of τ_s , pointing from the bottom left vertex to the top right vertex. Calculation 7 is the calculation parallel to Calculation 5.

Lemma 5.12 (Calculation 7) *Let $s \in [3/4, 1)$ and $u = T(s)$. Then ω_s conjugates $f_u|Y_u$ to $f_s|W_s$. Moreover, Z_s is a clean set.*

Calculation 8 is the calculation parallel to Calculation 6. Notice that there are some differences. Item 1 of Calculation 6 refers to τ_u . We will discuss the reason for this difference below. Item 2 of Calculation 8 refers to the modified set

$$(Z_s^0)^* = Z_s^0 - \tau_s. \quad (27)$$

We have to chop off the tile τ_s to make the statement true. Also, f_s appears in Item 2 of Calculation 8 whereas f_s^{-1} appears in Item 2 of Calculation 6. Item 3 is a slightly different statement, but the new statement works the same way in the proof of Lemma 5.11.

Lemma 5.13 (Calculation 8) *Let $s \in [3/4, 1)$. Then*

1. τ_s is a tile of Δ_s , having period 2.
2. $f_s(p) = p + \delta_s$ for all $p \in (Z_s^0)^*$.
3. $f_s(X_s - Z_s - W_s) \subset Z_s^*$.

5.5 Proof of Lemma 5.2

Let T be the map from Equation 26.

Lemma 5.14 *Let $s \in (3/4, 1)$ be any point. Then there is some positive k such that $T^k(s) \in (1/2, 3/4)$.*

Proof: Same proof as Lemma 5.7. ♠

The rest of the proof of Lemma 5.2 is like what we did for Lemma 5.1, but there are some small differences. First of all, this time we know that τ_s is a tile of Z_s , so all the nontrivial orbits intersect Z_s .

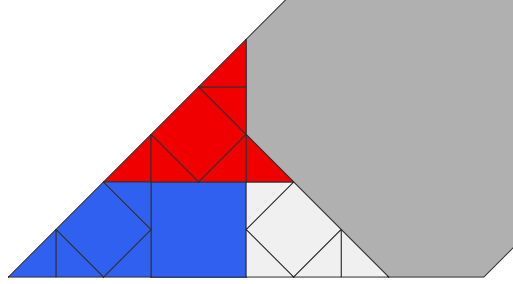


Figure 5.5: Half of W_s for $s = 4/5$.

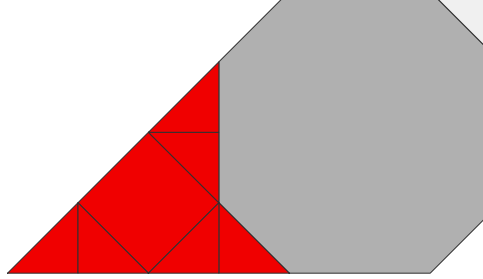


Figure 5.6: $\Delta_u \cap X_u^0$ for $u = 2/3$.

When $s \in [3/4, 5/6)$ and $u \in [1/2, 3/4)$ the tile τ_u does not exist. Figures 5.5 and 5.6 show the example of $s = 4/5$ and $u = 2/3$. However, we define

$$Z_s^* = (Z_s^0)^* \cup \iota((Z_s^0)^*) = Z_s - \tau_s - \iota(\tau_s). \quad (28)$$

and we use the pair (Z_s^*, Z_u) in place of the pair (Z_s, Z_u^*) . Making these changes, Lemmas 5.9, 5.10, and 5.11 go through without a problem.

6 Properties of the Tiling

6.1 The Rational Case

Even though we mainly care about the irrational case of Theorem 1.4, we find it convenient to prove the analogous result for the rational case. When $s = 1/2n$ we define

$$\phi_s(x, y) = \left(\frac{x}{2n}, \frac{y}{2n} \right). \quad (29)$$

This is a new definition, because the Main Theorem does not apply for $s = 1/2n$. When $s = 0$, we slightly abuse notation and define O_s to be (simultaneously) each of the 4 isosceles triangles having vertices $(0, 0)$ and $(\pm 1, \pm 1)$.

Lemma 6.1 *When $s \in (0, 1)$ is rational, a polygon arises in Δ_s if and only if it is translation equivalent to $T_n(O_{s_n})$ for some n .*

Proof: Our proof goes by induction on the value of n such that $T^n(s) = 0$.

Consider the base case. This corresponds to $s = 1/2n$, $n = 1, 2, 3, \dots$. For $s = 1/2$, we check that Δ_s consists of $O_{1/2}$ and each of the 4 triangles O_0 scaled down by a factor of 2. When $a = 1/2n$, we apply the Insertion Lemma and verify that the 4 triangles in $\Delta_{1/2n}$ have sizes consistent with the statement that they are translates of $T_0(O_0)$.

The general case follows from induction. Let $s = s_0$. By the Main Theorem, a tile appears in Δ_{s_0} if and only if it is either $O_{s_0} = T_0(O_{s_0})$ or if it is translation equivalent to a tile of the form

$$\phi_{s_0}(\sigma),$$

where σ is a tile of Δ_{s_1} . By induction, σ is translation equivalent to the tile

$$\phi_{s_1} \circ \dots \circ \phi_k(O_k),$$

for some k . Hence, τ is translation equivalent to the tile

$$\phi_{s_0} \circ \dots \circ \phi_k(O_k).$$

Conversely, all such tiles appear in Δ_{s_0} , by the same induction argument. ♠

6.2 The Irrational Case

Now we prove Theorem 1.4.

Let s be some irrational parameter. First of all, the argument in Lemma 6.1 applies *verbatim* to show that the a translate of the tile

$$T_k(O_u), \quad u = R^k(s)$$

does indeed appear in Δ_s . The argument is simply induction on k , combined with the Main Theorem.

We need to prove the converse, showing that these are the only tiles that appear in Δ_s when s is irrational. Let $\{{}_n s\}$ be a sequence of rationals converging to s .

P be a tile of Δ_s . By Lemma 3.5, we can find a tile ${}_n P$ of $\Delta_{{}_n s}$ such that ${}_n P \rightarrow P$ as $n \rightarrow \infty$. By Lemma 6.1, there is an integer k_n such that ${}_n P$ is translation equivalent to some tile of the form

$${}_n T_{k_n}(O_{u_n}), \quad u_n = R^{k_n}({}_n s).$$

Here ${}_n T_{0,n} T_{1,n} T_{2,n} \dots$ are the maps which arise in Lemma 6.1 relative to the parameter ${}_n s$.

Now, the scale factor of ${}_n T_k$ tends to 0 with k , and ${}_n P$ has uniformly large diameter. Therefore, the integer k_n is uniformly bounded from above. So, passing to a subsequence, we can assume that ${}_n k$ is independent of n . That is, P_n is a translation of

$${}_n T_k(O_{u_n}), \quad u_n = R^k({}_n s). \tag{30}$$

But

- ${}_n T_k \rightarrow T_k$,
- $u_n \rightarrow u = R^k(s)$,
- $O_{u_n} \rightarrow O_u$.

Hence P is a translate of $T_k(O_u)$.

The rest of this chapter is devoted to proving Theorem 1.1.

6.3 Existence of Square Tiles

Here we prove Statement 1 of Theorem 1.1. We will suppose that $s \neq \sqrt{2}/2$ and show that Δ_s has a square tile. We will first suppose that s is irrational.

Lemma 6.2 *Suppose that s and $t = R(s)$ lie in $(0, 1)$. If Δ_t has a non-central square tile, then so does Δ_s .*

Proof: By the Main Theorem, Δ_s has a similar copy of every non-central tile of Δ_t , and these similar copies are themselves non-central. ♠

Lemma 6.3 *Suppose that s is irrational. If $R^n(s) < 1/2$ for some even n , then Δ_s has a square tile.*

Proof: We choose n to be as small as possible. If $n = 0$ then $s < 1/2$ and the central tile of Δ_s is square. Suppose $n \geq 2$. Let $t = R^{n-2}(s)$ and $u = R^{n-1}(s)$ and $v = R^n(s)$. We know that $v < 1/2$. If $u > 1/2$ then $t < 1/2$, contradicting the minimality of n . So, $u < 1/2$. But then we apply the Main Theorem to the pair $(u, R(u))$ and conclude that some non-central tile of Δ_u is a square. Now we apply Lemma 6.2 repeatedly to conclude that Δ_s has a non-central square tile. ♠

Lemma 6.4 *Suppose that s is irrational. If $R^n(s) < 1/4$ for some odd n , then Δ_s has a square tile.*

Proof: If $n = 0$ then Δ_s has a central square tile. So, assume that $n > 0$. Let $t = R^{n-1}(s)$ and $u = R^n(s)$. Since $u < 1/4$, the tiling Δ_u has at least 3 central tiles, one of which is contained in the set $Y_t \subset \Delta_u$. But then $Z_t \subset \Delta_t$ contains a non-central square tile. Repeated applications of Lemma 6.2 finish the proof. ♠

Lemma 6.5 *Suppose that s is irrational and Δ_s has no square tiles. Then $s = \sqrt{2}/2$.*

Proof: We know that $R^n(s) > 1/2$ for every even n and $R^n(s) \in (1/4, 1/2)$ for every odd n . If $R^n(s) \in (1/3, 1/2)$ for some odd n , then $R^{n+1}(s) < 1/2$, because R maps $(1/3, 1/2)$ onto $(0, 1/2)$. Hence $R^n(s) \in (1/4, 1/3)$ for all odd n .

For $x \in (1/4, 1/3)$ we have the formula

$$R(x) = \frac{1}{2x} - 1 \quad (31)$$

Hence, if $x > 1/2$ and $R(x) \in (1/4, 1/3)$ we have

$$R^2(x) = \frac{1-2x}{-2+x} = Mx, \quad M = \begin{bmatrix} -\sqrt{2} & 1/\sqrt{2} \\ \sqrt{2} & -\sqrt{2} \end{bmatrix}. \quad (32)$$

Here M acts as a linear fractional transformation. Iterating, we have

$$R^{2n}(s) = M^n(s). \quad (33)$$

The map M , acting as a linear fractional transformation, fixes $\pm\sqrt{2}/2$ and is expanding in a neighborhood of $\sqrt{2}/2$. We conclude that there is some n such that $M^n(s) < 0$ unless $s = \sqrt{2}/2$. Since we never have $N^n(s) < 0$ we must have $s = \sqrt{2}/2$. ♠

Lemma 6.6 *If s is rational, the Δ_s has a square tile.*

Proof: The proof is the same as in the irrational case, except we have to worry about what happens if $R^n(s) \in \{1/4, 1/3, 1/2\}$ for some odd n . If $R^n(s) = 1/4$ for some odd n , then the same argument as in Lemma 6.4 applies. The point is that $\Delta_{1/4}$ still has 3 central square tiles.

If $R^n(s) = 1/2$ for some odd n , then $R^{n-1}(s) < 1/2$. But then the argument in Lemma 6.5 applies to the even iterate $R^{n-1}(s)$.

If $R^n(s) = 1/3$ for some odd n , then $R^{n+1}(s) = 1/2$. But then the argument in Lemma 6.5 applies to the even iterate $R^{n+1}(s)$. because $\Delta_{1/2}$ still has a central square tile. ♠

Putting together the last several lemmas, we finish the proof that Δ_s has a square tile as long as $s \neq \sqrt{2}/2$.

6.4 The Case of Squares

Here we prove Statement 2 of Theorem 1.1. We compare the map R with the *Gauss map*

$$\gamma(s) = 1/s - \text{floor}(1/s) \quad (34)$$

Lemma 6.7 *Let $s = [0, a_1, a_2, a_3, \dots]$ be the continued fraction expansion of s . Suppose that a_1 is even. Then $s, R(s) < 1/2$ and $R^2(s) = \gamma^2(s)$.*

Proof: Let $x = 1/s$. We write

$$x = a_1 + \frac{1}{a_2 + 1/y}.$$

The continued fraction expansion of $1/y$ is $[0, a_3, a_4, \dots]$. Hence $1/y = \gamma^2(s)$. Note, in particular, that $1/y < 1$. We need to show that $R^2(s) = 1/y$.

Since $a_1 > 1$, we have $s < 1/2$. Hence

$$R(s) = 1/(2s) - \text{floor}(1/(2s)) = x/2 - \text{floor}(x/2).$$

We have

$$x/2 = (a_1/2) + \frac{1}{2a_2 + 2/y}. \quad (35)$$

Hence

$$R(s) = \frac{1}{2a_2 + 2/y} < 1/2.$$

Since $R(s) < 1/2$ we have

$$R^2(s) = (a_2 + 1/y) - \text{floor}(a_2 + 1/y) = 1/y,$$

as desired. ♠

Let $[a_0, a_1, a_2, a_3, \dots]$ be the continued fraction expansion for s . We call s *oddly even* if s is irrational and a_k is even for all odd k . When $s \in (0, 1)$ we have $a_0 = 0$.

Lemma 6.8 *Let $s \in (0, 1)$ be irrational. Then s is oddly even if and only if $R^k(s) \in (0, 1/2)$ for all k .*

Proof: Suppose that s is oddly even. By the previous result, s and $R(s)$ lie in $(0, 1/2)$ and $R^2(s)$ is again oddly even. Hence $R^2(s)$ and $R^3(s)$ lie in $(0, 1/2)$ and $R^4(s)$ is oddly even. And so on.

Conversely, suppose that s is not oddly even. Applying Lemma 6.7 finitely many times if necessary, we reduce to the case where the first term in the continued fraction expansion of s is odd. If $s > 1/2$ we are done. Otherwise, s lies in one of the intervals $(1/3, 1/2)$, $(1/5, 1/4)$, $(1/7, 1/6)$, ..., and R maps each of these intervals onto $(1/2, 1)$. So $R(s) > 1/2$ in this case. Hence, if $R^k(s) \in (0, 1/2)$ for all k , then s is oddly even. ♠

Lemma 6.8 combines with Theorem 1.4 to prove Statement 2 of Theorem 1.1 in case $s \in (0, 1)$. But the case $s > 1$ now follows from the Inversion Lemma and from the fact that the map $x \rightarrow 1/(2x)$ preserves the set of oddly even numbers.

6.5 The Density of Shapes

Now we prove Statement 3 of Theorem 1.1. This result follows immediate from Theorem 1.4 and from the following lemma.

Lemma 6.9 *For almost all $s \in (0, 1)$, the orbit $\{R^n(s)\}$ is dense in $(0, 1)$.*

We will prove Lemma 6.9 through a series of smaller lemmas. We start with a classic result. See [BKS] for instance.

Lemma 6.10 *Almost every orbit of the Gauss map is dense in $(0, 1)$.*

This result has a well known geometric consequence. Let Σ_0 denote the trice-punctured sphere. Let $T_1(\Sigma)$ denote the unit tangent bundle of Σ . A geodesic in Σ_0 has a natural *lift* to the unit tangent bundle: One just keeps track of the points on the geodesic as well as their unit tangent vectors. We say that a geodesic on Σ_0 *emanates* from a cusp of Σ if one end of the geodesic is asymptotic with a cusp. The lift of such a geodesic to \mathbf{H}^2 has one endpoint on a parabolic fixed point of the surface fundamental group. There is a natural measure on the set of cusps emanating from one of the cusps of Σ_0 .

Corollary 6.11 *Almost every geodesic ray emanating from a cusp of Σ_0 lifts to a dense subset of $T_1(\Sigma_0)$.*

Proof: Let α be a geodesic emanating from a cusp of Σ_0 . By symmetry, it suffices to consider the case when some lift $\tilde{\alpha}$ of α is the vertical geodesic connecting ∞ to some $r \in (0, 1)$. The position of any given segment of $\tilde{\alpha}$ is determined, to arbitrary precision, by finite portions of the orbit of r under the Gauss map. If α is chosen so that this orbit is dense, then we can approximate any finite geodesic segment on Σ_0 , up to an arbitrarily small error, using a portion of α . ♠

Now let Σ be a finite normal covering surface of Σ_0 . That is, $\Sigma_0 = \Sigma/G$, where G is some finite group acting on Σ . There is again a natural measure on the set of geodesics emanating from a cusp of Σ .

Corollary 6.12 *Almost every geodesic ray emanating from the cusp of Σ lifts to a dense subset of $T_1(\Sigma)$.*

Proof: Let α be a geodesic emanating from our cusp of Σ . Let $\bar{\alpha}$ be the projection of α to Σ_0 . Almost every choice of α leads to $\bar{\alpha}$ having a dense lift in $T_1(\Sigma_0)$. But then the G -orbit of the lift of α is dense in $T_1(\Sigma)$. Let C be the closure of the lift of α in $T_1(\Sigma)$. We know that $G(C) = T_1(\Sigma)$. At the same time, we know that $\bar{\alpha}$ approximates, with arbitrary precision, any closed loop in Σ_0 . From this we see that in fact C is G -invariant. Hence $C = T_1(\Sigma)$, as desired. ♠

Let T be the $(2, 4, \infty)$ hyperbolic triangle generating our group Γ . One of the edges of T is contained in the geodesic circle C fixed pointwise by the map $z \rightarrow 1/(2\bar{z})$. We color C red. We color the other two edges blue. We then lift this coloring to the universal covering \mathbf{H}^2 . This gives us a pattern of geodesics that is invariant under the $(2, 4, \infty)$ triangle group. Among other colored geodesics in \mathbf{H}^2 , we have the red circle, and the blue lines connecting ∞ to half-integers.

Lemma 6.13 *Almost every geodesic emanating from the cusp of the $(2, 4, \infty)$ triangle has a billiard trajectory which hits the red edge in a dense set of points.*

Proof: We think of T as the $(2, 4, \infty)$ orbifold. There is a surface Σ (a 4-times punctured sphere) which covers T in the sense of orbifolds, and which also covers Σ_0 , the thrice punctured sphere. Say that a geodesic on Σ is good

if it emanates from a cusp of Σ and lifts to a dense set in $T_1(\Sigma)$. Almost every geodesic on T , emanating from the cusp of T , has a preimage which is a good geodesic. Hence, almost every geodesic emanating from the cusp of T has dense image in the unit tangent bundle of T . But such a geodesic would intersect each edge of T in a dense set of points. ♠

To prove that $\{R^n(s)\}$ is dense for almost every choice of $s \in (0, 1)$, it suffices to prove that $\{R^n(s)\}$ is dense for almost every choice of $s \in (0, 1/2)$. It is also useful to first consider the alternate map $R_1 : (0, 1/2) \rightarrow (0, 1/2)$, defined as follows:

- $R_1(s) = R(s)$ if $R(s) < 1/2$.
- $R_1(s) = 1 - R(s)$ if $R(s) > 1/2$.

One can describe R_1 like this. Starting with s_0 , we first reflect in the red circle C to produce the point s_1 . There is some nearest vertical blue line which separates s_1 from 0. We reflect in this blue line to produce s_2 . We now repeat these reflections in blue lines until we arrive at a point in $(0, 1/2)$, and this point is $R_1(s)$.

Each $s \in (0, 1/2)$ corresponds to a geodesic g_s of T , which emanates from the cusp. The recipe is that the lift of g_s to \mathbf{H}^2 is the geodesic connecting s to ∞ . From the description of R_1 above, we see that we can recover the action of R_1 by looking at the billiard path of g_s . The orbit $\{R^1(s)\}$ is dense provided that g_s intersects the red edge in a dense set. By Lemma 6.13, this happens for almost all $s \in (0, 1/2)$.

Knowing that $\{R_1^n(s)\}$ is dense is not quite the same as knowing the $\{R^n(s)\}$ is dense. However, there is a decomposition of the red edge of T into intervals $I_1, J_2, I_3, J_4, \dots$ such that an intersection point of g_s with I_j corresponds to a value s_k where $R_1(s_k) = R(s_k)$ and an intersection point of g_s with J_j corresponds to a value of s_k where $R_1(s_k) = 1 - R(s_k)$. In terms of billiards, the I intervals are such that g_s hits an even number of blue edges after hitting some I -interval.

The upshot of this interval decomposition is that, since g_s intersects both the I -intervals and the J -intervals densely, the orbit $\{R^n(s)\}$ is also dense.

7 Covering Results

7.1 An Area Estimate

Recall that X_s^0 is the portion of X_s to the left of the central tiles. Define

$$\lambda(s) = \frac{\text{Area}(\Delta_s \cap X_s^0)}{\text{Area}(X_s^0)}. \quad (36)$$

Lemma 7.1 (Area) *The function $\lambda(s)$ is uniformly bounded away from 0, for all $s \in (0, 1)$.*

Proof: By the Insertion Lemma, it suffices to take $s \in [1/4, 1)$. The case $s = 1/4$ is trivial, so we consider $s \in (1/4, 1)$. When s is bounded away from $1/2$ and 1 , the size of the largest square in X_s^0 is bounded away from 0 . (Figure 7.1 below shows a picture of the case when s is very near $1/4$, the other potential place to worry about.)

As $s \rightarrow 1$, the size of τ_s tends to 0 . However, the inductive argument given to prove Lemma 5.1 shows that the union of squares isometric to τ forms the following pattern. There is a bottom row of $2k + 1$ squares, then a row of $2k - 1$ squares, then a row of $2k - 3$ squares, and so on, all the way down to a single top square. When $s > 1$, the number k is such that $T^k(s) \in (5/4, 3/2)$. When $s < 1$, the number k is such that $T^k(s) \in (3/4, 5/6)$.

Technically, the argument we gave above establishes the existence of the left half of the picture (and the central column.) Combining the Inversion Lemma and the Bilateral Lemma, we see that the reflection ρ in the vertical line through the top vertex of X_s^0 maps the right half of $\Delta_s \cap X_s^0$ into the left half. This lets us deduce that the right half of X_0^s has the same pattern of squares as the left half.

As $s \rightarrow 1$, the bottom row is more and more nearly filled up with squares isometric to τ . Hence, the “triangular pile” of squares fills more and more of X_s^0 as $s \rightarrow 1$. Indeed, $\lambda(s) \rightarrow 1$ as $s \rightarrow 1$.

When $s \rightarrow 1/2$, we can again apply the Inversion Lemma to instead consider the case $s \rightarrow 1$, which we have already treated. ♠

Remark: The Area Lemma is really what is responsible for our result that $\widehat{\Lambda}_s$ always has measure 0 .

7.2 A Length Estimate

Say that a *special edge* is an edge of X_s^0 which is contained either in the bottom edge or the left edge of X_s . Let b_s and ℓ_s be the bottom and left edges of X_s^0 respectively. We will first focus on ℓ_s . When the dependence on the parameter is clear, we will set $\ell = \ell_s$ and $b = b_s$. Given a special edge E of X_s^0 , define

$$\lambda(E, s) = \frac{\text{length}(E \cap \Delta_s)}{\text{length}(E)} \quad (37)$$

This equation needs some interpretation because Δ_s , being the union of open tiles, is technically disjoint from E . What we are talking about here is the portion of E contained in edges of tiles of Δ_s .

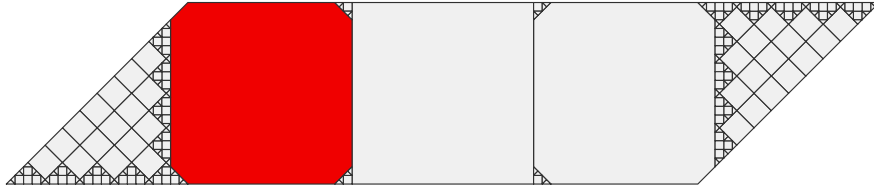


Figure 7.1 Δ_s for $s = 21/80$.

The area estimate given above has an analogue for lengths, but the result is more subtle. Figure 6.1 indicates some of the subtlety. Figure 7.1 shows the tiling for a parameter very near $1/4$. The edge ℓ is very nearly covered by the edges of square tiles, whereas the right half of b is nearly covered by the edge of a single tile and the left half meets the tiles in a jagged¹ kind of way. This “jagged edge” phenomenon is what makes our length estimate more subtle than the area estimate.

Lemma 7.2 (Length) *Let $s \in (0, 1)$. Then $\lambda(\ell, s)$ and $\lambda(b, s)$ are uniformly bounded away from 0 as long as $1/(2s) \bmod 1$ lies in a compact subset of $(0, 1)$.*

We will prove the Length Lemma through a series of smaller lemmas.

Lemma 7.3 *There is a uniform lower bound on $\lambda(\ell, s)$ for $s \in [1/4, 2/3]$.*

¹Technically, in the rational case, the special edges are completely covered by tile edges, but Figure 7.1 is supposed to suggest the kind of complicated phenomena which can arise in the irrational case.

Proof: Our analysis for the case of area gives us a uniform lower bound for (b_s, s) when $s \in [3/4, 3/2]$. By the Inversion Lemma, we get the same result for (ℓ_s, s) when $s \in [1/3, 2/3]$. So, we just have to worry about $s \in [1/4, 1/3]$.

When $s \in [1/4, 1/3]$ we have $t = R(s) > 1/2$. Let O_t be the trivial octagonal tile of Δ_t . By Statement 3 of the Main Theorem, ϕ_s extends to O_t and $\phi_s(O_t)$ has an edge in ℓ_s . As long as t is bounded away from 1, which corresponds to s being bounded away from $1/4$, there is a lower bound to the length of $\phi_s(O_t) \cap \lambda_s$. Again, we interpret O_t as a closed tile for this statement.

Consider what happens when $s \rightarrow 1/4$ from above. In this case $t \rightarrow 1$ from below. We check that Z_s nearly covers all of ℓ_s . All that is missing is a small portion of the very top of ℓ_s , coming from $\phi_s(O_t)$. See Figure 7.1. So, by the Main Theorem, and our analysis in the Area Lemma, $\lambda(\ell_s, s) \rightarrow 1$ as $s \rightarrow 1/4$ from above. ♠

Lemma 7.4 *$\lambda(\ell, s)$ is uniformly bounded away from 0 on any compact subset of $[2/3, 1)$.*

Proof: When $s = 2/3$, there is a large square diamond whose edge lies in ℓ_s . This tile is stable, as one can see from the arithmetic graph, so $\lambda(\ell, s)$ uniformly bounded away from 0 in a neighborhood of $2/3$. As long as t is bounded away from 0, the tile τ_t of Δ_t sharing a vertical edge with the trivial tile has an edge in β_s whose length is bounded away from 0. So, by the Main Theorem, we get a uniform lower bound on $\lambda(\ell_s, s)$ for $s \in (2/3, 1)$ as long as s stays away from 1. ♠

Combining the the results above, we see that $\lambda(\ell, s)$ is uniformly bounded away from 0 when $s \in (0, 1)$ is uniformly bounded away from 1. This result certainly implies the result for ℓ_s claimed in the Length Lemma. Now we turn our attention to the edge b_s .

Lemma 7.5 *There is a uniform lower bound on $\lambda(b, s)$ when s lies in a compact subset of $(1/2, 1)$.*

Proof: We have a uniform lower bound on $\lambda(\ell, s)$ for s in a compact subset of $(1/2, 1)$. Now we apply the Inversion Lemma, which maps s to $1/2s$ and switches the roles of ℓ and b . ♠

Lemma 7.6 *There is a uniform lower bound on $\lambda(b, s)$ when s lies in a compact subset of $(1/4, 1/2)$.*

Proof: Let $t = R(s) < 1$. The left edge of Y_t is all of ℓ_t . When $s \in (1/4, 1/2)$, the scale factor of ϕ_s , from the Main Theorem, is bounded uniformly away from 0. Hence, the bottom edge of Z_s is uniformly large. As long as t is bounded away from 1, the trivial tile in Δ_t has edges which take up a uniformly large fraction of the top and bottom edges of X_t . By the Main Theorem, the corresponding tile in Δ_s has a uniformly large edge in b_s . ♠

The Length Lemma for b_s now follows from the Insertion Lemma and the preceding two results.

7.3 The Covering Lemma

Let s be some parameter, and let t be some other parameter. We say that a *similar copy* of X_t^0 is a set of the form $T(X_t^0)$ where T is a similarity. We say that $A = T(X_t^0)$ *fits nicely* over X_s if

$$T^{-1}(\widehat{\Lambda}_s \cap A) \subset \widehat{\Lambda}_t. \quad (38)$$

We don't require that A is actually a subset of X_s^0 .

Say that a *nice covering* of X_s^0 is a covering of the form

$$X_s^0 \subset A_1 \cup \dots \cup A_m \cup B_1 \cup \dots \cup B_n, \quad (39)$$

where each A_i is a similar copy of X_t^0 which fits nicely over X_s^0 and each B_j is a periodic tile of Δ_s .

Lemma 7.7 (Covering) *Let $t = R(s)$. The set X_s^0 has a nice covering by similar copies of X_t^0 . All the similarities associated to the pieces in the cover have the form $I \circ \phi_s$, where I is an isometry and ϕ_s is as in the Main Theorem.*

We will prove this result through a series of smaller lemmas.

Lemma 7.8 *The Covering Lemma holds for $s \in (1/4, 1/3)$.*

Proof: Let A_s and B_s be the hexagon and triangle from the Bilateral Lemma. For $s \in (1/4, 1/3)$ we have $R(s) \in (1/2, 1)$. For these values, a calculation shows that $B_s \subset Z_s$. The largest tile in Z_s is an octagon, τ , the image of the central tile in Δ_t under ϕ_s . Figure 7.4 below shows the typical example of $s = 3/10$.

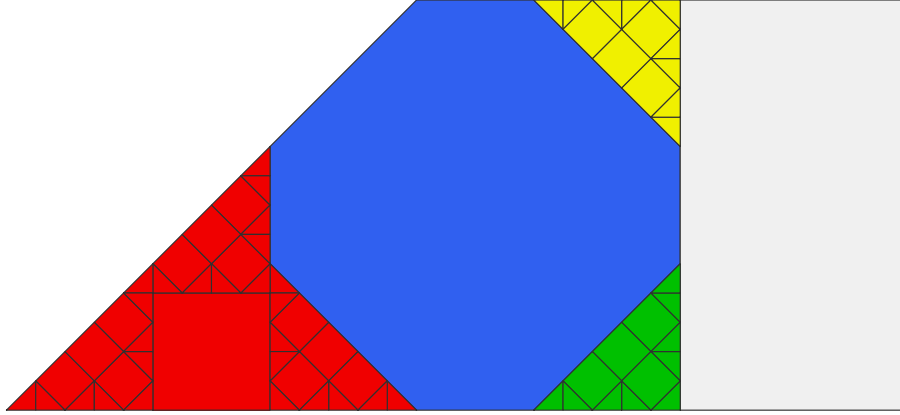


Figure 7.2 X_s (red) and τ (blue) and $X_s^0 - Z_s - \tau$ (yellow, green)

Let ρ_1 be the reflection in the line D_s from the Bilateral Lemma. The tiles in the collection $\rho_1(\Delta_s \cap Z_s) \cap X_s$ are again tiles of Δ_s by the Bilateral Lemma, and $\rho_1(Z_s) \cap X_s$ is precisely the region of X_s^0 lying above τ . This is the yellow region in Figure 7.2. Hence $\rho_2(Z_s)$ fits nicely over Δ_s .

Let ρ_2 be reflection in the line H_s from the Bilateral Lemma. By the Bilateral Lemma, $\rho_2 \circ \rho_1(Z_s)$ fits nicely over Δ_s . The intersection $\rho_2 \circ \rho_1(Z_s) \cap X_s$ is precisely the region of X_s^0 lying below and to the right of τ . This is the green region in Figure 7.2.

To finish the proof, we note that $Z_s = \phi_s(X_t^0)$. The point is that there is just one central tile in Δ_t . So, all the sets we are using have the form $I \circ \rho_s(X_t^0)$, where I is an isometry. ♠

Corollary 7.9 *The Covering Lemma holds for $s \in (3/2, 2)$.*

Proof: For s in this range, we have $R(s) = s - 1$. The result now follows from the Inversion Lemma. ♠

Lemma 7.10 *The Covering Lemma holds for $s \in (1/3, 2/5)$.*

Proof: Figure 7.5 shows a typical case, for the parameter $s = 19/50$.

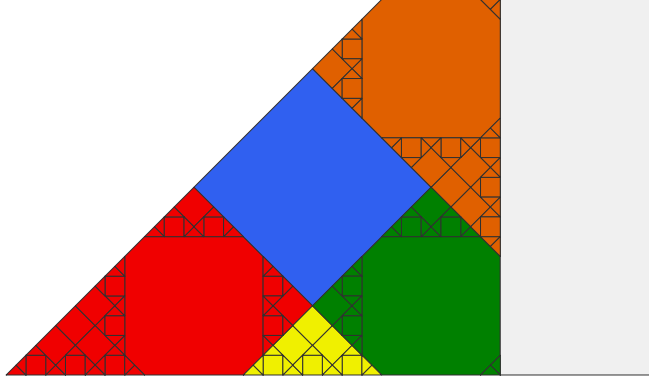


Figure 7.3 Z_s (red) and A_s (green, blue, orange) and B_s (red, yellow)

For $s \in (1/3, 2/5)$, the set Z_s covers the left half of the triangle B_s from the Bilateral Lemma, and also $Z_s \subset B_s$. Let ρ_1 be reflection in the vertical line of symmetry of B_s . By the Bilateral Lemma, the set $\rho_1(Z_s)$ fits nicely over Δ_s . The two pieces Z_s and $\rho_1(Z_s)$ cover B_s .

Let ρ_2 be reflection in the line D_s from the Bilateral Lemma. The pieces $\rho_2(Z_s)$ and $\rho_2 \circ \rho_1(Z_s)$ fit nicely over Δ_s . This is the orange region in Figure 7.3.

Aside from the blue tile τ , the only region not yet covered is the green region, and this is covered by $\rho_3 \circ \rho_2(Z_s)$, where ρ_2 is reflection in the x -axis, H . This last-mentioned piece also fits nicely over Δ_s .

To finish the proof, we note again that $Z_s = \phi_s(X_t^0)$. The point, again, is that there is just one central tile in Δ_t . So, all the sets we are using have the form $I \circ \rho_s(X_t^0)$, where I is an isometry. ♠

Corollary 7.11 *The Covering Lemma holds for $s \in (5/4, 3/2)$. Moreover, none of the similar copies of X_t^0 crosses the bottom edge of X_s^0 .*

Proof: This follows from the Inversion Lemma, and from the fact that the covering we constructed in Lemma 7.10 is such that no similar copy crosses the left edge of X_s^0 . ♠

Lemma 7.12 *The Covering Lemma holds for $s \in (1, 3/2)$.*

Proof: We give the same kind of inductive proof we used in the proof of Lemma 5.1. We already know the result holds for $s \in (5/4, 3/2)$. Given $s \in (1, 5/4)$ we let $u = T(s)$, where T is the map in Equation 20. We will show that the truth of the lemma for u implies the truth of the lemma for s . In all cases, we will use the fact that no tile in the covering crosses the bottom edge of the relevant region.

Let $t = R(s)$ and $v = R(u)$. Suppose that X_u^0 has a nice covering by similar copies of X_v^0 , with the additional property that no piece crosses the bottom edge of X_u^0 . Using the map $\omega_s : Y_u \rightarrow W_s$ from the proof of Lemma 5.1, we get a nice covering of W_s by finitely many tiles of Δ_s and finitely many similar copies of X_t^0 . We also have the piece Z_s .

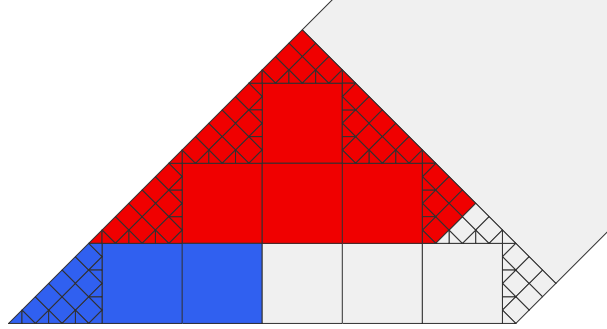


Figure 7.4: Half of W_s for $s = 22/19$.

For convenience, we repeat Figure 5.1 here. The union $Z_s \cup W_s$ covers the entire left half of X_s^0 , namely the half which lies to the left of the vertical line through the top vertex of X_s^0 . Moreover, as in the proof of Lemma 5.1, we note that reflection in this vertical line maps the left right half of the tiling into the left half. Thus, we can extend our covering to all of X_s^0 using this reflection. Some of the pieces slop over into the central tile of Δ_s , but this does not bother us.

As in the proof of Lemma 5.1, this lemma now follows from induction on the number k needed so that $T^k(s) \in (5/4, 3/2)$. ♠

Corollary 7.13 *The Covering Lemma holds for $s \in (0, 1/2)$.*

Proof: Combining the previous results, we see that the Covering Lemma holds for all $s \in (1, 2)$. By the Inversion Lemma, the Covering Lemma holds for all $s \in (1/4, 1/2)$. But then, by repeated applications of the Insertion Lemma, the Covering Lemma holds for all $s \in (0, 1/2)$. ♠

Remark: We have ignored the parameter $1/4$. The Covering Lemma is vacuous here, because $R(1/4) = 0$.

Lemma 7.14 *The Covering Lemma Holds for $s \in (1/2, 3/4)$.*

Proof: This case is similar to the case treated in Lemmas 7.8. Figure 7.5 shows the rather typical case of $s = 7/10$.

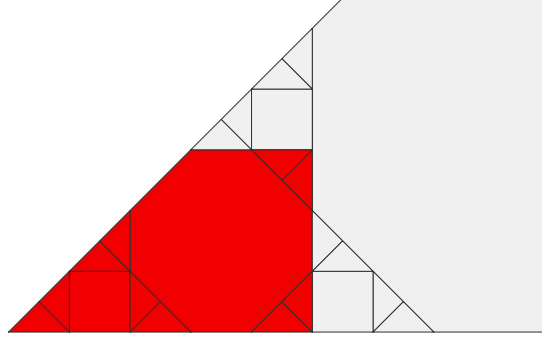


Figure 7.5: Δ_s (white, red) and Z_s (red) for $s = 7/10$.

Using reflections in the lines V_s and D_s from the Bilateral Lemma, we produce two isometric copies of Z_s which nicely fit over Δ_s . ♠

Lemma 7.15 *The Covering Lemma Holds for $s \in (3/4, 5/6)$.*

Proof: The proof is similar to the case for $s \in (1/2, 3/4)$. Figure 7.6 shows a typical example. ♠

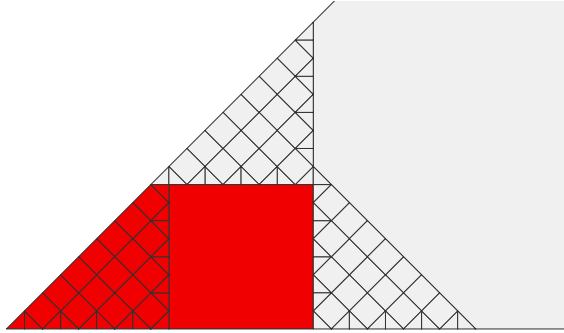


Figure 7.6: $\Delta)_s$ (white, red) and Z_s (red) for $s = 13/17$.

Lemma 7.16 *The Covering Lemma Holds for $s \in (5/6, 1)$.*

Proof: The proof here relates to the proof of Lemma 5.2 in the same way that the proof of Lemma 7.12 relates to the proof of Lemma 5.1. We omit the details. ♠

8 Properties of the Limit Set

8.1 Area Zero

Here we show that $\widehat{\Lambda}_s$ has zero area. It suffices to prove this for the left half of $\widehat{\Lambda}_s$, which we denote by S_s .

Lemma 8.1 *Let s be irrational. For any $\epsilon > 0$, the set X_s^0 has a nice covering by similar copies of X_t^0 , all having diameter at most ϵ .*

Proof: The nice fitting property is hereditary. If a similar copy $T_u(X_u^0)$ fits nicely over X_t^0 and a similar copy $T_t(X_t^0)$ fits nicely over X_s^0 , then the similar copy $T_t \circ T_u(X_u)$ fits nicely over X_s^0 . The boundary-adapted property is also hereditary. We let $s_n = R^n(s)$ and note that, by induction, X_s^0 has a nice and boundary adapted covering by similar copies of X_t^0 where $t = s_n$. The scale factor of the similarities involved is the product of the scales factors of ϕ_{s_i} , taken over $i = 0, \dots, (n-1)$. At least every other time, $s_i < 1/2$ and the corresponding scale factor is less than $\sqrt{2}/2$, so the total scale factor is less than $2^{-n/4}$. We can make this less than ϵ/D by taking n large enough. Here $D < 2$ is the maximum diameter of any set X_u^0 , taken over all $u \in (0, 1)$. ♠

Say that a *near disk* is a compact set D which is contained in a disk of radius $10r$ and contains a disk of radius r . For every s , the set X_s^0 is a near disk. Let μ denote the 2-dimensional Lebesgue measure. The following is an immediate consequence of the Lebesgue Density Theorem.

Lemma 8.2 *Suppose that $S \subset \mathbf{R}^2$ is a bounded measurable set of positive Lebesgue measure. Then almost every point $p \in S$ has the following property. If $\{D_n\}$ is a sequence of near disks containing p , having diameter shrinking to 0, then $\mu(D_n \cap S)/\mu(S) \rightarrow 1$, as $n \rightarrow \infty$.*

Suppose now that S_s has positive measure. We can find a point $p \in S_s$ satisfying the conclusion of Lemma 8.2. By Corollary 8.1 we can find a sequence $\{D_n\}$ of near disks such that $p \in D_n$ for all n , and the diameter of D_n tends to 0, and D_n is a similar copy of X_u^0 for some $u = u_n$. The Area Lemma now tells us that $\mu(S_s \cap D_n) < \lambda(1 - \epsilon)(D_n)$ for some universal constant $\epsilon > 0$. This contradicts Lemma 8.2. Hence Λ_s has zero area.

8.2 Characterization of the Limit Set

Now that we know $\widehat{\Lambda}_s$ has area zero, we can give a nicer characterization of the limit set.

Lemma 8.3 *A point belongs to $\widehat{\Lambda}_s$ if and only if every open neighborhood of the point contains infinitely many periodic tiles of Δ_s .*

Proof: Certainly, $\widehat{\Lambda}_s$ contains all such points. For the converse, suppose that $p \in \widehat{\Lambda}_s$. There exists a sequence of points $q_n \rightarrow p$ with the following property $f^1(q_n), \dots, f^n(q_n)$ are all defined and distinct. Since $\widehat{\Lambda}_s$ has measure 0, and the set of points with undefined orbits has measure 0, the set of periodic points has full measure. So, we can take a new sequence $\{q'_n\}$ of periodic points converging to p , and we can make $|q_n - q'_n|$ as small as we like. Making these distances sufficiently small, we guarantee that q'_n has periodic at least n . But then every neighborhood of p intersects infinitely many periodic tiles.

♠

8.3 Projections of the Limit Set

Let $s \in (0, 1)$ be irrational and let π denote projection onto the x -axis. We will show that $\pi(\widehat{\Lambda}_s)$ contains a line segment. Following this, we will deal with projections onto lines parallel to the other 8th roots of unity. We suppress the parameter s . Since $\widehat{\Lambda}$ is a closed set, it suffices to prove that $\pi(\Lambda)$ contains a dense subset of a line segment.

There are countably many vertical lines which contain vertices of tiles in Δ . We ignore such lines. Let L be a vertical line which contains both a point on the bottom edge b of X and a point on the left edge ℓ of X . Assume that L does not contain a tile vertex. We will prove that L contains a point of $\widehat{\Lambda}$. From this it follows that $\pi(\ell) \subset \pi(\widehat{\Lambda})$, which proves what we want.

Suppose L does not intersect $\widehat{\Lambda}$. Then L only intersects finitely many tiles, τ_1, \dots, τ_n . We order these tiles according to when L enters them as we move upwards along L . Note that L must leave τ_i and enter τ_{i+1} at the same point. Otherwise, the segment of L lying between these two tiles would be the accumulation point of infinitely many tiles. For the same reason, the bottom edge of τ_1 must lie in b and the top edge of τ_n must lie in ℓ .

Since L leaves τ_i and enters τ_{i+1} at the same point, τ_i and τ_{i+1} must share an edge, and this shared edge contains a point of L . In particular, if L leaves τ_i through a horizontal edge, then L enters τ_{i+1} through a horizontal edge.

Since L is a vertical line, and the tiles of Δ are semi-regular octagons with sides parallel to the 8th roots of unity, we get the following result: L enters τ_i through a horizontal edge if and only if L leaves τ_i through a horizontal edge.

We know that L enters τ_1 through a horizontal edge. Using the properties above, we see that L leaves τ_n through a horizontal edge. But the top edge of τ_n , which is contained in ℓ , is not horizontal. This is a contradiction. Hence L does intersect $\widehat{\Lambda}$.

Remark: When s is rational, our argument breaks down because of the existence of triangular tiles.

Now we deal with projection into a line parallel to a different 8th root of unity. Let ω be an 8th root of unity. Unless $\omega = \pm i$, we can find lines perpendicular to ω which intersect both a horizontal and a diagonal edge of X . Once we have such lines, the argument we gave for $\omega = \pm 1$ works in this new context.

We just have to worry about the case $\omega = \pm i$. In this case, we observe that some edge of the trivial tile in Δ is vertical. Thus, there are horizontal lines connecting ℓ to this vertical edge. Now we run the same argument again, interchanging the roles played by the horizontal and vertical directions.

8.4 Finite Unions of Lines

Let s be irrational. Let S_s denote the left half of $\widehat{\Lambda}_s$. We will assume that there exists an irrational parameter s such that S_s is contained in a finite union of lines, and we will derive a contradiction.

Say that an *essential cover* of S_s is a finite union of lines which covers all but finitely many points of S_s . Let $c(s)$ denote the cardinality of an essential cover of S_s having the fewest number of lines. We call s a *minimal failure* if $c(s)$ achieves the minimum possible value of the function ² $c : (0, 1) \rightarrow \mathbf{N}$. We call a cover realizing $c(s)$ a *minimal essential cover*. For the rest of our proof we assume that s is a minimal failure.

²We define $c(t) = \infty$ if S_t has no essential cover.

Referring to the Main Theorem, we can pull back essential covers by ϕ_s . Suppose that L is a line intersecting Z_s^0 in a segment. Then we define $\phi_s^{-1}(L)$ to be the line extending the segment $\phi_s^{-1}(L \cap Z_s^0)$. If L does not intersect Z_s^0 in a line segment we define $\phi_s^{-1}(L)$ to be the empty set.

Let $t = R(s)$. By the Main Theorem,

$$\phi_s(S_t) \subset S_s \cap Z_s^0. \quad (40)$$

for this reason, t is also a minimal failure, and the pullback of a minimal essential cover of S_s is a minimal essential cover of S_t .

Lemma 8.4 *Every line of a minimal essential cover of S_s . contains v_s , the bottom left vertex of X_s .*

Proof: Let $d(s, L)$ denote the distance from v_s to a line L of an essential minimal cover. Let $d(s)$ denote the maximum of $d(s, L)$, taken over all lines of L which appear in some essential minimal cover of S_s . Suppose that $d(s) > 0$. Since ϕ_s is a contraction, we have $d(s) < d(t)$. Also, setting $u = R(t)$, we have

$$d(s) < d(u)/\sqrt{2}. \quad (41)$$

This is true because at least one of the maps ϕ_s or ϕ_t contracts distances by at least a factor of $\sqrt{2}$.

Equation 41 is not possible for all choices of s . Note that X_s has diameter at most $1 + \sqrt{2}$. So, $d(s)$ is uniformly bounded. Hence, we can choose s so as to maximize $d(s)$, amongst all minimal counterexamples, up to a factor of (say) 9/10. But then $d(u)$ exceeds the maximum. This is a contradiction. The only way out is that $d(s) = 0$. ♠

Lemma 8.5 *Let A_s denote the hexagon from the Bilateral Lemma. Only finitely many points of S_s lie in the $A_s - \partial X_s$.*

Proof: Let S'_s denote the subset of S_s contained in the interior of A_s . Let U_s denote a minimal essential cover. Let ρ denote reflection in the x -axis, as in the Bilateral Lemma. $\rho(S'_s) = S'_s$. But then $S'_s \subset U_s \cap \rho(U_s)$. This is just a finite set of points, because all lines in U_s contain the vertex v_s and none of the lines in $\rho(U_s)$ contains v_s . Hence S'_s is a finite set.

Consider points of S_s lying on the edge of A_s that does not lie in ∂X_s . If this edge contained infinitely many points of S_s then U_s would have infinitely many lines. The point is that this edge of A_s does not contain the vertex v_s . ♠

Lemma 8.6 *Let B_s denote the triangle from the Bilateral Lemma. Only finitely many points of S_s lie in the $B_s - \partial X_s$.*

Proof: Same argument as above. ♠

Now we know that the interior of X_s contains only finitely many points of S_s .

Let ℓ_+ (respectively ℓ_-) denote the subset of the interior of ℓ lying above (respectively below) $(-1, 0)$, a common vertex of A_s and B_s . Let ρ be reflection in the x -axis. By the Bilateral Lemma,

$$\rho(S_s \cap \ell_+) \subset S_s \cap \text{interior}(X_s). \quad (42)$$

Hence $S_s \cap \ell_+$ is finite. A similar argument shows that $S_s \cap \ell_-$ is finite. Hence $S_s \cap \ell$ is finite.

But then S_s is contained in the top and bottom (horizontal) edges of X_s , except for finitely many points. But then the projection of S_s onto the y -axis does not contain a segment. This contradicts Statement 2 of Theorem 1.2. Hence a minimal failure cannot exist. This proves Statement 3 of Theorem 1.2.

8.5 Intersection with the Bad Set

Here we will show that $\widehat{\Lambda}_s - \Lambda_s$ has length 0 for almost every parameter s . What we will actually prove is that $\widehat{\Lambda}_s - \Lambda_s$ has length zero provided that the sequence

$$\left\{ \frac{1}{2R^n(s)} \mod 1 \right\}$$

has an accumulation point in $(0, 1)$. Almost every choice of s satisfies this criterion. Suppose now that $s \in (0, 1)$ is a parameter which satisfies the condition above.

Lemma 8.7 *Let s be irrational. For any $\epsilon > 0$, some open neighborhood of the special segments of X^0 has a nice covering by open subsets of similar copies of X_t^0 , all having diameter at most ϵ . Moreover, t can be chosen so that $1/(2t) \bmod 1$ is uniformly bounded away from 0 and 1.*

Proof: We simply restrict the covers produced in the Covering Lemma to neighborhoods of the special segments. This gives us everything in the lemma except the last statement. The last statement comes from the hypotheses on s . ♠

Lemma 8.8 $\widehat{\Lambda}_s \cap \partial X_s$ has length 0.

Proof: Referring to the Length Lemma from the previous chapter, it suffices to show that Λ_s intersects the special segments in sets of measure 0. The proof of this lemma is exactly like what we did for S_s , except that we use the Lebesgue Density Theorem for length instead of for area, and we use Lemma 8.7 in place of Corollary 8.1. ♠

Let $B_s \subset X_s$ denote the set of points where some iterate of f_s is undefined. Let B_s^+ (respectively B_s^-) denote the set of points where some positive (respectively negative) iterate of f is undefined. We will show that $\widehat{\Lambda} \cap B_s^+$ has length 0. The case of $\widehat{\Lambda}_s \cap B_s^-$ is quite similar.

Lemma 8.9 *Let $s > 1/2$. If $\widehat{\Lambda}_s \cap B_s^+$ has positive length, then $\Lambda_s \cap \partial X_s$ has positive length.*

Proof: We suppress the parameter s . Suppose that $\widehat{\Lambda} \cap B^+$ has positive length.

Recall that $X' = F_1 \cup F_2$ and $f' : X' \rightarrow X'$ is such that $f = (f')^2$. It is easier to work with f' because the discontinuity set is simpler. Let $S'_n \subset X'$ denote the set of points where one of the first n iterates of f' is not defined.

We have

$$B_+ \subset \bigcup_{n=1}^{\infty} S'_n \quad (43)$$

The set on the right is countable. So, if $\widehat{\Lambda} \cap B_+$ has positive length, there is some n such that $\widehat{\Lambda} \cup S'_n$ has positive length. We also have the equation

$$f'(S'_n - S'_1) \subset S'_{n-1}. \quad (44)$$

Using this equation, together with the fact that f' is a piecewise isometry, we see by induction that $\widehat{\Lambda} \cap S'_1$ has positive length.

By symmetry, the $\pi/2$ rotation carries F_1 to F_2 and $\widehat{\Lambda} \cap F_1$ to $\widehat{\Lambda} \cap F_2$ and $S'_1 \cap F_1$ to $S'_1 \cap F_2$. Hence, if $\widehat{\Lambda}$ has positive length intersection with S'_1 , then $\widehat{\Lambda}$ also has positive length intersection with $S'_1 \cap F_1$. (Recall that $X = F_1$.)

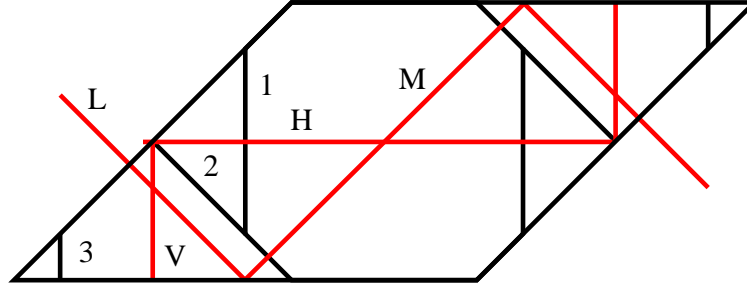


Figure 8.1: The set $S'_1 \cap X$ in black, and symmetry lines in red.

The red lines labelled H, V, L in Figure 8.1 are lines of symmetry from Bilateral Lemma I and Bilateral Lemma II. The fact that line M is a line of symmetry follows from the Inversion Lemma and the fact that L_t is a line of symmetry for A_t when $t = 1/2s$.

Let R_L denote reflection in line L , etc. We now have 3 cases.

1. Suppose $\widehat{\Lambda}$ intersects the segment labelled 1 in a set of positive length. We apply R_L . Lemma 8.3 and the Bilateral Lemma II combine to say that $\widehat{\Lambda} \cap \partial X$ has positive length.
2. Suppose $\widehat{\Lambda}$ intersects the line labelled 2 in a set of positive length. On at least one side of line 2 there are tiles of Δ_s which accumulate on line 2 in a set of positive length. Depending on which side has this property we either apply R_H or R_V . Lemma 8.3 and Bilateral Lemma I combine to say that $\widehat{\Lambda} \cap \partial X$ has positive length.
3. Suppose $\widehat{\Lambda}$ intersects the line labelled 3 in a set of positive length. This is the same argument as in Case 2, except we use one of the reflections $R_L \circ R_V$ or $R_M \circ R_V$.

If $\widehat{\Lambda}$ intersects S'_1 on the right hand side of the picture in a set of positive length, then we use the rotational symmetry to reduce to the cases above. ♠

Combining the previous result with Lemma 8.8, we see that $\widehat{\Lambda}_s \cap B_s^+$ has zero length when $s > 1/2$. Now consider the case $t < 1/2$. Suppose that $\widehat{\Lambda}_t \cap B_t^+$ has positive length. Let $s = 1 - t$ so that $t = R(s)$. By the Main Theorem, $\widehat{\Lambda}_s \cap B_s^+$ has positive length. But then, by the previous result, $\widehat{\Lambda}_s \cap \partial X_s$ has positive length. Lemma 8.8 rules this out.

8.6 Hyperbolic Symmetry

In this section, we prove Theorem 1.5. Let $i = \sqrt{-1}$, as usual. Let Γ' denote the group of maps of $\mathbf{C} \cup \infty$ generated by the following maps.

1. $z \rightarrow \bar{z}$.
2. $z \rightarrow -z$.
3. $z \rightarrow z - 1$.
4. $z \rightarrow 1/(2z)$.

Let $\Gamma \subset \Gamma'$ be the index 2 subgroup which preserves \mathbf{H}^2 .

Lemma 8.10 *If s and t lie in the same Γ' orbit, then (X_s, f_s) and (X_t, f_t) are locally equivalent.*

Proof: Local equivalence is an equivalence relation, so we just have to check this result on the generators of Γ . Note that local equivalence is an empty condition for rational parameters. So, we only work with irrational parameters.

Complex conjugation fixes \mathbf{R} pointwise. So, for this generator there is nothing to prove.

If $t = -s$ then the two systems are identical, by definition.

If $t = 1/2s$, then the two systems are conjugate, by the Inversion Lemma.

The one nontrivial case is when $t = s - 1$. There are several cases to consider. By symmetry, it suffices to consider the case when $s > 0$. There are several cases to consider. When $s > 2$, the result follows from the Insertion Lemma.

Suppose that $s \in (1, 2)$. By the Covering Lemma, X_s^0 is nicely covered by similar copies of X_t^0 . Moreover, in our construction, at least one of these similar copies, namely Z_s , lies entirely in X_s^0 . The local equivalence follows immediately in this case. To make this work, we need to throw out points on the finitely many lines extending the sides of the similar copies of X_t^0 .

Suppose that $s \in (1/2, 1)$ and $t' = s - 1$. Then $t' < 0$ and we can switch to the parameter $t = -t' = 1 - s$. Now we apply the Covering Lemma again, just as in the previous case.

Finally, suppose that $s \in (0, 1/2)$. Again, we consider $t = 1 - s \in (1/2, 1)$. Switching the roles of s and t we reduce to the previous case. ♠

It just remains to recognize Γ .

- Γ contains the element $\rho_1(z) = -\bar{z}$. This is the reflection in the geodesic joining 0 to ∞ .
- Γ contains the element $\rho_2(z) = \overline{1 - z}$. This is the reflection in the geodesic ray joining $1/2 + i/2$ to ∞ .
- Γ contains the element $\rho_3(z) = 1/(2\bar{z})$. This is a reflection in the geodesic joining $i/\sqrt{2}$ to $1/2 + i/2$.

In short, Γ contains ρ_j for $j = 1, 2, 3$, and these elements generate the $(2, 4, \infty)$ triangle group generated by reflections in the sides of the triangle with vertices $i/\sqrt{2}$, and $1/2 + i/2$, and ∞ . We omit the proof that these elements generate Γ , since what we have done already gives a proof of Theorem 1.5.

9 The Eight Calculations

9.1 The Fiber Bundle Picture

Our strategy is to reduce all our calculations to statements about convex lattice polyhedra. In this section, we explain the main idea behind this reduction. For the most part, we only need to make our calculations for parameters $a \in [1/4, 2]$, and so this interval will make a frequent appearance in the discussion.

In our standard normalization, X_s be the parallelogram with vertices

$$(\epsilon_1 + \epsilon_2 s, \epsilon_2 s), \quad \epsilon_1, \epsilon_2 \in \{-1, 1\}. \quad (45)$$

We define

$$\mathcal{X} = \{(x, y, s) \mid (s, y) \in X_s\} \subset \mathbf{R}^2 \times [1/4, 2] \quad (46)$$

The space \mathcal{X} is both a convex lattice polyhedron and a fiber bundle over $[1/4, 2]$ such that the fiber above s is the parallelogram X_s . See §10.1 for the list of vertices of \mathcal{X} . The maps $f_s : X_s \rightarrow X_s$ piece together to give a fiber-preserving map $F : \mathcal{X} \rightarrow \mathcal{X}$.

Lemma 9.1 *The map F is a piecewise affine map.*

Proof: Consider some point $p \in X_s$. There is some vector

$$V_s = (A + Bs, C + Ds)$$

Here A, B, C, D are integers. such that $f_s(p) = p + V_s$. If we perturb both V and s , the integers A, B, C, D do not change. So, in a neighborhood of p in \mathcal{X} , the map F has the form

$$(F(x, y, s) = (x + Bs, y + Ds, s) + (A, C, 0).$$

This is a locally affine map of \mathbf{R}^3 . ♠

Let $\mathcal{X}(S)$ be the subset of our fiber bundle lying over a set $S \subset [1/4, 2]$. Given the nature of the map, we find it useful to split our fiber bundle into 3 pieces, namely

$$\mathcal{X} = \mathcal{X}[1/4, 1/2] \cup \mathcal{X}[1/2, 1] \cup \mathcal{X}[1, 2]. \quad (47)$$

A *maximal domain* of $\mathcal{X}(S)$ is a maximal subset on which F is entirely defined and continuous. The map F acts as an affine map on each maximal subset. In §9.3 we explain how we verify the following experimentally discovered facts.

- $\mathcal{X}[1/4, 1/2]$ is partitioned into 19 maximal domains, each of which is a convex rational polytope. The vertices in the partition of \mathcal{X} are of the form $(a/q, b/q, p/q)$ where $a, b, p, q \in \mathbf{Z}$ and

$$(p, q) \in \{(1, 4), (2, 7), (3, 10), (1, 3), (1, 2)\}.$$

These polyhedra are permuted by the map $\iota_1(x, y, s) = (-x, -y, s)$.

- $\mathcal{X}[1/2, 1]$ is partitioned into 13 maximal domains, each of which is a convex rational polytope. The vertices in the partition of $\mathcal{X}[1/2, 1]$ are of the form $(a/q, b/q, p/q)$ where $a, b, p, q \in \mathbf{Z}$ and

$$(p, q) \in \{(1, 2), (2, 3), (3, 4), (1, 1)\}.$$

These polyhedra are permuted by ι_1 .

- The 19 polyhedra in the partition of $\mathcal{X}[1, 2]$ are all images of the polyhedra in the partition of $\mathcal{X}[1/4, 1/2]$ under the map $\iota_2 \circ F$, where

$$\iota_2(x, y, s) \rightarrow ((x + y)/2s, (x - y)/2s, 1/2s).$$

These polyhedra are permuted by ι_1 .

In §10.3 we will explain the action of the map F on each polyhedron. We scale all the polyhedra by a factor of $420 = 10 \times 7 \times 4$ so that we can make all our calculations using integer arithmetic. One can think of this rescaling as a way of clearing all denominators in advance of the calculations.

We will list the 420-scaled polyhedra in §10.2. For now, call them

$$\alpha_0, \dots, \alpha_{18}, \beta_0, \dots, \beta_{12}, \gamma_0, \dots, \gamma_{18}.$$

We have labeled so that list these so that

$$\alpha_i \subset \mathcal{X}[105, 210], \quad \beta_i \subset \mathcal{X}[210, 420], \quad \gamma_i \subset \mathcal{X}[420, 840]. \quad (48)$$

$\mathcal{X}[105, 210]$ is our name for the 420-scaled version of $\mathcal{X}[1/4, 1/2]$, etc. When we want to discuss these polyhedra all at once, we call them P_0, \dots, P_{50} .

9.2 Computational Methods

Here we describe the main features of our calculations. As we mentioned above, all our calculations boil down to calculations involving convex lattice polytopes.

Operations on Vectors: The only operations we perform on vectors are vector addition and subtraction, the dot and cross product, scaling a vector by an integer, and dividing a vector by $d \in \mathbf{Z}$ provided d divides all the coordinates. These operations in turn only use plus, minus, and times, and integer division.

Avoiding Computer Error: We represent integers as *longs*, a 64 bit integer data type. One can represent any integer strictly between -2^{63} and 2^{63} . (The extra bit gives the sign of the number.) There are two possible sources of error: overflow error and division errors.

We subject all our calculations to an overflow checker, to make sure that the computer never attempts a basic operation (plus, minus, times) in which either the inputs or the output is out of range. To give an example, if we want to take the cross product $V_1 \times V_2$, we first check that all entries in V_1 and V_2 are less than 2^{30} in size. This guarantees that all intermediate answers, as well as the final answer, will be in the legal range for longs.

We also check our division operations. Before we compute n/d , we make sure that $n \equiv 0 \pmod{d}$. The java operation $n\%d$ does this. Once we know that $n\%d = 0$, we know that the computer correctly computes the integer n/d .

No Collinearities: Given a polyhedron P , let P_1, \dots, P_n denote the vertices. We first check that

$$(P_k - P_i) \times (P_j - P_i) \neq 0, \quad \forall i < j < k \in \{1, \dots, n\}. \quad (49)$$

This guarantees that no three points in our vertex list of P are collinear. We found the polyhedra of interest to us in an experimental way, and initially they had many such collinearities. We detected collinearities by the failure of Equation 49, and then removed all the redundant points.

Face Lists: For each of our polyhedra P , we find and then store the list of faces of the polyhedron. To do this, we consider each subset $S = \{S_1, \dots, S_m\}$

having at least 3 members. We check for three things.

1. S lies in a single plane. We compute a normal $N = (S_2 - S_1) \times (S_3 - S_1)$ and then check that $N \cdot S_i$ is independent of i . Assuming this holds, let $D = N \cdot S_i$.
2. S lies on ∂P . To check this, we compute the normal N as above, and then check that either $\max N \cdot P_i \leq D$ or $\min N \cdot P_i \geq D$.
3. We check that S is maximal with respect to sets satisfying the first two properties.

Improved Normals: We noticed computationally that all of the normals to all of the polyhedron faces can be scaled so that they have the following form: At least two of the three coordinates lie in $\{-1, 0, 1\}$ and the third coordinate lies in $\{-8, \dots, 8\}$. When we use the normals in practice, we make this scaling. This is one more safeguard against overflow error.

No Face Redundancies: Once we have the face list, we check that each vertex of each polyhedron lies in exactly 3 faces. In particular, all the vertices of our polyhedra are genuine vertices.

Containment Algorithm: Suppose we want to check if a vector V lies in a polyhedron P . For each face S of P , we let N be the (scaled) normal to S . we set $D = N \cdot S_0$, and then we verify the following.

- If $\max N \cdot P_i \leq D$ then $V \cdot N \leq D$.
- If $\min N \cdot P_i \geq D$ then $V \cdot N \geq D$.

If this always holds then V lies on the same side of S as does P , for all faces S . In this case, we know that $V \in P$. If we want to check that $V \in \text{interior}(P)$, we make the same tests, except that we require strict inequalities.

Disjointness Algorithm: Let $\mathbf{Z}_{10} = \{-10, \dots, 10\}$. To prove that two polyhedra P and Q have disjoint interiors, we produce (after doing a search) an integer vector $W \in \mathbf{Z}_{10}^3$ such that

$$\max W \cdot P_i \leq \min W \cdot Q_j. \quad (50)$$

Volumes: For many of the lattice polytopes P we consider, we compute $6 \text{volume}(P) \in \mathbb{Z}$. To compute this volume, we decompose P into prisms by choosing a vertex of $v \in P$ and then computing

$$\sum_{f \in P} 6 \text{volume}([v, f]). \quad (51)$$

The sum is taken over all faces f of P and $[v, f]$ denotes the prism obtained by taking the convex hull of $v \cup f$. We compute the volumes of these prisms by taking various triple products of the vectors involved.

9.3 Verifying the Partition

Now we explain how we verify that the polyhedra we mention in §9.1 (and list in §10.2) really are correct. Let $\mathcal{R}\mathcal{X}$ denote the polytope obtained from \mathcal{X} by rotating 90 degrees. We have $F = (F')^2$, where F' is the original PET which swaps \mathcal{X} and $\mathcal{R}\mathcal{X}$.

Pairwise Disjointness: Using the Disjointness Algorithm, we check that P_i and P_j have disjoint interiors for all $i \neq j \in \{0, \dots, 50\}$. We check the same thing for $F(P_i)$ and $F(P_j)$.

Containment: Using the Containment Algorithm, we check that

- $P_i \subset \mathcal{X}$ for $i = 0, \dots, 50$.
- $F(P_i) \subset \mathcal{X}$ for $i = 0, \dots, 50$.
- $F'(P_i) \subset \mathcal{R}\mathcal{X}$ for $i = 0, \dots, 50$.

We also see, by inspection, that F has a different action on P_i and P_j whenever P_i and P_j share a (non-horizontal) face. These checks show that each P_i is a maximal domain for the action of F

Filling: It remains to check we check that \mathcal{X} is partitioned into P_0, \dots, P_{50} . We check that

$$\sum_{i=0}^{50} \text{volume}(P_i) = \text{volume}(\mathcal{X}). \quad (52)$$

The same equation shows that \mathcal{X} is also partitioned into $F(P_0), \dots, F(P_{50})$.

9.4 Calculation 1

Let $H = F^{-1}$, and let \mathcal{H} be the partition of $\mathcal{X}[1/4, 1]$ by the polyhedra $F(P_0), \dots, F(P_{31})$. Then \mathcal{H} is the partition by maximal domains for F^{-1} . We rename the members of \mathcal{H} as H_0, \dots, H_{31} .

We have the partition

$$\mathcal{X}[1/4, 1] = \mathcal{A}[1/4, 1] \cup \mathcal{B}[1/4, 1] \cup \mathcal{C}[1/4, 1] \quad (53)$$

Here \mathcal{A} is such that the fiber of \mathcal{A} over s is the hexagon A_s . The polyhedron \mathcal{B} has the same definition relative to the triangle β_s . The polyhedron \mathcal{C} is obtained from \mathcal{B} by reflecting in the line $x = y = 0$.

The map μ from Calculation 1 acts on each of \mathcal{A} and \mathcal{B} and \mathcal{C} as a reflection. We verify that each polyhedron α_i and β_i is a subset of one of these 3 big pieces. Thus, μ acts on each polyhedron as a reflection. The new partition

$$\mathcal{X}[1/4, 1] = \bigcup_{i=0}^{18} \mu(\alpha_i) \cup \bigcup_{i=0}^{12} \mu(\beta_i) \quad (54)$$

is the partition for the map

$$G = \mu \circ f \circ \mu^{-1}. \quad (55)$$

We call this partition \mathcal{G} , and we rename its members G_0, \dots, G_{31} .

So, in summary \mathcal{G} is the partition for G and \mathcal{H} is the partition for H . Next, we find a list of 48 pairs i, j so that

$$\text{interior}(G_i) \cap \text{interior}(H_j) \neq \emptyset$$

only if (i, j) lies on our list. More precisely, we use the Separation Algorithm to show that all other pairs have disjoint interiors.

Finally, we consider the grid

$$\Gamma = \{(20i, 20k, 105 + 10k) \mid i = -42, \dots, 42, \ j = -21, \dots, 21, \ k = 0, \dots, 31\}. \quad (56)$$

We check the identity $G = H$ on each point of Γ and we also check that at least one point of Γ is contained in each intersection $G_i \cap H_j$ for each of our 48 pairs. This suffices to establish the identity on all of $\mathcal{X}[1/4, 1]$.

9.5 Calculation 2

Calculation 2 follows the same scheme as Calculation 1. Here we just explain the differences in the calculation.

- We set $H = F$ and $G = \nu F^{-1}\nu$.
- \mathcal{H} is the partition consisting of $\alpha_0, \dots, \alpha_{18}$.
- $\mathcal{X}[1/4, 1/2]$ is partitioned into 5 smaller polyhedra, coming from P_s , Q_s , the central tile, $\iota(P_s)$ and $\iota(Q_s)$. the map ν acts as a reflection on each piece. For $i = 0, \dots, 18$, the polyhedron $F(\alpha_i)$ is contained in one of the 5 pieces, so that ν acts isometrically on $F(\alpha_i)$.
- \mathcal{G} be the partition of $\mathcal{X}[1/4, 1/2]$ by the polyhedra

$$\nu \circ F(\alpha_0), \dots, \nu \circ F(\alpha_{18}).$$

- We find a list of 27 pairs (i, j) such that G_i and H_j do not have disjoint interiors.

The rest of the calculation is the same.

9.6 Calculation 3

Let $s \in [5/4, 2]$ and let $t = s - 1 \in [1/4, 1]$. We want to show that ϕ_s conjugates $f_t|Y_t$ to $f_s|Z_s$ and that every orbit of f_s intersects Z_s , except the following orbits.

- Those in the trivial tile $(\alpha_0 \cup \beta_0)_s$ of Δ_s .
- Those in the set

$$\tau_s = \phi_s\left((\alpha_0 \cup \beta_0)_t\right).$$

Once we are done, we will know that τ_s is in fact a tile of Δ_s , and that τ_s has period 2.

For this section we set $\mathcal{X} = \mathcal{X}[5/4, 2]$. Let \mathcal{Y} denote the subset of \mathcal{X} whose fiber over s is the set Y_s . Define \mathcal{Z} in a similar way. The maps $\phi_s : Y_t \rightarrow Z_s$ piece together to give an isometry $\phi : \mathcal{Y} \rightarrow \mathcal{Z}$. The map is given by

$$\phi(x, y, z) = (x \pm 1, y \pm 1, z - 1) \tag{57}$$

Whether we add or subtract 1 to the first two coordinates depends on whether the point (x, y, z) lies in the left half of \mathcal{Y} or in the right half.

For what we describe next, we always refer to open polyhedra, and our equalities are meant to hold up to sets of codimension 1, namely the boundaries of our polyhedra.

We have

$$\mathcal{Y} = \alpha_1 \cup \dots \cup \alpha_{18} \cup \beta_1 \cup \dots \cup \beta_{12}. \quad (58)$$

For each $i = 1, \dots, 18$ we check computationally that there is some $k = k_i$ with the following three properties.

1. The first $k_i + 1$ iterates of F^{-1} are defined on $\phi \circ F(\alpha_i)$. This amounts to checking that

$$P_{ij} = F^{-i} \circ \phi \circ F(\alpha_i) \quad (59)$$

is contained in some α_a or β_b for suitable indices a and b , and for all $i = 0, \dots, k_i$.

- 2.

$$P_{ij} \cap \mathcal{Z} = \emptyset, \quad j = 1, \dots, k_i. \quad (60)$$

Equation 60 shows that

$$F|_{P_{i0}} = F^{k_i}$$

That is, on P_{i0} , the map F returns to \mathcal{Z} as F^{k_i} . To establish Equation 60, we use the Separation Algorithm so show that

$$P_{ij} \cap \phi(\alpha_a) = \emptyset, \quad P_{ij} \cap \phi(\beta_b) = \emptyset$$

for all $a = 1, \dots, 18$ and $b = 1, \dots, 12$, and all relevant indices i and j . This suffices because \mathcal{Z} is partitioned into the polyhedra

$$\mathcal{Z} = \phi(\alpha_\infty) \cup \dots \cup \phi(\alpha_{\infty\forall}) \cup \phi(\beta_\infty) \cup \dots \cup \phi(\beta_{\infty\epsilon}).$$

3. $P_{i,k_i+1} = \phi(\alpha_i)$.

We make all the same calculations for $\beta_1, \dots, \beta_{12}$, finding an integer ℓ_i which works for β_i . We define Q_{ij} with respect to β_i just as we defined P_{ij} with respect to α_i .

Our calculations above show that ϕ conjugates $F|_{\mathcal{Y}}$ to $F|_{\mathcal{Z}}$. Also, by construction, the boundary of \mathcal{Z} is contained in the union of the boundaries of the polyhedra $\phi(\alpha_i) \cup \phi(\beta_j)$. Hence, Z_s is a clean set for all $s \in [5/4, 2]$.

We still want to see that all orbits except those of period 1 and 2 actually intersect \mathcal{Z} . We check the following.

1. F is entirely defined on $\phi(\alpha_0)$ and has order 2.
2. Both $\phi(\alpha_0)$ and $F \circ \phi(\alpha_0)$ are disjoint from \mathcal{Z} . We use the same trick with the Separation Algorithm to do this.

We claim that the open polyhedra in the following union are pairwise disjoint.

$$\bigcup_{i=1}^{18} \bigcup_{j=0}^{k_i} P_{ij} \cup \bigcup_{i=1}^{12} \bigcup_{j=0}^{\ell_i} Q_{ij} \cup \bigcup_{j=0}^1 F^j \circ \phi(\alpha_0) \cup \bigcup_{j=0}^1 F^j \circ \phi(\beta_0) \cup \alpha_0 \cup \beta_0. \quad (61)$$

Suppose, for instance, that P_{ab} and P_{cd} were not disjoint. Then $P_{a,b+e}$ and $P_{c,d+f}$ would not be disjoint for $e > 0$ and $f > 0$ such that $b+e = k_a + 1$ and $c+f = k_b + 1$. But we know that these last polyhedra are disjoint because they respectively equal the disjoint polyhedra $\phi(\alpha_a)$ and $\phi(\alpha_c)$. Similar arguments work for the other cases.

Similar to Equation 52, we compute the sum of the volumes of the polyhedra in Equation 61 and see that it coincides with the volume of \mathcal{X} . Thus, \mathcal{X} is partitioned into the polyhedra in Equation 61. This fact implies the all orbits except those of period 1 and 2 actually intersect \mathcal{Z} .

Finally, we see by process of elimination that τ_s really is a tile of Δ_s . All other points not in the interior of τ_s either have undefined orbits, or lie in the trivial tile, or have orbits which intersect \mathcal{Z} . Thus f_s cannot be defined on any point of the boundary of τ_s . Since f_s is defined, and has period 2, on the interior of τ_s , we see that τ_s is a tile of Δ_s having period 2.

9.7 Calculation 4

Calculation 4 follows the same scheme as Calculation 3. Here we will describe the differences between the two calculations.

- We consider the behavior of polyhedra on the interval $s \in [1/2, 3/4]$ rather than on $[5/4, 1]$. Here $t = 1 - s \in [1/4, 1/2]$.
- The map ϕ is not an isometry here, but rather a volume preserving affine map. The formula is

$$\phi(x, y, z) = (x \pm (1 - 2z), y \pm (1 - 2z), 1 - z). \quad (62)$$

The choice of plus or minus again depends on whether (x, y, z) lies in the left of the right half of \mathcal{Y} .

- \mathcal{Y} is partitioned into the tiles $\alpha_1, \dots, \alpha_{18}$. The B -tiles are not needed here.
- The tiles τ and $\iota(\tau)$ already belong to \mathcal{Z} . The work in Calculation 3 shows that τ_s and ι_s are indeed period 2 tiles of Δ_s . This time, τ and $\iota(\tau)$ are amongst the images of $\alpha_1, \dots, \alpha_{18}$ under ϕ .
- Using the notation from the previous section, the partition in Equation 61 becomes

$$\bigcup_{i=1}^{18} \bigcup_{j=0}^{k_i} P_{ij} \cup \alpha_0 \quad (63)$$

The rest of the calculation is the same.

9.8 Calculation 5

Calculation 5 follows the same scheme as Calculation 3, except that we don't need to keep track of the volumes. Let T and ω be as in Calculation 5. Let $s \in (1, 4/3]$ and let $t = T(s) \in (1, 2]$.

We define \mathcal{W} and \mathcal{Y} as the global versions of W_s and Y_u , as in Calculation 3. We are interested in $\mathcal{Y}[1, 2]$ and $\mathcal{W}[1, 4/3]$. Similar to Calculation 3, we have a global map $\omega : \mathcal{Y} \rightarrow \mathcal{W}$. We have the formula

$$\omega(x, y, z) = (\omega_s(x, y), s), \quad s = T^{-1}(z). \quad (64)$$

We want to see that ω conjugates $F|_{\mathcal{Y}}$ to $F|_{\mathcal{W}}$.

We have

$$\mathcal{Y} = \gamma_1 \cup \dots \cup \gamma_{18}. \quad (65)$$

By the same methods used in Calculation 3, we check, for each $i = 1, \dots, 18$, that there is some $k = k_i$ with the following three properties.

1. The first $k_i + 1$ iterates of F^{-1} are defined on $\omega \circ F(\gamma_i)$. Define

$$P_{ij} = F^{-i} \circ \omega \circ F(\gamma_i) \quad (66)$$

- 2.

$$P_{ij} \cap \mathcal{W} = \emptyset, \quad j = 1, \dots, k_i. \quad (67)$$

3. $P_{i, k_i+1} = \omega(\alpha_i)$.

These facts imply that ω conjugates $F|\mathcal{Y}$ to $F|\mathcal{W}$.

Finally, the set Z_s is clean for each s for the following reasons.

- The top edge of Z_s^0 and the bottom edge of $\iota(Z_s^0)$ are contained in the union of slices of the sets $\omega \circ F(\partial\gamma_i)$.
- The vertical edges of Z_s are contained in the set $\partial\tau_s \cup \iota(\partial\tau_s)$.
- The remaining edges of Z_s lie in the ∂X_s .

9.9 Calculation 6

As we mentioned in §5, Calculation 6 practically amounts to inspecting the partition. For Statement 1, we let τ be the polyhedron which restricts to τ_s for $s \in [1, 3/2]$. We list this polyhedron in §10.1. We check that F is entirely defined on (the interior of) τ and that $F^2(\tau) = \tau$.

For each polyhedron P , let P_s denote the intersection of P with the horizontal plane of height s .

For Statement 2, let \mathcal{Z} be the polyhedron which restricts to Z_s^0 for $s \in [1, 5/4]$. We compute that

$$\mathcal{Z} \subset F(\gamma_{13}). \quad (68)$$

We also try a single point $(x, y, s) \in F(\gamma_{13})$ and check that $f_s^{-1}(p) = p + \delta_s$. Since $F(\gamma_{13})$ is a domain of continuity for F^{-1} , the same result holds for all points in $F(\gamma_{13})$, including all the points in \mathcal{Z} . This proves Statement 2.

For Statement 3, let \mathcal{K} be the union of two polyhedra which intersect the fiber X_s in $X_s - Z_s - W_s$, for $s = (1, 5/4]$. We see by inspection that

$$\mathcal{K} = F(\gamma_2) \cup F(\gamma_8) \cup F(\gamma_{11}) \cup F(\gamma_{17}); \quad \gamma_j \subset \mathcal{Z}, \quad j = 2, 8, 11, 17. \quad (69)$$

This proves Statement 3.

Remark: We could have made an explicit computation to establish Equation 69, but this is something that is obvious from a glance at just 2 planar pictures. We just have to check Equation 69 at the parameters $s = 1$ and $s = 3/2$ because every polyhedron P in sight, when restricted to the fibers above $[1, 5/4]$, is the convex hull of $P_1 \cup P_{5/4}$.

9.10 Calculation 7

Calculation 7 follows the same scheme as Calculation 5. Here are the differences.

- Here we are interested in $\mathcal{Y}[1/2, 1]$ and $\mathcal{W}[3/4, 1]$.
- Here we use the formula from 26 to define the map ω in Equation 64.
- Here we have

$$\mathcal{Y} = \beta_1 \cup \dots \cup \beta_{12}. \quad (70)$$

The rest of the calculation is the same.

9.11 Calculation 8

Calculation 8 works essentially the same as Calculation 6. For Statement 1, we let τ be the polyhedron which restricts to τ_s for $s \in [3/4, 1]$. We list this polyhedron in §10.1. We check that F is entirely defined on (the interior of) τ and that $F^2(\tau) = \tau$.

For Statement 2, we let \mathcal{Z}^* be the polyhedron which intersects X_s in $(Z_s^0)^*$ for $s \in [3/4, 1]$. We compute that

$$\mathcal{Z}^* \subset \beta_7 \quad (71)$$

and we finish the proof of Statement 2 just as in Calculation 6.

For Statement 3, we define \mathcal{K} as in Calculation 6 and we see by inspection that

$$\mathcal{K} = \beta_2 \cup \beta_6 \cup \beta_8 \cup \beta_{12}, \quad F(\beta_j) \subset \mathcal{Z}, \quad j = 2, 6, 8, 12. \quad (72)$$

This proves Statement 3.

10 The Raw Data

10.1 Auxilliary Polyhedra

Here we list the coordinates of the auxilliary polyhedra which arise in our calculations. All our polyhedra are scaled by a factor of 420.

Here is $\mathcal{X}[1/4, 2]$.

$$\begin{bmatrix} -525 \\ -105 \\ 105 \end{bmatrix} \begin{bmatrix} 315 \\ -105 \\ 105 \end{bmatrix} \begin{bmatrix} -315 \\ 105 \\ 105 \end{bmatrix} \begin{bmatrix} 525 \\ 105 \\ 105 \end{bmatrix} \begin{bmatrix} -1260 \\ -840 \\ 840 \end{bmatrix} \begin{bmatrix} -420 \\ -840 \\ 840 \end{bmatrix} \begin{bmatrix} 420 \\ 840 \\ 840 \end{bmatrix} \begin{bmatrix} 1260 \\ 840 \\ 840 \end{bmatrix}$$

Here is $\mathcal{A}[1/4, 1]$. This set intersects the fiber X_s in the hexagon A_s , for $s \in [1/4, 1]$.

$$\begin{bmatrix} 315 \\ 105 \\ 105 \end{bmatrix} \begin{bmatrix} -315 \\ 105 \\ 105 \end{bmatrix} \begin{bmatrix} -315 \\ -105 \\ 105 \end{bmatrix} \begin{bmatrix} 315 \\ -105 \\ 105 \end{bmatrix} \begin{bmatrix} 420 \\ 0 \\ 105 \end{bmatrix} \begin{bmatrix} -420 \\ 0 \\ 105 \end{bmatrix} \begin{bmatrix} 0 \\ 420 \\ 420 \end{bmatrix} \begin{bmatrix} 420 \\ 0 \\ 420 \end{bmatrix} \begin{bmatrix} -420 \\ 0 \\ 420 \end{bmatrix} \begin{bmatrix} 0 \\ -420 \\ 420 \end{bmatrix}$$

Here is $\mathcal{B}[1/4, 1]$. This set intersects the fiber X_s in the triangle β_s , for $s \in [1/4, 1]$.

$$\begin{bmatrix} -315 \\ -105 \\ 105 \end{bmatrix} \begin{bmatrix} -420 \\ 0 \\ 105 \end{bmatrix} \begin{bmatrix} -525 \\ -105 \\ 105 \end{bmatrix} \begin{bmatrix} -840 \\ -420 \\ 420 \end{bmatrix} \begin{bmatrix} -420 \\ 0 \\ 420 \end{bmatrix} \begin{bmatrix} 0 \\ -420 \\ 420 \end{bmatrix}$$

Here is $\mathcal{P}[1/4, 1/2]$. This set intersects the fiber X_s in the pentagon P_s , for $s \in [1/4, 1/2]$.

$$\begin{bmatrix} -315 \\ -105 \\ 105 \end{bmatrix} \begin{bmatrix} -105 \\ -105 \\ 105 \end{bmatrix} \begin{bmatrix} -105 \\ 105 \\ 105 \end{bmatrix} \begin{bmatrix} -315 \\ 105 \\ 105 \end{bmatrix} \begin{bmatrix} -630 \\ -210 \\ 210 \end{bmatrix} \begin{bmatrix} -210 \\ -210 \\ 210 \end{bmatrix} \begin{bmatrix} -210 \\ 210 \\ 210 \end{bmatrix}$$

Here is $\mathcal{Q}[1/4, 1/2]$. This set intersects the fiber X_s in the triangle Q_s , for $s \in [1/4, 1/2]$.

$$\begin{bmatrix} -525 \\ -105 \\ 105 \end{bmatrix} \begin{bmatrix} -315 \\ -105 \\ 105 \end{bmatrix} \begin{bmatrix} -315 \\ 105 \\ 105 \end{bmatrix} \begin{bmatrix} -630 \\ -210 \\ 210 \end{bmatrix}$$

Here is the period 2 tile $\tau[1, 5/4]$ from Calculation 6.

$$\begin{bmatrix} -525 \\ -315 \\ 315 \end{bmatrix} \begin{bmatrix} -315 \\ -315 \\ 315 \end{bmatrix} \begin{bmatrix} -315 \\ -105 \\ 315 \end{bmatrix} \begin{bmatrix} -525 \\ -105 \\ 315 \end{bmatrix} \begin{bmatrix} -420 \\ -420 \\ 420 \end{bmatrix}$$

Here is the period 2 tile $\tau[3/4, 1]$ from Calculation 8.

$$\begin{bmatrix} -420 \\ -420 \\ 420 \end{bmatrix} \begin{bmatrix} -210 \\ -630 \\ 630 \end{bmatrix} \begin{bmatrix} -210 \\ -210 \\ 630 \end{bmatrix} \begin{bmatrix} -630 \\ -210 \\ 630 \end{bmatrix} \begin{bmatrix} -630 \\ -630 \\ 630 \end{bmatrix}$$

Here is the domain $\mathcal{Z}[1, 5/4]$ from Calculation 6.

$$\begin{bmatrix} -420 \\ -420 \\ 420 \end{bmatrix} \begin{bmatrix} -840 \\ -420 \\ 420 \end{bmatrix} \begin{bmatrix} -945 \\ -525 \\ 525 \end{bmatrix} \begin{bmatrix} -525 \\ -525 \\ 525 \end{bmatrix} \begin{bmatrix} -525 \\ -315 \\ 525 \end{bmatrix} \begin{bmatrix} -735 \\ -315 \\ 525 \end{bmatrix}$$

Here is the domain $\mathcal{Z}[3/4, 1]$ from Calculation 8.

$$\begin{bmatrix} -420 \\ -420 \\ 420 \end{bmatrix} \begin{bmatrix} -840 \\ -420 \\ 420 \end{bmatrix} \begin{bmatrix} -945 \\ -525 \\ 525 \end{bmatrix} \begin{bmatrix} -525 \\ -525 \\ 525 \end{bmatrix} \begin{bmatrix} -525 \\ -315 \\ 525 \end{bmatrix} \begin{bmatrix} -735 \\ -315 \\ 525 \end{bmatrix}$$

10.2 The Polyhedra in the Partition

Define

$$\iota_1(x, y, s) = (-x, -y, s), \quad \iota_2(x, y, s) = \left(\frac{x+y}{2s}, \frac{x-y}{2s}, \frac{1}{2s} \right). \quad (73)$$

The partition of $\mathcal{X}[1/4, 1/2]$ consists of the 19 polyhedra

$$\alpha_0, \alpha_1, \dots, \alpha_9, \iota_1(\alpha_1), \dots, \iota_1(\alpha_9). \quad (74)$$

The partition of $\mathcal{X}[1/2, 1]$ consists of the 13 polyhedra

$$\beta_0, \beta_1, \dots, \beta_6, \iota_1(\beta_1), \dots, \iota_1(\beta_6). \quad (75)$$

The partition of $\mathcal{X}[1, 2]$ consists of the 19 polyhedra

$$\iota_2 \circ F(\alpha_i), \quad i = 0, \dots, 18. \quad (76)$$

Here $\alpha_0, \dots, \alpha_{18}$ are the polyhedra from Equation 74.

As we mentioned in the last chapter, we scale each polyhedron by a factor of 420 so that all the entries are integers. Here are the polyhedra.

$$A_0 = \begin{bmatrix} 105 \\ 105 \\ 105 \end{bmatrix} \begin{bmatrix} -105 \\ 105 \\ 105 \end{bmatrix} \begin{bmatrix} -105 \\ -105 \\ 105 \end{bmatrix} \begin{bmatrix} 105 \\ -105 \\ 105 \end{bmatrix} \begin{bmatrix} 210 \\ 210 \\ 210 \end{bmatrix} \begin{bmatrix} -210 \\ 210 \\ 210 \end{bmatrix} \begin{bmatrix} -210 \\ -210 \\ 210 \end{bmatrix} \begin{bmatrix} 210 \\ -210 \\ 210 \end{bmatrix}$$

$$A_1 = \begin{bmatrix} 420 \\ 0 \\ 105 \end{bmatrix} \begin{bmatrix} 525 \\ 105 \\ 105 \end{bmatrix} \begin{bmatrix} 315 \\ 105 \\ 105 \end{bmatrix} \begin{bmatrix} 280 \\ 140 \\ 140 \end{bmatrix}$$

$$A_2 = \begin{bmatrix} 105 \\ 105 \\ 105 \end{bmatrix} \begin{bmatrix} 280 \\ 140 \\ 140 \end{bmatrix} \begin{bmatrix} 140 \\ 140 \\ 140 \end{bmatrix} \begin{bmatrix} 210 \\ -210 \\ 210 \end{bmatrix}$$

$$A_3 = \begin{bmatrix} 280 \\ 140 \\ 140 \end{bmatrix} \begin{bmatrix} 140 \\ 140 \\ 140 \end{bmatrix} \begin{bmatrix} 210 \\ 210 \\ 210 \end{bmatrix} \begin{bmatrix} 210 \\ -210 \\ 210 \end{bmatrix} \begin{bmatrix} 420 \\ 0 \\ 210 \end{bmatrix}$$

$$A_4 = \begin{bmatrix} 525 \\ 105 \\ 105 \end{bmatrix} \begin{bmatrix} 420 \\ 0 \\ 140 \end{bmatrix} \begin{bmatrix} 420 \\ 0 \\ 210 \end{bmatrix} \begin{bmatrix} 630 \\ 210 \\ 210 \end{bmatrix} \begin{bmatrix} 210 \\ 210 \\ 210 \end{bmatrix}$$

$$A_5 = \begin{bmatrix} 315 \\ -105 \\ 105 \end{bmatrix} \begin{bmatrix} 420 \\ 0 \\ 105 \end{bmatrix} \begin{bmatrix} 315 \\ 105 \\ 105 \end{bmatrix} \begin{bmatrix} 420 \\ 0 \\ 120 \end{bmatrix} \begin{bmatrix} 378 \\ -42 \\ 126 \end{bmatrix}$$

$$A_6 = \begin{bmatrix} 420 \\ 0 \\ 120 \end{bmatrix} \begin{bmatrix} 462 \\ 42 \\ 126 \end{bmatrix} \begin{bmatrix} 420 \\ 0 \\ 140 \end{bmatrix} \begin{bmatrix} 420 \\ 140 \\ 140 \end{bmatrix} \begin{bmatrix} 280 \\ 140 \\ 140 \end{bmatrix} \begin{bmatrix} 210 \\ 210 \\ 210 \end{bmatrix}$$

$$A_7 = \begin{bmatrix} 315 \\ 105 \\ 105 \end{bmatrix} \begin{bmatrix} 420 \\ 0 \\ 120 \end{bmatrix} \begin{bmatrix} 378 \\ -42 \\ 126 \end{bmatrix} \begin{bmatrix} 420 \\ 0 \\ 140 \end{bmatrix}$$

$$A_8 = \begin{bmatrix} 315 \\ -105 \\ 105 \end{bmatrix} \begin{bmatrix} 315 \\ 105 \\ 105 \end{bmatrix} \begin{bmatrix} 105 \\ 105 \\ 105 \end{bmatrix} \begin{bmatrix} 105 \\ -105 \\ 105 \end{bmatrix} \begin{bmatrix} 420 \\ 0 \\ 140 \end{bmatrix} \begin{bmatrix} 280 \\ 140 \\ 140 \end{bmatrix} \begin{bmatrix} 210 \\ -210 \\ 210 \end{bmatrix} \begin{bmatrix} 420 \\ 0 \\ 210 \end{bmatrix}$$

$$\begin{aligned}
A9 &= \begin{bmatrix} 420 \\ 0 \\ 105 \end{bmatrix} \begin{bmatrix} 525 \\ 105 \\ 105 \end{bmatrix} \begin{bmatrix} 420 \\ 0 \\ 120 \end{bmatrix} \begin{bmatrix} 462 \\ 42 \\ 126 \end{bmatrix} \begin{bmatrix} 420 \\ 140 \\ 140 \end{bmatrix} \begin{bmatrix} 280 \\ 140 \\ 140 \end{bmatrix} \\
B0 &= \begin{bmatrix} 105 \\ 105 \\ 105 \end{bmatrix} \begin{bmatrix} -105 \\ 105 \\ 105 \end{bmatrix} \begin{bmatrix} -105 \\ -105 \\ 105 \end{bmatrix} \begin{bmatrix} 105 \\ -105 \\ 105 \end{bmatrix} \begin{bmatrix} 210 \\ 210 \\ 210 \end{bmatrix} \begin{bmatrix} -210 \\ 210 \\ 210 \end{bmatrix} \begin{bmatrix} -210 \\ -210 \\ 210 \end{bmatrix} \begin{bmatrix} 210 \\ -210 \\ 210 \end{bmatrix} \\
B1 &= \begin{bmatrix} 420 \\ 0 \\ 105 \end{bmatrix} \begin{bmatrix} 525 \\ 105 \\ 105 \end{bmatrix} \begin{bmatrix} 315 \\ 105 \\ 105 \end{bmatrix} \begin{bmatrix} 280 \\ 140 \\ 140 \end{bmatrix} \\
B2 &= \begin{bmatrix} 105 \\ 105 \\ 105 \end{bmatrix} \begin{bmatrix} 280 \\ 140 \\ 140 \end{bmatrix} \begin{bmatrix} 140 \\ 140 \\ 140 \end{bmatrix} \begin{bmatrix} 210 \\ -210 \\ 210 \end{bmatrix} \\
B3 &= \begin{bmatrix} 280 \\ 140 \\ 140 \end{bmatrix} \begin{bmatrix} 140 \\ 140 \\ 140 \end{bmatrix} \begin{bmatrix} 210 \\ 210 \\ 210 \end{bmatrix} \begin{bmatrix} 210 \\ -210 \\ 210 \end{bmatrix} \begin{bmatrix} 420 \\ 0 \\ 210 \end{bmatrix} \\
B4 &= \begin{bmatrix} 525 \\ 105 \\ 105 \end{bmatrix} \begin{bmatrix} 420 \\ 0 \\ 140 \end{bmatrix} \begin{bmatrix} 420 \\ 0 \\ 210 \end{bmatrix} \begin{bmatrix} 630 \\ 210 \\ 210 \end{bmatrix} \begin{bmatrix} 210 \\ 210 \\ 210 \end{bmatrix} \\
B5 &= \begin{bmatrix} 315 \\ -105 \\ 105 \end{bmatrix} \begin{bmatrix} 420 \\ 0 \\ 105 \end{bmatrix} \begin{bmatrix} 315 \\ 105 \\ 105 \end{bmatrix} \begin{bmatrix} 420 \\ 0 \\ 120 \end{bmatrix} \begin{bmatrix} 378 \\ -42 \\ 126 \end{bmatrix} \\
B6 &= \begin{bmatrix} 420 \\ 0 \\ 120 \end{bmatrix} \begin{bmatrix} 462 \\ 42 \\ 126 \end{bmatrix} \begin{bmatrix} 420 \\ 0 \\ 140 \end{bmatrix} \begin{bmatrix} 420 \\ 140 \\ 140 \end{bmatrix} \begin{bmatrix} 280 \\ 140 \\ 140 \end{bmatrix} \begin{bmatrix} 210 \\ 210 \\ 210 \end{bmatrix}
\end{aligned}$$

10.3 The Action of the Map

In this section we explain the action of the map on each of the polyhedra listed above. To each polyhedron we associate a 4-tuple of integers. The list $V = (u_1, v_1, u_2, v_2)$ tells us that

$$F_V \begin{bmatrix} x \\ y \\ s \end{bmatrix} = \begin{bmatrix} 1 & 0 & 2v_1 - 2v_2 \\ 0 & 1 & 2v_1 + 2v_2 \\ 0 & 0 & 1 \end{bmatrix} \begin{bmatrix} x \\ y \\ s \end{bmatrix} + \begin{bmatrix} -2u_1 \\ 2u_2 \\ 0 \end{bmatrix}. \quad (77)$$

Remark; Equation 77 gives the equation for the action on the unscaled polyhedra. When we acts on the scaled polyhedra listed above, we need to scale the translation part of the map by 420. That is, $-2u_1$ and $2u_2$ need to be replaced by $-840u_1$ and $840u_2$.

The polyhedra α_0 and β_0 correspond to the trivial tiles. The vectors associated to these are $a_0 = b_0 = (0, 0, 0, 0)$. Below we will list the vectors $a_1, \dots, a_9, b_1, \dots, b_6$. We have the relations

$$a_{9+i} = -a_i, \quad b_{6+i} = -b_i. \quad (78)$$

The vector c_i associated to $\iota_2 \circ F(\alpha_i)$ is given by the following rule:

$$a_i = (u_1, v_1, u_2, v_2) \implies c_i = (-v_2, -u_2, -v_1, -u_1). \quad (79)$$

Recall that the map F is really the composition $(F')^2$, where F' maps the bundle $\mathcal{X}[1/4, 2]$ to the polyhedron obtained by rotating $\mathcal{X}[1/4, 2]$ by 90 degrees about the z -axis. To get the action of F' we simply replace each vector $V = a_1, a_2, \dots$ by V' , where

$$V = (u_1, v_1, u_2, v_2) \implies V' = (u_1, v_1, 0, 0). \quad (80)$$

Here are the vectors.

$$\begin{aligned} a_1 &= (1, 2, 0, -2), & a_2 &= (0, -1, -1, -2) & a_3 &= (0, -1, -1, -1). \\ a_4 &= (1, 1, 0, -1), & a_5 &= (0, -2, -1, -2) & a_6 &= (1, 2, 1, 1). \\ a_7 &= (0, -2, -1, -1), & a_8 &= (0, -1, 0, 1) & a_9 &= (1, 2, 1, 2). \\ b_1 &= (1, 0, -1, -1), & b_2 &= (1, 1, 0, -1) & b_3 &= (1, 1, 1, 0). \\ b_4 &= (0, -1, -1, 0), & b_5 &= (0, -1, -1, -1) & b_6 &= (1, 1, 1, 1). \end{aligned}$$

11 References

- [AG] A. Goetz and G. Poggiaspalla, *Rotations by $\pi/7$* , Nonlinearity **17** (2004) no. 5 1787-1802
- [AKT] R. Adler, B. Kitchens, and C. Tresser, *Dynamics of non-ergodic piecewise affine maps of the torus*, Ergodic Theory Dyn. Syst **21** (2001) no. 4 959-999
- [BKS] T. Bedford, M. Keane, and C. Series, eds., *Ergodic Theory, Symbolic Dynamics, and Hyperbolic Spaces*, Oxford University Press, Oxford (1991).
- [B] J. Buzzi, *Piecewise isometries have zero topological entropy (English summary)* Ergodic Theory and Dynamical Systems **21** (2001) no. 5 pp 1371-1377
- [GH1] E Gutkin and N. Haydn, *Topological entropy of generalized polygon exchanges*, Bull. Amer. Math. Soc., **32** (1995) no. 1., pp 50-56
- [GH2] E Gutkin and N. Haydn, *Topological entropy polygon exchange transformations and polygonal billiards*, Ergodic Theory and Dynamical Systems **17** (1997) no. 4., pp 849-867
- [H] H. Haller, *Rectangle Exchange Transformations*, Monatsh Math. **91** (1985) 215-232
- [Hoo] W. Patrick Hooper, *Renormalization of Polygon Exchange Maps arising from Corner Percolation* Invent. Math. 2012.
- [LKV] J. H. Lowenstein, K. L. Koupsov, F. Vivaldi, *Recursive Tiling and Geometry of piecewise rotations by $\pi/7$* , nonlinearity **17** (2004) no. 2. [Low] J. H. Lowenstein, *Aperiodic orbits of piecewise rational rotations of convex polygons with recursive tiling*, Dyn. Syst. **22** (2007) no. 1 25-63
- [R] G. Rauzy, *Exchanges d'intervalles et transformations induites*, Acta. Arith. **34** 315-328 (1979)
- [S0] R.E. Schwartz *The Octagonal PET II: Topology of the Limit Sets*,

preprint (2012)

[S1] R.E. Schwartz *Outer Billiards, Quarter Turn Compositions, and Polytope Exchange Transformations*, preprint (2011)

[S2] R. E. Schwartz, *Outer Billiards on Kites*, Annals of Math Studies **171**, Princeton University Press (2009)

[S3] R. E. Schwartz, *Outer Billiards on the Penrose Kite: Compactification and Renormalization*, Journal of Modern Dynamics, 2012.

[T] S. Tabachnikov, *Billiards*, Société Mathématique de France, “Panoramas et Synthèses” 1, 1995

[VL] F. Vivaldi and J. H. Lowenstein, —it Arithmetical properties of a family of irrational piecewise rotations, *Nonlinearity* **19**:1069–1097 (2007).

[Y] J.-C. Yoccoz, *Continued Fraction Algorithms for Interval Exchange Maps: An Introduction*, Frontiers in Number Theory, Physics, and Geometry Vol 1, P. Cartier, B. Julia, P. Moussa, P. Vanhove (editors) Springer-Verlag 4030437 (2006)

[Z] A. Zorich, *Flat Surfaces*, Frontiers in Number Theory, Physics, and Geometry Vol 1, P. Cartier, B. Julia, P. Moussa, P. Vanhove (editors) Springer-Verlag 4030437 (2006)